# Novel insights into the infection mechanism of oomycete *Pythium* spp. in the host *Arabidopsis thaliana*.

A Thesis Submitted to the College of

Graduate and Postdoctoral Studies

in Partial Fulfillment of the Requirements

for the Degree of Master of Science

in the Department of Biology

University of Saskatchewan

Saskatoon, Canada

By:

Wilhelmina Gerarda Hendrica Maria Hendriks

(Anouk Hendriks)

2020

## PERMISSION TO USE

In presenting this thesis in partial fulfilment of the requirements for a Postgraduate degree from the University of Saskatchewan, I agree that the Libraries of this University may make it freely available for inspection. I further agree that permission for copying of this thesis in any manner, in whole or in part, for scholarly purposes may be granted by the professor or professors who supervised my thesis work or, in their absence, by the Head of the Department or the Dean of the College in which my thesis work was done. It is understood that any copying or publication or use of this thesis/dissertation or parts thereof for financial gain shall not be allowed without my written permission. It is also understood that due recognition shall be given to me and to the University of Saskatchewan in any scholarly use, which may be made of any material in my thesis.

Requests for permission to copy or to make other uses of materials in this thesis/dissertation in whole or part should be addressed to:

Head of the Department of Biology
University of Saskatchewan
112 Science Place
Saskatoon, Saskatchewan S7N5E2
Canada

OR

College of Graduate and Postdoctoral Studies
University of Saskatchewan
116 Thorvaldson Building,
Saskatoon, Saskatchewan S7N 5C9
Canada

# ABSTRACT

Phytopathogenic *Pythium* spp. cause seedling damping-off of a wide range of plant species worldwide and are traditionally considered necrotrophs. In this study, novel pathogenicity was discovered involving the oomycete *Pythium cryptoirregulare* and the model plant *Arabidopsis thaliana*. This pathogen was isolated from *A. thaliana* seedlings that were showing damping-off symptoms and was later identified as *Pythium cryptoirregulare* based on morphological and molecular characterization alongside reference species *P. irregulare* and *P. ultimum* var. *ultimum*. To examine its infection strategy, *A. thaliana* was inoculated with *P. cryptoirregulare* and studied using a microscopy approach. Viable colonized cells were observed based on neutral red uptake and the ability to undergo cell plasmolysis after infection. This biotrophic interaction contradicts the previously reported necrotrophic lifestyle of *Pythium* spp., which is characterized by killing the host cells prior to colonization. In addition, inhibition of root growth was detected prior to colonization by *P. cryptoirregulare*, suggesting that *P. cryptoirregulare* secreted growth inhibitors. Potentially, these inhibiting metabolites facilitate infection by delaying plant development and, thereby, extending the seedling stage that is targeted by this pathogen. Notably, *P. cryptoirregulare* culture filtrates disturbed transport and distribution of auxins, indicated by altered GFP expression in the *A. thaliana* lines PIN1-GFP, PIN2-GFP, PIN3-GFP, PIN7-GFP and DR5::GFP which visualize the auxin efflux. This disturbance was further confirmed by a reduced inhibitory effect on the auxin-insensitive *A. thaliana* mutants *axr1-3*, *axr4-2*, and *aux1-7*. Metabolic activity assay results suggested that *P. cryptoirregulare* secretes auxin-related metabolites that are involved in reprogramming plant growth. Overall, the characterization of *P. cryptoirregulare* as a novel pathogen on *A. thaliana* gives new insights into understanding the pathogenic mechanisms and interactions between oomycetes and plants.



**Keywords:** *Pythium (cryptoirregulare)*, infection strategy, hemibiotrophy, metabolic activity, auxin homeostasis

# ACKNOWLEDGEMENTS

First, I would like to thank my supervisor, Dr. Yangdou Wei, for his guidance, support, and knowledge in my journey to obtaining an M.Sc degree. He was and still is a very knowledgeable mentor, and I am very thankful for sharing his knowledge with me during my project.

Secondly, I would like to thank my advisory committee, Drs. Sabine Banniza and Art Davis for their guidance and advice in my course work, my research project, and other related matters. Also, I would like to thank Dr. Zamir Punja for acting as an external examiner during my thesis defence.

Confocal microscopy techniques were taught by Dr. Guosheng Liu, who taught me how to use the Confocal 510 and Confocal 880 microscope, and Dr. Chris Ambrose, who taught me how to use the Confocal 880 and how to analyse the pictures with the imaging software "ImageJ". They are therefore greatly thanked for their support.

I would also like to thank my lab members Dr. Lijiang Lui and Li Qin, who practically helped whenever and wherever this was requested.

The National Research Council (NRC) Canada is also appreciated for supporting this project financially and Agriculture and Agri-Food Canada (AAFC) for providing the two *Pythium* reference strains from their Canadian Collection of Fungal Cultures (DAOMC).

Finally, I would like to thank my family, friends, colleagues, and remaining Biology faculty and staff for all their care, support, and patience throughout my graduate studies by creating a home away from home. Of this list, special thanks go to my parents and other family members who were my greatest motivators to complete this degree at the University of Saskatchewan in Canada.

# TABLE OF CONTENTS

**PERMISSION TO USE** ..... **i**

**ABSTRACT** ..... **ii**

**ACKNOWLEDGEMENTS** ..... **iii**

**TABLE OF CONTENTS** ..... **iv**

**LIST OF FIGURES** ..... **vii**

**LIST OF TABLES** ..... **x**

**LIST OF ABBREVIATIONS** ..... **xii**

**CHAPTER 1 GENERAL INTRODUCTION** ..... **1**

1.1 Research objectives ..... 2

**CHAPTER 2 LITERATURE REVIEW** ..... **4**

2.1 An overview of plant-pathogen interactions ..... 4

2.1.1 Biotrophy ..... 5

2.1.2 Necrotrophy ..... 6

2.1.3 Hemibiotrophy ..... 6

2.2 Infection mechanism and host-response ..... 8

2.3 Plant-oomycete pathosystems ..... 9

2.4 Plant-*Pythium* interactions ..... 10

2.4.1 The genus *Pythium* ..... 11

2.4.2 The life cycle of *Pythium* species ..... 15

2.4.3 Infection strategy of *Pythium* species ..... 16

2.4.4 *Pythium* interaction with the host *Arabidopsis thaliana* ..... 17

2.4.5 The importance of damping-off and root rot disease caused by *Pythium* species ..... 23

2.4.6 Management strategy ..... 24

**CHAPTER 3 ISOLATION, GROWTH, AND IDENTIFICATION OF *PYTHIUM CRYPTOIRREGULARE*** ..... **26**

3.1 Introduction ..... 26

3.2 Materials and methods ..... 28
3.2.1 Plant and pathogen materials ..... 28
3.2.2 Isolation of *Pythium cryptoirregulare* from *Arabidopsis thaliana* ..... 31
3.2.3 Media optimization to induce *Pythium* structure development ..... 31
3.2.4 Morphological characterization and identification ..... 32
3.2.5 Molecular characterization and identification ..... 33
3.3 Results ..... 36
3.3.1 Optimized media for the structure development of *Pythium* species ..... 36
3.3.2 Hyphal characteristics of *Pythium* species ..... 39
3.3.3 Characteristics of the reproductive structures of *Pythium* species ..... 40
3.3.4 Characteristics of the asexual reproductive structures ..... 42
3.3.5 Appressoria characteristics ..... 43
3.3.6 Morphological similarities and differences of the *Pythium* candidate with the reference species *P. irregulare* and *P. ultimum* var. *ultimum* ..... 44
3.3.7 Molecular characteristics and phylogeny of the *Pythium* candidate compared to *Pythium* reference species ..... 46
3.4 Discussion ..... 50

**CHAPTER 4 PATHOGENICITY AND INFECTION STRATEGIES OF *PYTHIUM CRYPTOIRREGULARE* ..... 52**

4.1 Introduction ..... 52
4.2 Materials and Methods ..... 54
4.2.1 Plant and pathogen materials ..... 54
4.2.2 Inoculation procedures ..... 54
4.2.3 Material preparation and microscopy techniques ..... 55
4.2.4 Mutant and host-specific screening for resistance ..... 57
4.3 Results ..... 59
4.3.1 Sensitivity of *Arabidopsis thaliana* to *Pythium cryptoirregulare* ..... 59
4.3.2 Colonization and reproduction on *Arabidopsis thaliana* ..... 60
4.3.3 Hemibiotrophy versus necrotrophy ..... 63
4.3.4 Resistance against *Pythium cryptoirregulare* ..... 67
4.4 Discussion ..... 68

**CHAPTER 5 AUXIN-LIKE METABOLITE EXTRACTION AND CHARACTERIZATION FROM *PYTHIUM CRYPTOIRREGULARE* ..... 70**

5.1 Introduction ..... 70

5.2 Materials and methods ..... 72

5.2.1 Plant and pathogen materials ..... 72

5.2.2 Metabolite extraction and media preparation ..... 72

5.2.3 Seedling development assessment ..... 73

5.2.4 Visualization of the auxin homeostasis with the use of confocal microscopy ..... 74

5.2.5 Auxin insensitivity assay ..... 75

5.3 Results ..... 78

5.3.1 Growth inhibition in response to *Pythium* culture filtrates ..... 78

5.3.2 Altered auxin homeostasis in response to *Pythium* metabolites ..... 83

5.3.3 Reduced root growth inhibition in auxin insensitive mutants in the presence of metabolites secreted by *Pythium* species ..... 89

5.4 Discussion ..... 97

**CHAPTER 6 GENERAL DISCUSSION AND CONCLUSION ..... 101**

**CHAPTER 7 FUTURE PERSPECTIVE ..... 104**

**LITERATURE CITED ..... 106**

**APPENDIX A ..... 119**

**APPENDIX B ..... 124**

**APPENDIX C ..... 129**

# LIST OF FIGURES

**Figure 2.1** Diagrams and photos of biotrophic, necrotrophic and hemibiotrophic infection strategies. ..... 8
**Figure 2.2** Phylogenetic tree presenting the re-classification of oomycetes separately from the kingdom Fungi. ..... 13
**Figure 2.3** Phylogeny of *Pythium* species based on the ITS region and the D1 to D3 regions of the nuclear large ribosomal subunit. ..... 14
**Figure 2.4** Life cycle of a root-infection by *Pythium* species. ..... 16
**Figure 2.5** Auxin distribution mediated by the PIN efflux carriers. ..... 23
**Figure 3.1** *Arabidopsis thaliana* transgenic line *FH1-YFP* showing damping-off symptoms upon infection by the *Pythium* candidate. ..... 36
**Figure 3.2** Structure induction of *Pythium cryptoirregulare* through media composition. ..... 38
Figure **3.3** The influence of surface contact on the appressoria formation of *Pythium cryptoirregulare*. ..... 39
**Figure 3.4** Hyphae characteristics of *Pythium cryptoirregulare* ..... 39
**Figure 3.5** Mycelial growth of *Pythium cryptoirregulare* in water droplets. ..... 40
**Figure 3.6** Oogonium development of *Pythium cryptoirregulare*. ..... 40
**Figure 3.7** A variety of *Pythium cryptoirregulare* oogonium fertilizations by paragynous antheridium or antheridia. ..... 41
**Figure 3.8** Differences in morphological characteristics of *Pythium cryptoirregulare* oospores. 42
**Figure 3.9** Terminal sporangia of *Pythium cryptoirregulare*. ..... 43
**Figure 3.10** *Pythium cryptoirregulare* appressoria formation upon contact with a hydrophobic surface. ..... 43
**Figure 3.11** Differences in appressoria abundance between the *Pythium* species of this study. . 44
**Figure 3.12** Comparison of morphological characteristics of *Pythium cryptoirregulare*, *Pythium irregulare* and *Pythium ultimum* var. *ultimum*. ..... 45
**Figure 3.13** PCR amplification products from the *Pythium* candidate (*P.ci.*), *Pythium irregulare* (*P.i.*, DOAMC 870 BR) and *Pythium ultimum* var. *ultimum* (*P.u.*, DAOMC 628 BR). ..... 46
**Figure 3.14** Evolutionary relationships between the *Pythium irregulare* and *Pythium cryptoirregulare* taxa. ..... 48

**Figure 3.15** Evolutionary relationships of *Pythium* taxa..... 49
**Figure 4.1** Disease development of *Arabidopsis thaliana* seeds and seedlings after inoculation with *Pythium cryptoirregulare* at time points 0.5, 3 and 7 days post-seeding (dps). ..... 59
**Figure 4.2** Infection of the root tissue of *Arabidopsis thaliana* seedlings after inoculation with *Pythium cryptoirregulare*..... 60
**Figure 4.3** Colonization of *Pythium cryptoirregulare* within *Arabidopsis thaliana* hypocotyl tissue associated with intracellular and intercellular hyphae. ..... 61
**Figure 4.4** *Pythium cryptoirregulare* hyphae exiting and re-entering *Arabidopsis thaliana* root tissue. ..... 62
**Figure 4.5** *Pythium cryptoirregulare* oospore development inside *Arabidopsis thaliana* host tissue. ..... 62
**Figure 4.6** *Pythium cryptoirregulare* hyphae exiting *Arabidopsis thaliana* tissues by penetration of epidermal surface..... 63
**Figure 4.7** Plasmolyzed and neutral red-stained *Arabidopsis thaliana* cotyledon cells infected by *Pythium cryptoirregulare*..... 64
**Figure 4.8** Plasmolyzed and neutral red-stained *Arabidopsis thaliana* root cells surrounded by *Pythium cryptoirregulare* hyphae. ..... 65
**Figure 4.9** Plasmolysis and GFP expression in the hypocotyl of the *Arabidopsis thaliana* plasma membrane marker line PMA-GFP after hyphal infection by *Pythium cryptoirregulare*..... 66
**Figure 4.10** *Arabidopsis thaliana* plasma membrane marker line LTI6b-GFP infected by *Pythium cryptoirregulare* hyphae. ..... 66
**Figure 4.11** *Arabidopsis thaliana* mutant screening for resistance against *Pythium cryptoirregulare* hyphae. ..... 67
**Figure 5.1** Inhibition of *Arabidopsis thaliana* seedling development caused by unknown metabolites in *Pythium cryptoirregulare* culture filtrate. ..... 80
**Figure 5.2** Germination and development of *Brassica napus* cv. Westar seeds and seedlings in the presence of *Pythium cryptoirregulare* culture filtrate..... 81
**Figure 5.3** Development of *Arabidopsis thaliana* root tips in the presence of different concentrations and treatments of *Pythium cryptoirregulare* culture filtrate..... 82
**Figure 5.4** Development of *Arabidopsis thaliana* PIN1-GFP marker line in the presence of uninoculated ½ Murashige and Skoog broth (½ MSB) and *Pythium cryptoirregulare* (*P.ci.*),

*Pythium irregulare* (*P.i.*, DOAMC 870 BR) and *Pythium ultimum* var. *ultimum* (*P.u.*, DAOMC 628 BR) culture filtrates..... 83
**Figure 5.5** Altered auxin transport in root tissues of *Arabidopsis* seedlings upon exposure to culture filtrates of *Pythium* species. ..... 85
**Figure 5.6** Altered auxin concentrations in the root tips of *Arabidopsis* DR5::GFP seedlings upon exposure to culture filtrates of *Pythium* species. ..... 88
**Figure 5.7** Auxin sensitivity assay presenting the difference in root growth inhibition between *Arabidopsis thaliana* Col-0 roots and roots from the auxin insensitive mutants *axr3-1*, *axr4-2* and *aux1-7*, all grown in the presence of *Pythium cryptoirregulare* (*P.ci.*), *Pythium irregulare* (*P.i.*, DOAMC 870 BR) and *Pythium ultimum* var. *ultimum* (*P.u.*, DAOMC 628 BR) culture filtrates or IAA. ..... 90
**Figure 5.8** Standard curve, generated from mean root lengths (mm) after incubation in the presence of different IAA concentrations. ..... 91
**Figure 5.9** Assessment of the effect of additional IAA on the inhibition of *Arabidopsis thaliana* root growth caused by *Pythium cryptoirregulare* (*P.ci.*), *Pythium irregulare* (*P.i.*, DOAMC 870 BR) and *Pythium ultimum* var. *ultimum* (*P.u.*, DAOMC 628 BR) culture filtrate. ..... 95
**Figure 5.10** *Arabidopsis thaliana* Col-0 wildtype and auxin-insensitive mutant seedlings showing differences in gravitropism adjustments upon exposure to IAA or *Pythium cryptoirregulare* (*P.ci.*), *Pythium irregulare* (*P.i.*, DOAMC 870 BR) and *Pythium ultimum* var. *ultimum* (*P.u.*, DAOMC 628 BR) culture filtrate. ..... 96

# LIST OF TABLES

**Table 3.1** *Pythium* reference strains ordered from the Canadian Collection of Fungal Cultures (DOAMC) ..... 28
**Table 3.2** *Pythium* strains used for differentiation between *Pythium irregulare* and *Pythium cryptoirregulare* ..... 29
**Table 3.3** Isolates used for the phylogenetic tree construction in this study.The isolate that was obtained during this study is underlined ..... 30
**Table 3.4** Alignment with reference sequences for differentiation between *Pythium irregulare* (*P.i.*) and *Pythium cryptoirregulare* (*P.ci*.),where the differences in sequence are highlighted in grey ..... 47
**Table 5.1** Summary of the metabolite function assessments ..... 77
**Table 5.2** ANOVA (One-way) results of the linear mixed-effects model based on *Brassica napus* root length upon exposure to ½ MSB or *Pythium cryptoirregulare* CF ..... 81
**Table 5.3** Mean fluorescence intensity of the root cap and epidermis region of DR5::GFP ..... 86
**Table 5.4** Tukey's HSD post-hoc results of the DR5::GFP root cap and epidermis fluorescence intensity upon exposure to ½ Murashige and Skoog broth (½ MSB) or *Pythium cryptoirregulare* (*P.ci.*), *Pythium irregulare* (*P.i.*, DOAMC 870 BR) or *Pythium ultimum* var. *ultimum* (*P.u.*, DAOMC 628 BR) culture filtrate (CF) ..... 86
**Table 5.5** Mean fluorescence intensity of the columella region of DR5::GFP ..... 87
**Table 5.6** Tukey's HSD post-hoc results of the DR5::GFP columella fluorescence intensity upon exposure to ½ Murashige and Skoog broth (½ MSB) or *Pythium cryptoirregulare* (*P.ci.*), *Pythium irregulare* (*P.i.*, DOAMC 870 BR) or *Pythium ultimum* var. *ultimum* (*P.u.*, DAOMC 628 BR) culture filtrates (CF) ..... 87
**Table 5.7** List of differences according to R using the difflsmeans function for pairwise comparison between the root length of *Arabidopsis thaliana* Col-0 seedlings grown on media containing uninoculated ½ Murashige and Skoog broth, and media containing *Pythium* culture filtrates or IAA, all after 14 days of incubation ..... 89
**Table 5.8** Estimated concentrations (nM) of auxin-like metabolites secreted by *Pythium* spp. after 10 days of incubation in ½ MSB ..... 92

**Table 5.9** List of differences according to R using the difflsmeans function for pairwise comparison between the root length of *Arabidopsis thaliana* Col-0 seedlings and auxin insensitive mutants grown on media containing IAA, all after 14 days of incubation..... 92
**Table 5.10** List of differences according to R using the difflsmeans function for pairwise comparison between the root length of *Arabidopsis thaliana* Col-0 seedlings and auxin insensitive mutants grown on media containing 0.25x CFs, all after 14 days of incubation..... 93

# LIST OF ABBREVIATIONS

| | |
|---|---|
| 3D | 3-dimensional |
| ABA | abscisic acid |
| AGI | *Arabidopsis* Genome Initiative |
| BLAST | basic local alignment search tool |
| bp | base pair |
| BP filter | band pass filter |
| CBS | Centraalbureau voor Schimmelculturen |
| CF | culture filtrate |
| CFW | calcofluor white |
| CMA | cornmeal agar |
| CMB | cornmeal broth |
| CMGPA | cornmeal/glucose/peptone agar |
| CMGPB | cornmeal/glucose/peptone broth |
| Col-0 | Columbia-0 |
| *cox* | cytochrome oxidase c subunit |
| cv. | cultivar |
| CWDE | cell wall degrading enzymes |
| DIC | differential interference contrast |
| DNA | deoxyribonucleic acid |
| dNTP | deoxynucleoside triphosphate |
| DOAMC | Canadian collection of fungal cultures |
| dpi | days post-inoculation |
| dps | days post-seeding |
| EDTA | ethylenediaminetetraacetic acid |
| EHM | extrahaustorial membrane |
| EHMx | extrahaustorial matrix |
| ET | ethylene |
| ETI | effector-triggered immunity |
| GA | gibberellin |
| GFP | green fluorescent protein |
| GI | GenInfo identifier |
| GUS | β-glucuronidase |
| $H_2O$ | dihydrogen monoxide (water) |
| HPLC | high-performance liquid chromatography |
| HR | hypersensitive response |
| IAA | indole-3-acetic acid |
| IFM | interfacial extracellular matrices |
| ITS | internal transcriber spacer |
| JA | jasmonic acid |
| $K_2HPO_4$ | dipotassium phosphate |
| Kb | kilo base pair |
| KCl | potassium chloride |
| $KH_2PO_4$ | Potassium dihydrogen phosphate |
| LLR | leucine-rich repeat |

| | |
|---|---|
| LP filter | long pass filter |
| LSM | laser scanning microscope |
| LSU | large nuclear ribosomal unit |
| MAMP | microbe-associated molecular pattern |
| MEGA x | Molecular Evolutionary Genetics Analysis x |
| MSA | Murashige and Skoog agar |
| MSB | Murashige and Skoog broth |
| MUSCLE | MUltiple Sequence Comparison by Log-Expectation |
| MYPA | maltose/yeast extract/peptone agar |
| MYPB | maltose/yeast extract/peptone broth |
| NBS | nucleotide-binding sites |
| NCBI | National Center for Biotechnology Information |
| NR | neutral red |
| NRC | National Research Council |
| PAMP | pathogen-associated molecular pattern |
| *P.ci.* | *Pythium cryptoirregulare* |
| PCR | polymerase chain reaction |
| PDA | potato dextrose agar |
| PDB | potato dextrose broth |
| PI | propidium iodide |
| *P.i.* | *Pythium irregulare* |
| PRR | pattern recognition receptors |
| PTI | PAMP-triggered immunity |
| *P.u.* | *Pythium ultimum* var. *ultimum* |
| R | resistance |
| RA | rice agar |
| RB | rice broth |
| rDNA | ribosomal deoxyribonucleic acid |
| RNA | ribonucleic acid |
| ROS | reactive oxygen species |
| rpm | rounds per minute |
| rRNA | ribosomal ribonucleic acid |
| SA | salicylic acid |
| UV | ultraviolet |
| V | volts |
| v/v | volume per volume |
| WGA | wheat germ agglutinin |

# CHAPTER 1

## GENERAL INTRODUCTION

A wide range of plant pathogens form a global threat to agricultural and natural plant systems, partially due to the increased spread because of human mobility and globalization of trade (Lacomme, 2015). Since the world population is increasing by the year, global agricultural demand has also grown (Bennett, 2015). High-impact research with innovative approaches and broad applications are required to satisfy the higher demands for safe and nutritious food.

The study of plant pathology plays a crucial role in meeting these higher demands by creating an understanding of plant pathogens that cause a threat to food production. Knowledge of the genotypic and phenotypic variation of plant pathogens contributes to disease management and the promotion of plant health, including plant resistance, without the use of chemicals that cause harm to the environment. Modern genomic approaches provide us with information about the changes in the genome of the plant as well as the pathogen. This information is valuable in disease management for predicting the durability of any plant resistance.

Also, for diagnosis of pathogens that pose threats, methods were developed such as morphological identification, molecular identification, bioassays and serological methods. Often, a multitude of these methods are used to increase the reliability of these diagnoses because many pathogens cause similar disease symptoms. Especially differentiation within a pathogen genus can require quite detailed and precise diagnostic approaches.

Overall, knowledge in the field of plant pathology is essential for keeping up with the forever growing agricultural and ornamental plant production worldwide.

In 2017, damping-off symptoms were observed on *Arabidopsis thaliana* (L.) Heynh in the growth chambers of the Department of Biology at the University of Saskatchewan, Saskatoon, Canada. After morphological and molecular characterization of this isolate was performed, the causal agent was identified as *Pythium cryptoirregulare* (Garzón, Yánez & G.W. Moorman sp.

nov). Interestingly, this pathogen has not been recorded as a pathogen to the model plant *A. thaliana,* before now.

## 1.1 Research objectives

The discovery of the novel pathogenicity of *P. cryptoirregulare* on *A. thaliana* formed an opportunity to carefully study the infection mechanism of *P. cryptoirregulare* as *A. thaliana* is a model organism that is used to study many diseases that occur on agricultural crops (Meinke *et al.*, 1998). The goal of this study was to establish a better understanding of the infection strategy of *P. cryptoirregulare* on this host, which is crucial for future damping-off disease management in field crops. In addition, a strain of *P. irregulare* Buisman (DAOMC 870 BR) and a strain of *Pythium ultimum* var. *ultimum* (DAOMC 628 BR) were obtained from the Canadian Collection of Fungal Cultures (DAOMC) to be investigated and compared as close and distant relatives of the *P. cryptoirregulare* isolate.

The following objectives were addressed as a part of this M.Sc. research project by employing various cellular, genetic, and molecular approaches.

1) **Morphological and molecular identification of *P. cryptoirregulare* as a novel oomycete pathogen on *A. thaliana*.** After the pathogen was isolated from *A. thaliana* and maintained on media plates, the growth conditions of the media were optimized for morphological characterization and identification by light and confocal laser-scanning microscopy. Molecular identification was based on ITS sequencing of DNA extracted from *P. cryptoirregulare* mycelia.

2) **Establishment of a better understanding of the infection strategy of *P. cryptoirregulare* on the host *A. thaliana* by using histological approaches, including live-cell imaging and fixed cell imaging, to illustrate the infection process.** The infection structures of *P. cryptoirregulare* were examined on and in host tissues of *A. thaliana* seedlings, mainly, to determine whether *P. cryptoirregulare* follows a hemibiotrophic or a necrotrophic infection strategy. Live cell imaging was used to clearly locate the initial hyphal structures on a cellular level after plasmolysis and staining were performed to show the infected cell's viability. After further advanced infection, an

additional fixed cell imaging was also used to illustrate the colonization of hyphal and reproductive structures.

3) **Examination of biological activities of secreted metabolites of *P. cryptoirregulare* that are affecting *A. thaliana* development**. Culture filtrates of *P. cryptoirregulare* exhibited inhibitory effects on seedling development of the host *A. thaliana*. Standardized experiments were designed, including the conditions of culture filtrate production and activity assays to determine metabolite activity. The auxin homeostasis of the seedlings affected by the culture filtrates was observed using transgenic fluorescent protein-tagged lines and auxin-insensitive mutants of *A. thaliana*. The results of these approaches contributed to an understanding of the function of the secreted metabolites and, potentially, their identification.

Due to the typical damping-off symptoms of the diseased seedlings that were found in the growth chambers it was hypothesized that the causal agent was a *Pythium* sp. Despite that the majority of previous studies presented *Pythium* species as necrotrophic pathogens, in this study, hyphae were found inside viable cells. This led to the hypothesis of a biotrophic phase being part of the infection cycle of *P. cryptoirregulare*, which contradicts the overall description of *Pythium* as a necrotroph. During these infection assays, a reduced seedling development was also observed when *P. cryptoirregulare* was present, suggesting that *P. cryptoirregulare* secreted growth inhibitors. Because the secretion of the yet unknown metabolites led to a reduced seedling development and root growth, it was hypothesized that the secreted metabolites either were auxins or exhibited an auxin-like function. The reduced seedling development potentially contributes to a greater infection success as *Pythium* species target seedlings. A delay in development would cause a longer seedling stage and therefore a longer period for the pathogen to infect.

# CHAPTER 2

# LITERATURE REVIEW

## 2.1 An overview of plant-pathogen interactions

Dean *et al.* (2012) released a list of the top 10 fungal pathogens in molecular plant pathology based on scientific and economic importance. This list includes (1) *Magnaporthe oryzae*; (2) *Botrytis cinerea*; (3) *Puccinia* spp.; (4) *Fusarium graminearum*; (5) *Fusarium oxysporum*; (6) *Blumeria graminis*; (7) *Mycosphaerella graminicola*; (8) *Colletotrichum* spp.; (9) *Ustilago maydis*; (10) *Melampsora lini*. These pathogens became part of this list due to their devastating effect on economically important crops, or due to their wide host range. This statement is supported by the two pathogens at the top of the list as *M. oryzae* affects rice, on which half of the world relies on as a source of calories, and *B. cinerea*, which has a wide host range while also exhibiting beneficial properties that can be used for wine production. The latter increased the number of votes for this pathogen for scientific reasons. Overall, to minimize the devastating effect of these parasitic plant pathogens, an understanding of their infection mechanisms is required. Therefore, the study of plant pathology focusses on increasing the understanding of interactions between hosts and pathogens.

In 1866, the German known as “father of plant pathology” Anton de Bary reported the ability of plant pathogenic fungi to alter their hyphal morphology for penetration, depending on the physiological features of the host tissue (de Bary, 1866). These alterations are specialized structures that play a crucial role during the infection phases such as the host-surface attachment, host recognition, penetration, colonization, and nutrient uptake. Several different parasitic colonization strategies are exhibited by plant pathogenic fungi which are divided into three major types: biotrophic, necrotrophic, or hemibiotrophic infection strategies (Kahmann & Basse, 2001).

### 2.1.1 Biotrophy

Fungus-like plant pathogens that exhibit biotrophic relationships with their hosts will do so because they either are only residing in the host for a short time, or because they need a living host until sporulation (Kahmann & Basse, 2001). This need for a living host is what characterizes the biotrophic lifestyle. Within this infection strategy, there are also different sub-strategies to maintain this lifestyle. Examples of these strategies include colonization methods that are either inter- or intracellular, extracellular, or subcuticular (Figure 2.1). Both extracellular and intercellular colonization can also include the formation of haustoria, which, during extracellular colonization, can be found in the epidermal cells, and during intercellular colonization, in the parenchyma cells. These haustoria are an example of the morphological alterations mentioned by de Bary (1866) as these structures are specialized hyphae for nutrient absorption and metabolism. However, most of these haustorium-forming pathogens are obligate biotrophs, which means that they cannot be cultured in artificial media, and they could, therefore, not be studied *ex planta* morphologically (Mendgen & Hahn, 2002).

Besides the formation of haustoria and other highly developed infection structures, the biotrophic fungi are also recognized by numerous other characteristics, prior, during, and after penetration of the host. First is the limited secretory activity, including lytic enzymes that degrade cell walls and cell membranes (Centis *et al.*, 1997). Instead of degrading these protective layers to move from cell-to-cell, hyphae are either located between the cells (extracellular), between the cuticle layer and epidermal cells, or in the apoplast between the cell wall and the cell membrane (intercellular). However, the latter introduces another physiological feature biotrophs exhibit, which, in contrast to the earlier mentioned limited secretory activity, requires secretory activity to separate the fungal plasma membrane from the plant plasma membrane. This thin, newly generated interfacial matrix consists of carbohydrate and protein components (Heath, 1976; Mendgen & Hahn, 2002). This extrahaustorial matrix (EHMx) also contributes to the host-biotroph recognition and interacting during the infection phase (Hahn & Mendgen, 2001; Mendgen & Hahn, 2002). Despite the minimal damage a biotroph causes to the host during infection, the host's defence system will be activated nevertheless to eradicate this pathogenic threat. It is therefore crucial for biotrophs to suppress this host defence long-term to not provoke host cell death before completing the biotroph's life cycle. Overall, due to the complexity of the biotroph-host interaction, the understanding of the mechanism of biotrophy is still limited. On

the other hand, recently developed molecular methods have expanded this understanding by creating opportunities to investigate this mechanism at the molecular level, even in studies that focus on obligate biotrophs.

### 2.1.2 Necrotrophy

In comparison to biotrophs, necrotrophs will kill the host cells rapidly to feed off the dead material as saprotrophs (Figure 2.1) (Mendgen & Hahn, 2002). The goal of these pathogens is thus to overpower its host by secreting the previously mentioned cell wall degrading enzymes (CWDE's) and other lytic enzymes and toxins, which often result in necrotic lesions on the plant host (Walton, 1996). Because necrotrophs do not need to live in co-existence with their host as biotrophs do, they produce fewer specialized infection structures. However, the early stages of infection by necrotrophs are not fundamentally different than from those biotrophs. Both start with the conidial attachment, germination, and host penetration (Prins *et al.*, 2000). Hereby, the latter can involve the active formation of appressoria or passively enter the host tissue through prior infection or stomates. However, necrotrophs are more likely to achieve successful penetration by enzymatic degradation than biotrophs are. After this penetration phase, necrotrophs will further degrade cell components with the usage of the initial enzymatic activity and by producing phytotoxic metabolites like reactive oxygen species (ROS) or proteins to induce necrosis (Prins *et al.*, 2000; Pemberton & Salmond, 2004). Secretion of other metabolites manipulates the host's defence response for better disease development, for example, by disturbing defence signalling or inactivating host metabolites that interfere with the necrotroph's virulence (Morrissey & Osbourn, 1999; Prins *et al.*, 2000). The manipulation of the host defence response is also a factor that can differentiate necrotrophs from biotrophs very well, especially when focused on the hypersensitive response (HR) cell death. Whereas biotrophs are inclined to suppress host cell death to maintain its viability, necrotrophs promote it as they obtain nutrients from the dead plant material (Govrin & Levine, 2000). During infection, necrotrophs will induce symptoms related to the HR-mechanism to cause programmed cell death.

### 2.1.3 Hemibiotrophy

Next to the obligate biotrophs, the arbusculars (who form intercellular haustoria-like structures), and the facultative biotrophs, the hemibiotrophs form a fourth group that exhibit a biotrophic

phase during their life cycle. In this particular group only, the biotrophic phase is followed by a necrotrophic phase several days post infection.

As previously described, the biotrophic phase often includes the formation of specialized infection structures such as haustoria, intracellular or intercellular hyphae (Figure 2.1) (Heath, 1976; Centis *et al.*, 1997). The advantage of intracellular hyphae and haustoria is the access to the cytoplasmic content, including important solutes for water and nutrient acquisition. However, the presence of the pathogen inside the cell requires a very specialized pathogen-host interaction. This interaction is established through the extrahaustorial membrane (EHM) in case of haustoria formation whereas interfacial extracellular matrices (IFMs) are involved in host interactions of intracellular hyphae (Heath, 1976; Perfect & Green, 2001). The appearance and composition of these matrices are organism-specific. Detecting the presence of the matrices has been challenging due to this variety among matrices. Lectin wheat germ agglutin (WGA) binds to N-acetyl glucosamine groups found in chitin and can therefore be used as a tool to label a fungal cell wall. However, a study done by Green *et al.* (1995) showed that lectin WGA does not appear to bind to the EHM of *Erysiphe pisi,* thus indicating the absence of the EHM. Another similar observation was made earlier in 1990 when O'Connel and Ride discovered that lectin WGA labelled the fungal cell wall of *Colletotrichum lindemuthianum* but not the IFM (O'Connell & Ride, 1990). Overall, many *Colletotrichum* species follow a hemibiotrophic lifestyle, but the ones without a biotrophic phase have no intracellular hyphae surrounded by an IFM (Bailey *et al.*, 1992; Münch *et al.*, 2008). The ones that develop an IFM establish either a biotrophic phase within a single host cell where the initial infection took place, or colonize multiple surrounding host cells with intracellular primary mycelium.

Meanwhile, the necrotrophic phase that is initiated several days later after the so-called "biotrophic-necrotrophic switch" is characterized by necrotrophic hyphae that kill host tissue prior to colonization. these hyphae are often smaller in diameter, breach the plasma membrane and secrete cell-wall degrading enzymes. The degradation of the cell walls releases a wide variety of sugars that will then become available to the pathogen. Compared to the biotrophic phase, the hyphae formed in the necrotrophic phase aim to kill the host instead of preventing recognition and host defence. This also explains the reason for hemibiotrophs to exhibit biotrophic properties before switching to necrotrophic colonization as earlier recognition could

cause an immediate defence-response leading to an inhibition in pathogen development and incompatible interaction (Thon *et al.*, 2002).

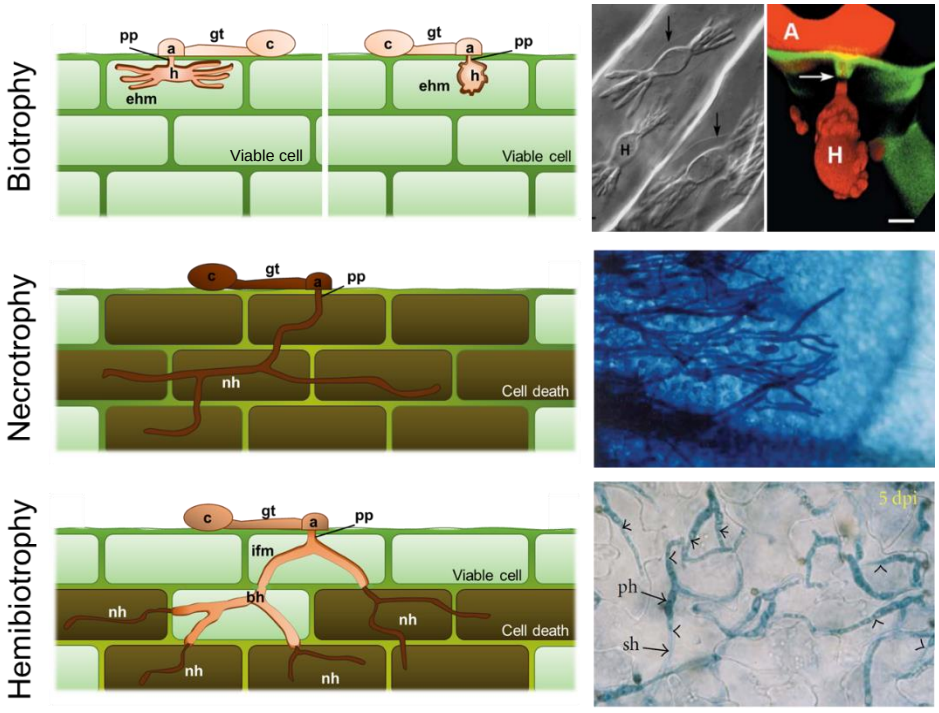


**Figure 2.1 Diagrams and photos of biotrophic, necrotrophic and hemibiotrophic infection strategies.** Diagrams: c = conidium, gt = germ tube, a = appressorium, pp = penetration peg, bh = (primary) biotrophic hypha(e), ifm = interfacial extracellular matrices, nh = (secondary) necrotrophic hypha(e), h = haustorium, ehm = extrahaustorial membrane. Photos from top to bottom: *Blumeria graminis* f.sp. *avenae* and *Erysiphe cichoracearum*, *Sclerotinia sclerotiorum*, *Colletotrichum higginsianum*, *Erysiphe cichoracearum* where A = appressorium, H = haustorium, ph = primary hypha(e), and sh = secondary hypha(e), Photos retrieved from: O'Connell & Panstruga (2006) and Koh *et al*. (2005) for biotrophic structures and Bhadauria *et al.* (2009) for necrotrophic and hemibiotrophic structures.

## 2.2 Infection mechanism and host-response

The previously mentioned infection strategies (biotrophy, necrotrophy and hemibiotrophy) present distinct differences host-wise including infection symptoms, host range, and secretion of effector proteins that are involved in pathogenicity (Laluk & Mengiste, 2010; Stergiopoulos *et al.*, 2013). The latter are produced by the pathogens while the host responds by activating its defence mechanism. Examples of this defence mechanism can include programmed cell death, accumulation of ROS and callose, or secretion of metabolites and hormones such as gibberellin (GA), jasmonic acid (JA), salicylic acid (SA), abscisic acid (ABA), and ethylene (ET). The host recognizes the microbe/pathogen-associated molecular pattern (MAMP/ PAMP) with their pattern recognition receptors (PRRs) and then responds with a PAMP-triggered immunity (PTI),

an effector-triggered immunity (ETI), mediated through phytohormone signalling (Hückelhoven, 2007; Bent & Mackey, 2007; Hardison & Brown, 2012). Additionally, R genes, consisting of leucine-rich repeat (LRR) domains and nucleotide-binding sites (NBS), can also recognize the presence of pathogens by detecting another category of pathogen effectors called "*Avr* genes".

## 2.3 Plant-oomycete pathosystems

At least four of the pathogens listed in the top 10 fungal pathogens in molecular plant pathology cause a condition called "damping-off", a typical symptom observed in seedlings where the seedling emerges and collapses, resulting in yield losses of a wide range of plants in fields as well as greenhouses. (Mao *et al.*, 1997; Nowicki, 1997; Begum *et al.*, 2010). Another pathogen species that is very well-known to cause this condition, which is not mentioned in the top 10, is *Pythium*, which is the focus of this study. *Pythium* is a genus of soil-borne phytopathogens that belongs to the class *Oomycota*, which were originally classified as fungi due to their morphology and infection mechanisms (Money *et al.*, 2004). However, a distinction between the two was made later on based on biochemistry, cell structure and development. Another list was thus released by Kamoun *et al.* (2015) that presented the top 10 oomycete pathogens in molecular plant pathology. The order of this top 10 is as follows: (1) *Phytophthora infestans*, (2, tied) *Hyaloperonospora arabidopsidis*, (2, tied) *Phytophthora ramorum*, (4) *Phytophthora sojae*, (5) *Phytophthora capsici*; (6) *Plasmopara viticola*, (7) *Phytophthora cinnamomic*, (8, tied) *Phytophthora parasitica*; (8, tied) *Pythium ultimum*, and (10) *Albugo candida*. Undoubtedly, *Phytophthora* poses the biggest threat among the oomycete pathogens as the majority of the list belong to this particular genus. *Phytophthora* and *Pythium*, listed as number 9, appear to share a common ancestor (Thines & Kamoun, 2010).

Among others, a community known as the "Oomycete Molecular Genetics Network", was founded two decades ago in response to the increasing knowledge about the class *Oomycota*. This community took advantage of molecular methods by coordinating transcriptome and genome sequence projects, thus contributing to the understanding of host-microbe interactions (Pais *et al.*, 2013). A community that focuses on these pathogens is of great importance as these pathogens affect economically important crops. The hemibiotroph *P. infestans* has been well-known historically for causing late-blight in potatoes, and continues to do so to this very day, thus causing a continuous threat to food security (Fisher *et al.*, 2012). This pathogen is notorious

for causing the “Great Irish Famine” in the 1840s, which was a period of great hunger and starvation in Ireland (Yoshida *et al.*, 2013). Other examples of plants affected by pathogens from the oomycete top 10 list include: soybean, which is threatened by root rot disease caused by *P. sojae*; solanaceous (pepper, tomato), legume (lima and snap beans) and most cucurbit hosts, affected by *P. capsici* (Hausbeck & Lamour, 2004); grapes with grape downy mildew caused by *Pl. viticola*; tobacco and citrus fruits, where damage is inflicted by *P. parasitica* (= *P. nicotianae*; Erwin & Ribeiro, 1996), which is known to cause tobacco black shank, citrus root rot and gummosis, and affects many more plants in forestry, horticulture and the nursery industry (Cline *et al.*, 2008) due to its wide host range (Kamoun *et al.*, 2015). Other oomycete pathogens including *Pythium ultimum* and *Albugo candida* are not as host-specific as the previously mentioned oomycetes and therefore also pose a great threat to food security but are not as well-studied as the forefront pathogenic oomycete *Phytophthora infestans*.

## 2.4 Plant-*Pythium* interactions

Even though *Pythium* and *Phytophthora* share a common ancestor, there are many important differences. Besides the absence of haustoria-like structures during infection of the host, *Pythium* species appear to produce 25% fewer effectors, including the RXLR effectors that are often released in these haustoria-like structures and mainly serve as suppressors against host immunity (Janardhanan & Husain, 1974; Whisson *et al.*, 2007; Anderson *et al.*, 2015; Kamoun *et al.*, 2015).

In contrast to *Phytophthora*, *Pythium* species have a wide host range and have therefore caused diseases worldwide. Examples of diseases caused by this genus are root-rot, seed-rot, lower stem-rot, damping-off, blackleg, cavity spot, cottony-leak disease and blighted foliar disease (Winstead & McCombs, 1961; Moore & Couch, 1968; Lumsden & Locke, 1989; Daughtrey & Benson, 2005). These diseases often have devastating effects such as damaged root systems, reduced yields, decreased winter survival, shortened lifespan and complete crop losses (Hancock, 1983). After infection, symptoms on seedlings, which are mostly affected by this pathogen, included soft radicles and lesions on the cotyledons and flaccid hypocotyls and roots which cause the seedlings to collapse and die. The reason for specifically targeting seedlings is likely because this opportunistic pathogen can then infect before the host tissue suberizes and lignifies. These processes would complicate infection by *Pythium* due to the lack of enzyme

production, such as cutinases and pectin esterases, which are required for penetrating such tissues (Clark & Harris, 1981; Chun & Schneider, 1998; Zerillo *et al.*, 2013). Meanwhile, older plants are more resistant to the infection by *Pythium*, but their nutrient uptake, nitrogen fixation and water absorption are still impaired due to the damage the pathogen afflicts to the finer roots and root hairs, thereby decreasing total root surface.

### 2.4.1 The genus *Pythium*

The genus *Pythium* is a group of soil-borne oomycete phytopathogen that was established by Pringsheim in 1858 and placed in the family *Saprolegniaceae*, but was later classified as part of the *Pythiaceae* family, also called "watermolds" (Sideris, 1932; Hendrix & Campbell, 1973). Since the early 1900s, pathologists found that *Pythium* spp. were consistently associated with root diseases. At the end of this century, taxonomic details of this genus had been clarified, and many new species had been described. To date, over 140 recognized saprobic and parasitic species have been described (Bala *et al.*, 2010). The monograph by van der Plaats Niterink (1981) and "Keys to *Pythium*" by Dick (1991) are to this very day commonly used tools for the identification of *Pythium* species. However, the lack of distinctive morphological structures limits the differentiation between the species. Recently, molecular methods were developed to identify *Pythium* species genomically based on their internal transcribed spacer (ITS) regions (Lévesque & de Cock, 2004; Tambong *et al.*, 2006; Garrido Haro & Garzón, 2016). Since then, more than 120 species have been confirmed within this genus, of which most are associated with root rot. In some cases, species share identical or nearly identical ITS regions. Therefore, a complete analysis of both morphological and non-morphological methods must be used for description of new species.

#### 2.4.1.1 Morphological characteristics

Before molecular methods were developed, and even to this very day, *Pythium* species have been identified through morphological characteristics (van der Plaats-Niterink, 1981; Dick, 1991). This identification is based on distinctive differences of the mycelia, sporangia, oogonia and antheridia, type and size of spores, homothallism versus heterothallism, growth habit, and rate of growth in culture media. Environmental conditions can also affect morphology.

Examples of the *Pythium* characteristics are the following: The mycelia of *Pythium* species are colourless, sometimes lustrous, occasionally slightly yellowish or greyish lilac. The hyphae

are hyaline and primary hyphae are mostly five to seven-, and occasionally up to 10 µm wide. Cross walls (septa) are absent, except in older degrading hyphae or where septa formation delimits the cytoplasm for the development of reproductive organs. In the younger non-septate hyphae, protoplasmic streaming is often clearly visible. The production of aerial mycelium depends on the media that is used.

The sporangia are either filamentous with different inflation levels and long discharge tubes, or spherical with short discharge tubes. Spherical sporangia can be distinguished into two kinds, sporangia that proliferate at the bottom followed by the formation of a new sporangium inside the old sporangial wall, or a new sporangium is formed outside the old one. The oogonia (female sexual reproduction organs) are spherical to limoniform and are intercalary or terminal. Its wall could either be smooth or ornamented with projections. The antheridia (male sexual reproduction organs) consist of an antheridial cell that can be sessile on a hypha, intercalary, or formed terminally on an antheridial stalk. They can originate from the oogonial stalk (monoclinous) or a different hypha not closely connected with the one subtending the oogonium (diclinous).

#### 2.4.1.2 Molecular characteristics and phylogeny

As described previously, *Pythium* species were traditionally classified and identified based on morphological features of the vegetative and reproductive structures (van der Plaats-Niterink, 1981). Due to the great morphological similarities among the species, molecular methods such as sequencing of the ITS regions became a necessity for differentiation between particular species. Unfortunately, even this method alone is occasionally insufficient, as the genetic code of *Pythium* species can contain many repeats and single base deletions and insertions which complicates proper alignment (Schroeder *et al.*, 2013). Therefore, an additional molecular identification involving the mitochondrial cytochrome oxidase c subunit 1 or 2 genes (*cox* 1/*cox* 2) and/or the large nuclear ribosomal unit (LSU) is required.

*Oomycota*, to which *Pythium* belongs, were initially classified among fungi based on their morphology, focussing on the vegetative filamentous hyphae, and infection mechanisms (Money et al., 2004). Besides a distinction based on biochemistry, cell structure (non-septate and diploid hyphae) and development, phylogenetic studies revealed that oomycetes belonged on a separate eukaryotic branch on the phylogenetic tree (Figure 2.2) and that oomycetes were in fact closer

related to algae than to fungi (Kamoun *et al.*, 1999; Baldauf *et al.*, 2000). Within the *Oomycota*, oomycetes are divided in either *Saprolegniomycetidae*, *Rhipidiomycetidae,* or *Peronosporomycetidae* (Van West *et al.*, 2003). The latter includes many plant pathogens in the *Peronosporales* and *Pythiales* order of which *Peronosporales* are all obligate plant pathogens. *Pythium* and the majority of other root pathogens are classified in the family *Phytiaceae*, together with *Phytophthora*.

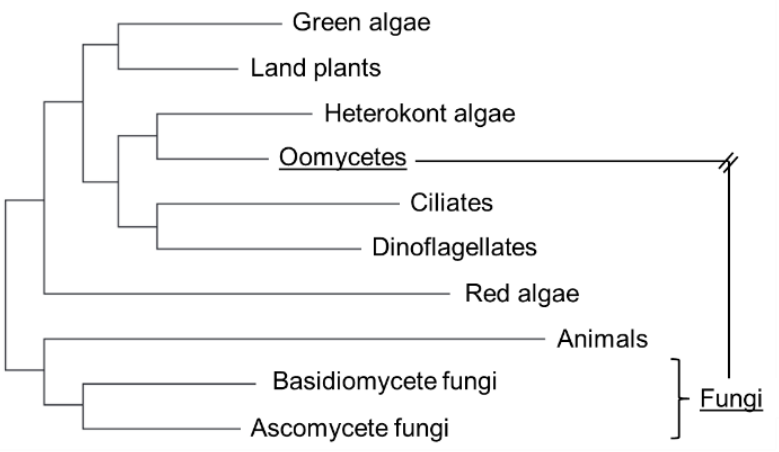


**Figure 2.2 Phylogenetic tree presenting the re-classification of oomycetes separately from the kingdom Fungi.** Retrieved and edited from Kamoun *et al.* (1999).

Since the genus *Pythium* was initially described by Pringsheim in 1858, many studies have contributed to dividing the *Pythium* species into several subgenera. These divisions were often based on either sporangium morphology or phylogeny (Fisher, 1892; Lévesque & de Cock, 2004; Uzuhashi *et al.*, 2009). Nuclear rDNA is the main region that has been used in phylogenetic studies within the genus *Pythium* (Lévesque and de Cock, 2004) and according to parsimony analysis, two major clades were generated in the *Pythium* species with either filamentous or globose sporangia. Later, a total of 11 smaller clades (Clade A-K) was recognized (Figure 2.3). These clades often correlated with either host-type or substrate, and morphological characteristics were also similar within the clade. Previous studies demonstrated that *Pythium* was phylogenetically isolated from other genera of oomycetes. The primary species in clade F include *P. spinosum, P. irregulare, and P. sylvaticum* which correspond to results from an earlier study done by Matsumoto *et al.* in 1999.

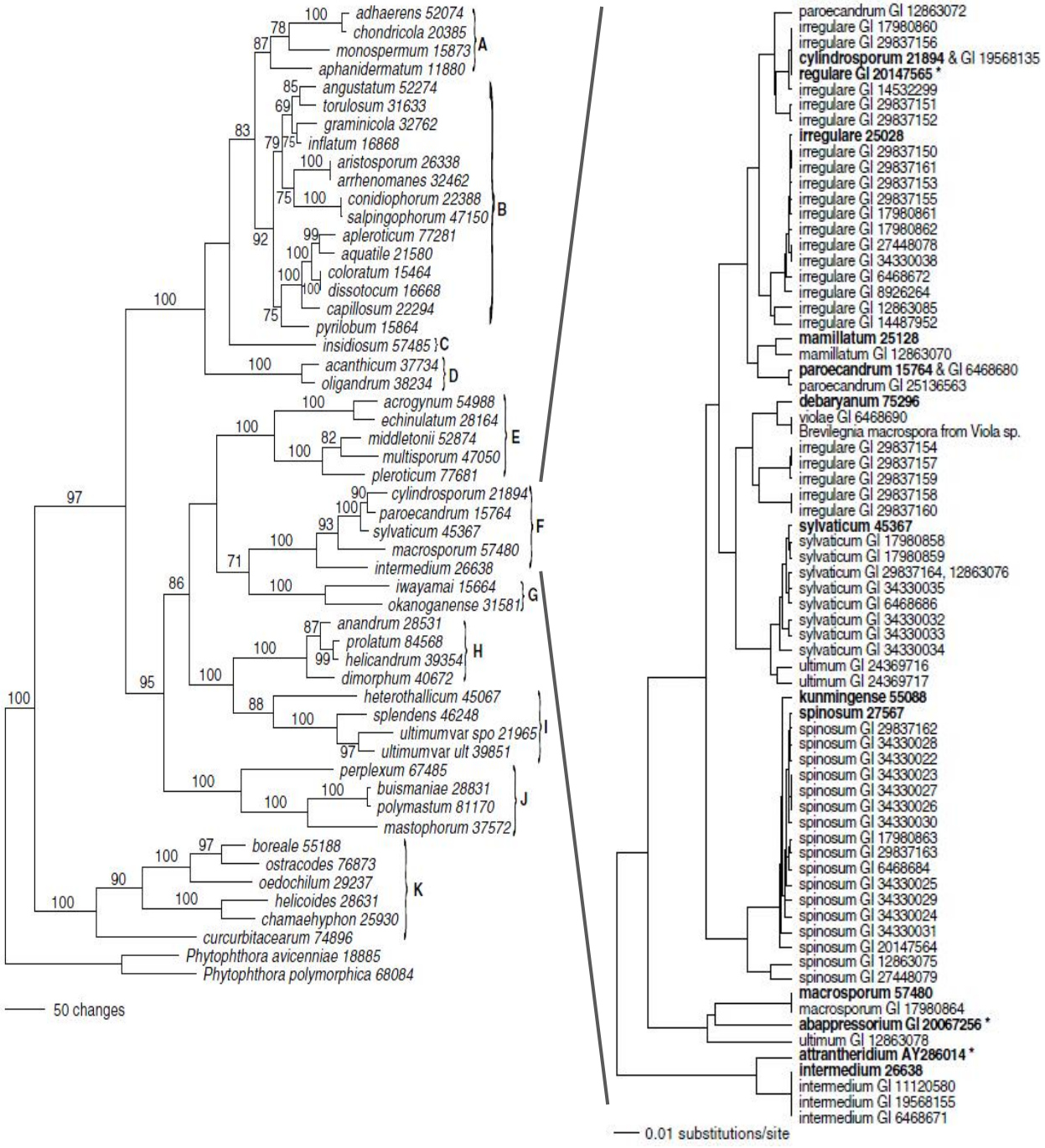


**Figure 2.3 Phylogeny of *Pythium* species based on the ITS region and the D1 to D3 regions of the nuclear large ribosomal subunit. On the left:** The percentage of replicate trees in which the associated taxa clustered together in the bootstrap test (1000 replicates) are shown next to the branches and branches that had less than 50% support show no bootstrap value. Length=4546, CI=0.502, RCI=0.383, and RI=0.764. **On the right**: An enlarged phylogenetic illustration of the F clade, constructed with the unweighted pair group method with arithmetic mean (UPGMA). Representative strains of the study of Lévesque & de Cock (2004) are presented in bold and include all available entries in Genbank (GI numbers). Ex-type strains with their sequences deposited in Genbank are in bold with an asterisk after the GI number and entries with identical sequence or nearly identical are represented by two GI numbers or by the extensions of the last digits. Numbers beside species names are the CBS numbers without decimal point. Both phylogenetic trees were retrieved and edited from Lévesque & de Cock (2004).

#### 2.4.1.3 *Pythium cryptoirregulare*, re-identified as a new pathogenic oomycete species

A new species within the *P. irregulare* complex was described in 2007 by Garzón *et al.* based on molecular and morphological data. According to these studies, *P. irregulare sensu lato* was clearly separated into two distinct groups: *P. irregulare sensu stricto* and *Pythium sp.*, which was recognized as the new species *P. cryptoirregulare* in that study. According to Garzón *et al.* (2007), subtle differences could be observed in morphology as *P. cryptoirregulare* featured wider hyphae and larger oogonia, oospores, ooplast diameter, and sporangia compared to *P. irregulare*. Additionally, a significant genetic difference was found between the two species based on polymorphic markers during amplification fragment length polymorphism (AFLP) analysis and ITS region analysis. *Pythium cryptoirregulare* was placed in a subclade along with *P. regulare* and *P. cylindrosporum* in the F clade described by Lévesque and de Cock in 2004.

### 2.4.2 The life cycle of *Pythium* species

As *Pythium* sp. can produce asexually, as well as sexually, it can follow two distinct life cycles (Figure 2.4) (Van West *et al.*, 2003).

The asexual cycle is recognized by the formation of sporangia and zoospores that develop in, and are released from these sporangia. While sporangia can germinate directly by forming a germ tube outside or on the host tissue, the production of zoospores is an indirect germination process. In several *Pythium* species, the zoospores are developed and released from a discharge vesicle. After this release, zoospores move in water to new host tissue with their heterokont flagella consisting of one tinsel and one whiplash flagella (van der Plaats-Niterink, 1981; Barr, 1983). Upon contact with this new host tissue, the zoospores will develop into a cyst to infect the host tissue with or without the formation of appressoria, followed by internal colonization by mycelia. New sporangia will then develop from these mycelia to restart the asexual cycle.

During the sexual cycle, mycelia form oogonia instead of sporangia which are then fertilized by one antheridium or multiple antheridia, which empty their content into the oogonia. These antheridia can either originate from the same hypha as the oogonia (homothallic) or from a different hypha (heterothallic) (Erwin & Ribeiro, 1996). Also, upon fusion with the oogonium, an antheridium can either surround the oogonial stalk (amphigynous) or fuse with the oogonia elsewhere on the oogonial wall (paragynous). The oospore resulting from this sexual reproduction is thick-walled and can go into dormancy as a resting spore for an extended period

for over-wintering. Whenever the oospore germinates under conducive conditions, it will either release the zoospores directly from the oospores or create a vesicle for the release. Identical to the asexual cycle, each zoospores may develop into a cyst for infection of the host tissue, followed by internal colonization by mycelia. New oogonia and antheridia will then develop from these mycelia to restart the sexual cycle.

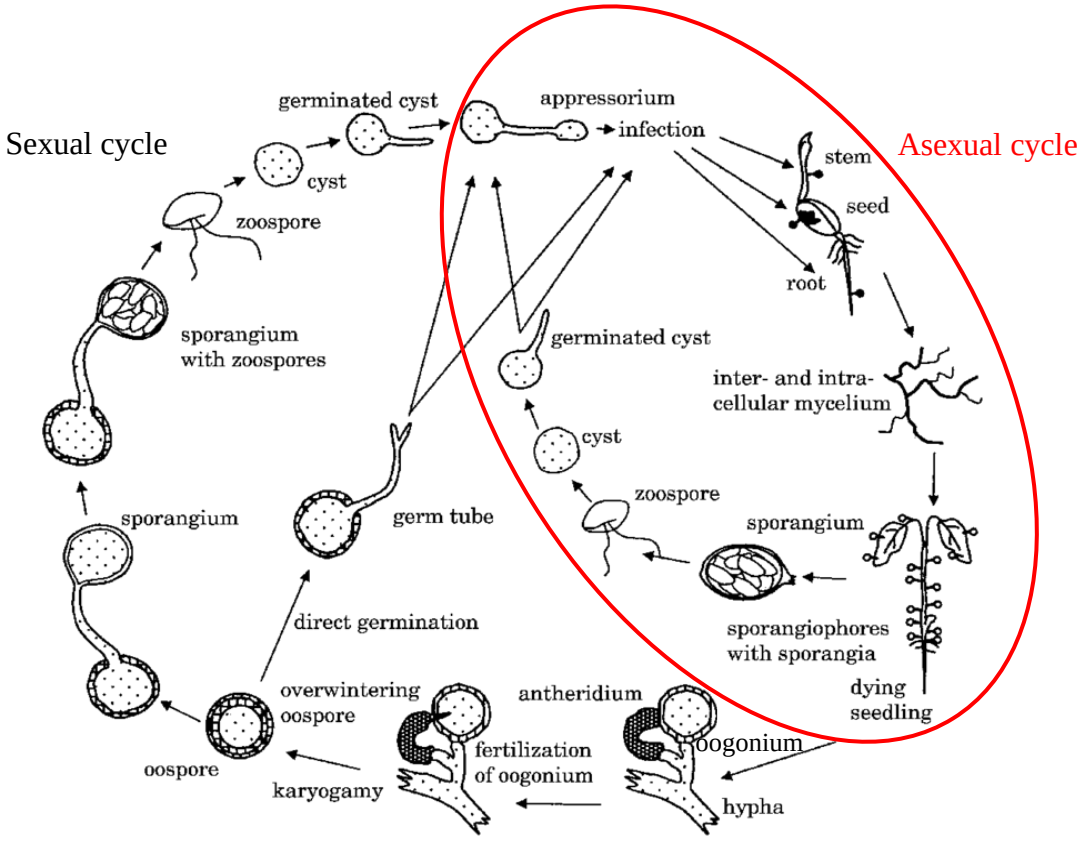


**Figure 2.4 Life cycle of a root-infection by *Pythium* species.** Retrieved and edited from: Van West *et al.* (2003)

### 2.4.3 Infection strategy of *Pythium* species

Within the genus *Pythium*, several disease cycles can arise depending on the species. Infection can either occur by zoospores, mycelia, or oospores (Sutton *et al.*, 2006). Oospores are produced in each species sexually by the formation of an antheridium and oogonium in infected roots and in the rhizosphere. Zoospores are produced asexually in sporangia and associated vesicles, and the production rate varies per species, and this is the initial (primary) inoculum in root rot. The primary sources of infection are plant residues, soil, hydroponic pipes and tubing, and insects,

basically, in a water-rich environment. Zoospores can feature flagella, which are either retracted or shed upon contact with the host tissue, followed by the zoospores developing into a cyst. It is still unclear whether *Pythium* species produce appressoria structures or not, as a swelling on the outside of the host tissue occurs prior to penetration of the host but does not exhibit the particular characteristics of true appressoria.

*Pythium* species have mostly been described as necrotrophic pathogens (Laluk & Mengiste, 2010; Adhikari *et al.*, 2013; Chen *et al.*, 2015). *Pythium ultimum* is one of these *Pythium* species, whose complement of metabolic and effector proteins is tailored to the pathogenic lifestyle of necrotrophs, even though the *P. ultimum* genome has similarities to related non-necrotroph oomycete plant pathogens (Lévesque *et al.*, 2010). Furthermore, according to Adhikari *et al.* (2013), *Pythium* is a great model to study plant-necrotroph interactions for the identification of genes involved in interspecific variation in pathogenicity. Laluk & Mengiste, (2010a) described *Pythium* as a major soilborne necrotrophic pathogen with an extensive host range and a diverse virulence, which causes pre-/post-emergence damping-off in seedlings and is responsible for root and vascular diseases. According to the same publication, *P. irregulare* and *P. sylvaticum* have been used to study *Arabidopsis* immune responses by different laboratories worldwide. One of these studies showed that *P. irregulare* develops haustoria-like structures after penetration of the host tissue, which is usually seen in biotrophic pathogens (Adie *et al.*, 2007). Biotrophic colonization by *P. aphanidermatum* and *P. dissotocum* have also been observed, but only at a temperature between 19-22 ºC (Owen-Going *et al.*, 2008). There are only a few publications where *Pythium* species were described with biotrophic characteristics. Two other main studies involving *P. irregulare* describe the increase of susceptibility in *Arabidopsis* jasmonate signalling mutants, and the role of strigolactones and ethylene as a defence against the pathogen (Staswick *et al.*, 1998; Blake *et al.*, 2016).

### 2.4.4 *Pythium* interaction with the host *Arabidopsis thaliana*

Since *Pythium* spp. have such a wide host range, causing devastating damage to economically important crops and ornamental plants, it is important to understand their infection mechanism. However, not all of the many hosts have their genome sequenced or have a variety of ecotypes or mutants available to explore differences in interactions.

Therefore, the model organism *Arabidopsis thaliana* has been used for many studies to increase the knowledge of host-pathogen interactions, including that of *Pythium* species.

#### 2.4.4.1 *Arabidopsis thaliana*, a model plant organism

*Arabidopsis thaliana* is a model plant that has been used in a wide range of studies (Meinke *et al.*, 1998). It is a small plant in the mustard family (*Cruciferae* or *Brassicaceae*) and is preferred because it is a relatively simple angiosperm which represents biological structures and functions that are common to all eukaryotes. Another reason why this model plant is used for many studies is its ability to regenerate in a short time as its lifecycle can be completed in six weeks. This short time span is very efficient for the transformation of the model plant by, for example, the use of *Agrobacterium*.

The usage rate of *Arabidopsis* for research started increasing in the 1980s when a genetic linkage map was released, presenting five linkage groups, corresponding to the five chromosomes (Koornneef *et al.*, 1983). In the year 2000, the genome of *A. thaliana* was sequenced and analysed by the *Arabidopsis* Genome Initiative (AGI). This organization included the following factions: the genome sequencing faction that sequenced and annotated assigned chromosomal regions, the genome analysis faction that carried out the analyses, and the contributing authors that interpreted the genome analyses and incorporated other data and analyses, with respect to selected biological topics (The *Arabidopsis* Genome Initiative, 2000). According to their study, the genome of *A. thaliana* includes 25,498 genes encoding proteins from 11,000 families. This amount is 5000 more genes than what studies of Meinke *et al.* had described in 1998.

In plant pathology, the use of *A. thaliana* is very convenient due to the wide variety (ecotypes) collected from the Northern Hemisphere (Innes, 1995). Since *Arabidopsis* is primarily self-fertilizing, genetic variation is preserved, and therefore populations are expected to have independently evolved by pathogenic pressure, resulting in ecotypes with specific phenotypic pathogen responses. These ecotypes could contribute to the knowledge of plant-pathogen interactions when these differences in ecotypes are imbedded in a genetic code that can be located and analysed. To this day, over 750 accessions of *A. thaliana* have been collected from natural populations that are available for experimental analyses, of which Colombia (Col) and Landsberg erecta (Ler) are the most commonly used (Agrawal, 2018). *Arabidopsis* is therefore

essential for studies when pathogens are isolated from their natural host but also show virulence on *Arabidopsis.* Studying these pathogens on *Arabidopsis* will increase the speed of gaining knowledge and understanding of the pathogen.

#### 2.4.4.2 *Pythium* infection and host response of *Arabidopsis thaliana*

*Arabidopsis thaliana* has been involved in studies of many *Pythium* species and the *Arabidopsis* host responses involving the putative sugar transporter SWEET2 is one of the many host responses upon infection by this plant pathogen (Chen *et al.,* 2015). This transporter is already highly expressed in *Arabidopsis* roots, but it was induced more than 10-fold during *Pythium* infection, and SWEET2-deficient mutants showed an increased susceptibility. In contrast, resistance to *Pythium* was increased by high amounts of the SWEET2 transporter, causing a lower amount of sugar availability for the pathogen in the rhizosphere.

A study by Adie *et al.* (2007) focussed on the infection of *P. irregulare* and the respective host response of *A. thaliana*. Despite this species being described as a necrotrophic pathogen, the infection could not be characterized as either necrotrophic or biotrophic. Hyphae of this pathogen invade the vascular tissues (xylem) and potentially block the water transport throughout the host, causing wilting and death of seedlings (Martin, 1995; Geraats *et al.*, 2002). The lack of water transport could also be the cause of the seedling collapse, a common symptom of damping-off.

More importantly, phytohormones such as JA appear to play a significant role in disease resistance against *P. irregulare*, which has been reported by several other studies (Staswick *et al.*, 1998; Tiryaki & Staswick, 2002; Oliver & Ipcho, 2004; Oliver *et al.*, 2009; Castro *et al.*, 2016). This defence-related signalling hormone has been associated with a plant's response against necrotrophs. It is noteworthy, however, that profiles of responses to the hemibiotrophic bacteria *Pseudomonas syringae* were also very closely related to the *P. irregulare*–wild type profile.

Abscisic acid, ethylene and salicylic acid were also part of the defence response against *Pythium* (Geraats *et al.*, 2002; Adie *et al.*, 2007). The important role of ABA in the defence response was demonstrated when ABA-deficient mutants, which were either impaired in ABA biosynthesis or insensitive to ABA, showed increased susceptibility to *Pythium* infection. This phytohormone can positively or negatively influence plant defence as it is a direct regulator of R protein activity (Adie *et al.*, 2007; Sánchez-Vallet *et al.*, 2012) and it is also required for JA

biosynthesis and JA-dependent defence gene expression after infection by *P. irregulare* (Adie *et al.*, 2007). The role of ethylene, however, is more ambiguous as ethylene production in the host is often increased upon infection by *Pythium* where it induces disease development. In contrast, ethylene insensitivity also increases susceptibility to *Pythium* infection (Geraats *et al.*, 2002). The latter could be explained by the contribution of ethylene to cell wall synthesis as cell wall formation prevents *Pythium* penetration. Meanwhile, when *Pythium* infection is already established, the pathogen might induce ethylene production of the host to increase disease symptoms for further colonization of the host. Salicylic acid is mostly regulating the activation of the host response. Deficiencies in producing this phytohormone lead to a decreased resistance (Vlot *et al.*, 2009; Denancé *et al.*, 2013). Moreover, while it regulates the activation of the host response, it also reduces an associated fitness cost that causes negative effects on the overall plant development (Walters & Heil, 2007). Aside from the intervention of phytohormone signalling, there are also plant pathogens that can produce plant hormones to cause a hormonal imbalance and disturb the hormone signalling (Möbius & Hertweck, 2009; Chanclud & Morel, 2016).

#### 2.4.4.3 Secretion of auxins as secondary metabolites

Some fungal pathogens can produce phytohormones or metabolites that mimic phytohormones. During infection, their production can disturb hormone signalling and thus alter the host cell response (Inomata *et al.*, 2004; Möbius & Hertweck, 2009; Brodhun *et al.*, 2013). *Pythium* spp. were reported to disturb the hormone signalling. In rice, *Pythium* spp. can induce the brassinosteroid signalling pathway to suppress the production of gibberellins (Biemelt *et al.*, 2004; De Vleesschauwer *et al.*, 2012). Gibberellin is involved in cell wall fortification, so by preventing this fortification, the cell wall is easier to penetrate when an infection is being established. This disruption of the fortification is a crucial mechanism for oomycetes that target seedlings.

Many *Pythium* species are capable of producing auxins as part of their infection mechanism. Most auxin-related studies focus on the compound “Indole-3-acetic acid” (IAA) (Hopkins, 1995). In host-pathogen interaction, this compound can have beneficial effects for the host, as well as for the pathogen. Regulation of the IAA levels within the host can be crucial for host resistance but can also be manipulated by the pathogen.

Auxin-rich regions in the root tips and lateral root initials are often targeted by soil-borne pathogens, such as *Pythium*, for penetration. The production of IAA advances lateral root and root hair development, thus the number of favourable means of entry into the host tissue increases. According to Cosgrove *et al.* (2002), IAA induces the production of expansins that are involved in cell elongation, resulting in less rigid cell walls that are easier to penetrate by pathogens. Apart from causing irregularities in the cell wall, pathogens can also use IAA for regulating their own pathogenicity genes, but also for downregulating auxin signalling in the host, e.g. causing growth inhibition, to increase susceptibility (Ludwig-Müller, 2015).

The effect of IAA is highly dependent on which pathogen is infecting which host, even within the same genus. For example, increased levels of IAA can be toxic for microbes and lead to growth inhibition of *Pythium debaraynum* in *Physcomitrella patens* while in case of *P. ultimum* infection, IAA caused an increase of the disease symptoms in *Lycopersicon esculentum* (Gravel *et al.*, 2007; Ludwig-Müller, 2015; Mittag *et al.*, 2015). Opinions are divided whether *P. ultimum* is capable of producing IAA, or if it produces toxins that cause similar symptoms (Blok, 1973; Rey *et al.*, 2001; Gravel *et al.*, 2007). A study involving *P. aphanidermatum* even concluded that the IAA produced by the pathogen, rather than the pathogen physically, was the cause of *Pythium* red blight symptoms on bentgrass (Shimada *et al.*, 1999). Among many other *Pythium* species, *P. sylvaticum* and *P. oligandrum* can also produce IAA which causes the disease symptoms in seedlings including growth inhibition, swelling close to the root tip and increased root hair development (Blok, 1973; Le Floch *et al.*, 2003). The study by Blok (1973) also suggested that *P. irregulare* and *P. paroecandrum* produce IAA, too.

For decades, many *Pythium* species have been observed to produce auxin, but the mechanism behind it remains the topic of many studies. Many of the microorganisms that produce IAA can do so because of the addition of IAA precursors, such as tryptophan, into the growth media, suggesting that the tryptamine-pathway is involved in the production of IAA (Rey *et al.*, 2001; Le Floch *et al.*, 2003; Gravel *et al.*, 2007). Only very few microorganisms are known to produce low amounts of IAA without these precursors.

#### 2.4.4.4 Auxin homeostasis

Indole-acetic acid is the most common and crucial natural auxin found in plants (Taiz & Zeiger, 1991; Hopkins, 1995). Together with cytokinins, it plays an important role in the development of calli, cell suspension, cell elongation, cell division and tissue differentiation. On a whole-organism level, it is also responsible for the polarity and maintenance of apical dominance and tropism (George *et al.*, 2008). Distribution of auxin throughout the plant is essential to provide auxin to the regions where the previously mentioned functions need to be executed. This transport is believed to occur in many ways. Firstly, active long-distance transportation is believed to occur through the vascular tissue, specifically the phloem (Hopkins, 1995). The transportation towards the root is partially driven by a concentration gradient but is primarily driven by a highly complex polar mechanism. Rubery & Sheldrake (1974) and Raven (1975) created the basis for this mechanism called the "chemiosmotic model". According to this model, the auxin distribution from cell-to-cell is based on three main components: a pH gradient or proton motive to drive IAA uptake, an IAA influx carrier, and an IAA efflux carrier. Of these components, the focus will be on the latter two.

The membrane protein responsible for the influx of auxin is called "AUX1", which is believed to serve as an auxin/proton symporter (Hopkins, 1995). Defects in this gene lead to a loss of gravitropism and reduced lateral root development. The *aux1* mutants, such as *aux1-7*, show an insensitivity to IAA, which can be beneficial in the presence of excessive amounts of it (The *Arabidopsis* Information Resource [TAIRb], 2007). AXR4 is also important for the effectiveness of this influx protein because it is required for localization of the AUX1 protein (TAIRc, 2006; Hobbie & Estelle, 1995; Dharmasiri *et al.*, 2006). Mutants of AXR4, such as *axr4-2*, therefore, show similarities in deficiencies as to *aux1* mutants. Another protein that is involved in the signal transduction is AXR1. It is required for jasmonate and auxin signalling and response (TAIRa, 2007; Lincoln *et al.*, 1990; Tiryaki & Staswick, 2013). Therefore, *axr1* mutants, show an insensitivity to IAA and a phenotype similar to *aux1* and *axr4* mutants. Overall, all these proteins contribute to the transmission of IAA into the cell.

Meanwhile, the membrane proteins responsible for the efflux of auxin are more complicated and consists of an entire family of PIN genes. Figure 2.5 shows where the PIN carriers are located and the direction of the auxin efflux (Feraru & Friml, 2008). PIN1, PIN4 and PIN7 are

root apex-facing and play a role in the downward efflux towards the root apex and the distribution in the columella and quiescent centre. Auxin efflux by these PIN proteins occurs thus predominantly in the stele and columella region. In contrast, PIN2 is located in the cortical cells on the basal side of the cell and in the epidermal cells, facing the shoot apex. This PIN carrier and the region where it is located in are typically known to be involved in the cell elongation. The DR5 promoter in combination with the green fluorescence protein (GFP) or β-glucuronidase (GUS) is commonly used as an auxin-responsive reporter to visualize and monitor the auxin distribution by these PIN carriers (Chen *et al.*, 2013).

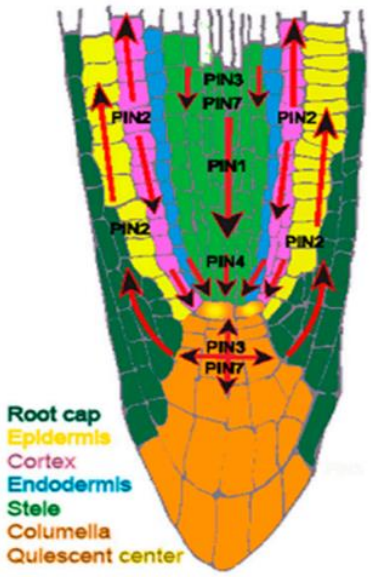


**Figure 2.5 Auxin distribution mediated by the PIN efflux carriers.** PIN1, PIN4 and PIN 7, located at the basal side of the cell, thus responsible for the auxin efflux towards the root, while PIN 3 is located apolarly in the columella and PIN2 regulates efflux towards the root in the cortical cells and towards the shoot in the epidermal cells. Figure is retrieved from Feraru & Friml (2008).

### 2.4.5 The importance of damping-off and root rot disease caused by *Pythium* species

Phytopathogenic *Pythium* sp. causes seedling root rot and damping-off on a wide range of crop species worldwide, and therefore, this results in significant yield losses. In a study by Nowicki (1997), 120 parsley plantations were evaluated for four years and *Alternaria* spp., *Fusarium* spp. and *Pythium* spp. were responsible for causing damping-off among the seedlings, of which *Pythium* spp. caused approximately 17% of the seedling loss. In ornamental production *Pythium* spp. also cause a reduction in seedling development, loss of seedlings or cuttings and reduced

crop quality (Garzón *et al.*, 2011). Among many other floral crops, geranium and poinsettias appeared to be major hosts for *P. irregulare* (45%), *P. aphanidermatum* (29%) and *P. ultimum* (10%) in Pennsylvania greenhouses, while snapdragons and begonias accounted for most of the remaining percentage (Moorman *et al.*, 2002; Moorman & Kim, 2004). Additionally Stephens & Powels (1982) recorded damping-off on the bedding plants impatiens, celosia and vinca, predominantly caused by *P. ultimum*.

*Pythium* spp. are also considered as the most damaging pathogen to alfalfa (*Medicago sativa*), an economically important crop that is used for multiple purposes (Hancock, 1983; Berg *et al.*, 2017). It causes reduced yields, fewer winter survival, and shortened stand life. Apart from the damping-off symptoms, affected seedlings also show lesions on the cotyledons and a lack of root hairs. The latter prevents proper nitrogen and water uptake from the soil. Depending on the region, a variety of *Pythium* species were responsible for causing damage to seedlings, but *P. ultimum* and *P. irregulare* were predominantly present in each region.

These ornamental and agricultural crops are only a few of the many crops that are affected by *Pythium* species. Almost all greenhouse crops are susceptible to one or more species (Stephens & Powels, 1982). Greenhouses and other environments that make use of irrigation systems are particularly at risk due to *Pythium*'s formation of zoospores, which spread through these watering systems. Any humid and warm environment is favourable for causing disease, and because of its development of oospores, *Pythium* is also capable of surviving less favourable conditions (Van West *et al.*, 2003). Due to the tremendous impact of this pathogen on such a wide variety of hosts, it is important that the infection mechanism of this pathogen is well-understood, so that the spread of this pathogen can be controlled.

### 2.4.6 Management strategy

*Pythium* species have a wide host range and therefore a pernicious effect on agriculture in several countries. The losses caused by this pathogen need to be controlled, but disease management is very challenging, as many ways to exterminate this pathogen have not been found yet. Studies that include finding resistance are still ongoing to this very day, and it is essential to create a better understanding of this pathogen so that this knowledge can contribute to better disease management.

Currently, chemical fungicides are mainly used for disease management because management practices such as cultivar resistance and crop rotation are not employed (Martin & Loper, 1999). However, these fungicide applications are limited and not desirable as they are expensive, cause environmental pollution and can potentially induce pathogen resistance or affect the crops treated with the fungicide (Jones, 1985; Matteoni, 1987; Van Iersel & Bugbee, 1996). It is also challenging for farmers to use fungicides due to the heavy regulations and registration processes that differ per country (Larson, 1987).

Examples of fungicides include the different C14 DMI, Nikkomycin and Polyoxin D, which control all the listed ascomycete and basidiomycete species (Latijnhouwers *et al.*, 2003; Oliver & Ipcho, 2004). Unfortunately, these fungicides do not control oomycetes such as *Pythium*. The difference in cell wall composition between fungal pathogens and oomycetes determines fungicide efficacy. The majority of fungicides target the chitin and sterol synthesis, which is not present in most oomycetes, and this makes the fungicides therefore ineffective (Latijnhouwers *et al.*, 2003). Also, it has been reported that several *Pythium* species exhibit resistance to the fungicides propamocarb and mefenoxam and that their growth is even enhanced in the presence of sublethal doses of these fungicides (Moorman & Kim, 2004; Garzón *et al.*, 2011). *Pythium irregulare* isolates in a study by Garzón *et al.* (2005) were sensitive to metalaxyl/mefenoxam, while resistance was present among *P. cryptoirregulare* isolates.

On the other hand, strobilurin fungicides control some ascomycetes and some basidiomycetes, but all the oomycetes as well (Oliver & Ipcho, 2004). Phenylamides such as metalaxyl are another application that is highly effective against oomycetes, because they interfere with RNA polymerases (Schwinn & Urech, 1986).

Another method of disease management is using biological control. This exists primarily of non-pathogenic *Pythium* spp. and bacterial antagonists (Lumsden & Locke, 1989; Mao *et al.*, 1997; Martin & Loper, 1999). Of these antagonists, *Pseudomonas* spp. and *Bacillus subtilis* are most effective in reducing disease severity. Additionally, *Streptomyces griseoviridis*, *Trichoderma harzianum* and *Gliocladium catenulatum* have also been reported as effective biocontrol agents against *Pythium* spp. (Paulitz & Belanger, 2001; Punja & Yip, 2003).

# CHAPTER 3

## ISOLATION, GROWTH, AND IDENTIFICATION OF *PYTHIUM CRYPTOIRREGULARE*

### 3.1 Introduction

Phytopathogenic *Pythium* is one of the several genera that can cause seedling root rot and a condition called "damping-off". This disease causes yield loss in a wide range of hosts and is recognized by seedlings that collapse after they emerged (Mao *et al.*, 1997; Nowicki, 1997; Begum *et al.*, 2010). Worldwide, this disease has affected crops in fields and greenhouses, resulting in significant economic losses.

The genus *Pythium* was first established by Springheim in 1858 and is now classified in the *Pythiaceae* family (Sideris, 1932; Hendrix & Campbell, 1973). The monography by van der Plaats-Niterink (1981) and "Keys to *Pythium*" by Dick (1991) have often been used to characterize and identify this soil-borne oomycete. Their differentiation of species was based on distinctive features of vegetative growth, (a)sexual reproduction structures, growth habit and growth rate in designated culture media. These distinctive features include sizes, shapes and types of mycelia, sporangia, oogonia, antheridia and spores. Additionally, van der Plaats-Niterink (1981) and Dick (1991) also acknowledge the importance of the effect of environmental factors on these features.

Despite the detailed morphological description available for *Pythium* species, multiple species share similar or identical structures that limit their identification. Therefore, methods involving molecular characterization were developed based on ITS regions (Tambong *et al.*, 2006). Phylogenetic studies by Lévesque and de Cock (2004) revealed 11 sub-clades (A-K) within two major distinctive clades within the genus *Pythium*. *Pythium irregulare sensu lato* is one of the species that resides in the F-clade. Further studies separated this species into

*P. irregulare sensu stricto* and a species that was recognized as a new species named *P. cryptoirregulare* (Garzón *et al.*, 2007).

In 2017, damping-off symptoms were observed on *A. thaliana* seedlings in the growth chambers of the Department of Biology at the University of Saskatchewan. It was suspected that a phytopathogenic *Pythium* sp. was the causal agent of these symptoms and seedling loss. The pathogen was isolated from the infected seedlings and identified through ITS sequencing. However, in some cases, *Pythium* species share identical or nearly identical ITS regions. Therefore, both morphological and non-morphological methods were applied for the identification of the *Pythium* candidate, which is presented in this research chapter.

Firstly, growth conditions and cultivation media were optimized for morphological characterization and identification by light and confocal laser-scanning microscopy. The morphological characteristics were all compared to the characteristics of the two obtained *Pythium* reference species "*P. irregulare*" and "*P. ultimum* var. *ultimum*". Secondly, molecular characterization and identification were based on ITS sequencing of DNA extracted from *P. cryptoirregulare* mycelia. The *P. cryptoirregulare* DNA sequences were aligned and compared with the *Pythium* reference species originating from the studies by Lévesque and de Cock (2004) and Garzón *et al.* (2007).

## 3.2 Materials and methods

### 3.2.1 Plant and pathogen materials

**Host** – For *Colletotrichum* related projects, unrelated to this study, the *A. thaliana* transgenic line *FH1-YFP* was grown in growth chambers at 22 °C with a 16-h photoperiod and approximate 55% RH on soil (Sunshine mix #1, Sungro®) in approximately 9 cm pots. Seedlings showing root rot disease symptoms were subjected to this study for the initial isolation of the *Pythium* candidate.

**Pathogen** – The *Pythium* candidate was isolated from *Arabidopsis* seedlings in 2017 and maintained on potato dextrose agar (PDA) until further examination at the end of 2018 when this project was initiated. Shortly after, two reference strains, *Pythium irregulare* (DOAMC 870 BR) and a more distantly related species *Pythium ultimum* var. *ultimum* (DAOMC 628 BR), were obtained from the Canadian Collection of Fungal Cultures (DOAMC). According to the DOAMC records, both these strains had initially been isolated from canola. Information about these strains can be found in Table 3.1.

**Table 3.1 *Pythium* reference strains ordered from the Canadian Collection of Fungal Cultures (DOAMC)**

| | *Pythium irregulare* Buisman | *Pythium ultimum* var. *ultimum* Throw |
|---|---|---|
| DOAMC identifier | DAOMC 870 BR | DAOMC 628 BR |
| Isolated from | Canola | Canola with seedling blight |
| Collected by | - | A.I. Calman AC 3 |
| Location | Alberta, Canada | Alberta, Canada |
| Determined by | D.J.S. Barr | D.J.S. Barr |
| Identification year | 1991 | 1989 |
| Isolate code | 91M-162 | 89M-19 |
| Received from | - | J.P. Tewari |

Internal transcriber spacer sequences of the five *P. irregulare* and five *P. cryptoirregulare* isolates that were used for the re-identification of *P. cryptoirregulare* as a new species by Garzón *et al*. (2007) were obtained from the National Center for Biotechnology Information (NCBI) for molecular differentiation between *P. irregulare* and *P. cryptoirregulare* during the identification of the isolate. Table 3.2 lists the collection designation, species, country and host/substrate origin, and Genbank accession and GI code of these reference strains.

**Table 3.2 *Pythium* strains used for differentiation between *Pythium irregulare* and *Pythium cryptoirregulare***

| Collection designation | Species | Host or substrate | Origin | GenBank ITS | |
|---|---|---|---|---|---|
| | | | | Accession | GI |
| *P.ci* Wei2017 | *P. cryptoirregulare* | *Arabidopsis thaliana* | Canada | – | – |
| 325393* | *P. cryptoirregulare* | *Anigozanthus* | Australia | AY907901 | 60203112 |
| P50 (CBS 118731) | *P. cryptoirregulare* | *Euphorbia pulcherrima* | PA, USA | AY907893 | 60100306 |
| 13-12* | *P. cryptoirregulare* | *Pelargonium* | NY, USA | AY907902 | 60100315 |
| 13-32* | *P. cryptoirregulare* | *Pelargonium* | CN, USA | AY907904 | 60100317 |
| 13-58* | *P. cryptoirregulare* | *Pelargonium* | FL, USA | AY907906 | 60100319 |
| 363670 R* | *P. irregulare* | *Allium* | Taiwan | AF452143 | 17980862 |
| 2076-80* | *P. irregulare* | *Capsicum annuum* | PA, USA | AY907907 | 60100320 |
| 13-7* | *P. irregulare* | *Pelargonium* | MI, USA | AY907912 | 60100325 |
| 13-10* | *P. irregulare* | *Pelargonium* | MI, USA | AY907913 | 60100326 |
| 13-59 | *P. irregulare* | – | – | AY907917 | 60100330 |

* Information partially obtained from Garzón *et al*. (2007)

For the phylogenetic tree construction in this study, one strain per species of the F-clade and a *P. ultimum* var. *ultimum* strain of the I-clade were included from the strains that were listed in the UPGMA phylogenetic trees constructed by Lévesque and de Cock (2004). *Pythium cryptoirregulare* strains "CBS 118731", "CBS 118731 clone 10", and "13-32" were also included based on their close relatedness to the pathogen isolated during this study to identify the isolate's place in the newly constructed phylogenetic tree. The strains that were obtained from the DOAMC and *Phytophthora infestans*, acting as the outgroup, were also included. Collection designation, clade, origin, and Genbank accession and GI numbers of all strains can be found in Table 3.3.

**Table 3.3 Isolates used for the phylogenetic tree construction in this study.The isolate that was obtained during this study is underlined**

| Collection designation | Species | *Pythium* genus clade | Host or substrate | Origin | GenBank ITS | |
|---|---|---|---|---|---|---|
| | | | | | Accession | GI |
| CBS 120920 | *Phytophthora infestans* | outgroup | *Solanum tuberosum* | The Netherlands | MF680417.1 | 1251770548 |
| B10-2 | *Pythium abappressorium* | F | – | USA | HQ643408.2 | 573007525 |
| DAOM 230383[a*] | *Pythium attrantheridium* | F | – | – | AY286014 | 33591054 |
| *P.ci*. Wei2017 | *Pythium cryptoirregulare* | F | *Arabidopsis thaliana* | Canada | – | – |
| CBS 118731 | *Pythium cryptoirregulare* | F | – | USA | HQ643515.2 | 573007528 |
| CBS 118731 clone 10 | *Pythium cryptoirregulare* | F | – | – | GQ410367.1 | 299764525 |
| 13-32[b] | *Pythium cryptoirregulare* | F | – | – | AY907906.1 | 60100319 |
| CBS 218.94[a*] | *Pythium cylindrosporum* | F | soil | Germany | AY598643.2 | 505574775 |
| CBS 752.96[a] | *Pythium debaryanum* | F | *Tulipa* sp. | UK | AY598704.2 | 531037412 |
| CBS 266.38[a] | *Pythium intermedium* | F | *Agrostis stolonifera* | The Netherlands | AY598647.4 | 1012146179 |
| BR870/ DAOMC 870 BR | *Pythium irregulare* | F | – | Canada | HQ643621.1 | 323301887 |
| CBS 250.28[a] | *Pythium irregulare* | F | *Phaseolus vulgaris* | The Netherlands | AY598702.2 | 531037411 |
| CBS 550.88[a*] | *Pythium kunmingense* | F | soil under *Vicia faba* | China | AY598700.1 | 51235554 |
| CBS 574.80[a] | *Pythium macrosporum* | F | flower bulb | The Netherlands | AY598646.2 | 505574778 |
| CBS 251.28[a] | *Pythium mamillatum* | F | *Beta vulgaris* | The Netherlands | AY598703.1 | 51235557 |
| CBS 157.64[a] | *Pythium paroecandrum* | F | soil | Australia | AY598644.2 | 505574776 |
| CI-34[a] | *Pythium regulare* | F | | Spain | AF492018.1 | 20147565 |
| CBS 275.67[a] | *Pythium spinosum* | F | compost | The Netherlands | AY598701.2 | 531037410 |
| CBS 453.67[a] | *Pythium sylvaticum* | F | soil | USA | AY598645.2 | 505574777 |
| CBS 219.65[a] | *Pythium ultimum* var. *sporangiiferum* | | *Chenopodium album* | USA | AY598656.1 | 51235510 |
| BR628/ DAOMC 628 BR | *Pythium ultimum* var. *ultimum* | | | Canada | HQ643936.1 | 323302199 |
| CBS 398.51[a] | *Pythium ultimum* var. *ultimum* | I | *Lepidium sativum* | The Netherlands | AY598657.2 | 505574787 |
| OPy6[a] | *Pythium violae* | F | – | – | AJ233463.1 | 6468690 |

[a] Information partially obtained from Lévesque and de Cock (2004)

[b] Information partially obtained from Garzón et al. (2007)

[*] Ex-type strain

### 3.2.2 Isolation of *Pythium cryptoirregulare* from *Arabidopsis thaliana*

For the isolation of the pathogen, infected *A. thaliana* transgenic FH1-YFP seedlings showing symptoms of root rot disease were selected based on poor seedling establishment, damping-off, stunting, premature defoliation, deterioration of leaves or plant wilt and death. Seedlings showing any of these symptoms were then removed from the soil, surface sterilized with 70 % ethanol for 30 seconds and 10 % bleach for 2 minutes, washed three times with sterilized water, and placed on potato dextrose agar (PDA). Purification of the *Pythium* candidate was carried out by cutting a small piece of media from the edge of the colony that originated from the specimen and thereby collecting hyphal tips that were subcultured onto new PDA until a pure culture was obtained.

### 3.2.3 Media optimization to induce *Pythium* structure development

As part of the morphological characterization and identification procedures, an optimal medium composition had to be established for efficient growth of the *Pythium* candidate. The following liquid and solid media were tested: potato dextrose broth (PDB) and agar (PDA), maltose yeast peptone broth (MYPB) and agar (MYPA), cornmeal broth (CMB) and agar (CMA), cornmeal glucose peptone broth (CMGPB) and agar (CMGPA), rice broth (RB) and agar (RA) and Murashige and Skoog broth (MSB) and agar (MSA).

Potato dextrose broth was created with 24 g PDB powder per litre $H_2O$ according to Difco™ instructions, whereas MYPB was manually prepared and composed of 1 g maltose, 0.5 g yeast extract and 1 g peptone in 500 mL $H_2O$ (Agricultural Research Service - ARS, 2015). The protocol of Waller *et al.*, 1998 was modified to obtain cornmeal broth by boiling 30 g cornmeal in 200 mL $H_2O$ for an hour and filtering it with cheesecloth and Miracloth by pouring $H_2O$ through the cloths until a final volume of 1 L was reached. Cornmeal glucose peptone broth was obtained similarly, by boiling 10 g cornmeal in 500 mL for an hour, filtering the mixture with $H_2O$ until a final volume of 500 mL was reached, followed by an additional 10 g of glucose and 10 g of peptone according to (ARS, 2015). The same amount (10 g) of rice was boiled in 500 mL $H_2O$ for an hour and filtered with cheesecloth and Miracloth to create RB. Lastly, ½ MSB with 1 % sucrose was made by adding 1.1 g MS powder (Sigma-Aldrich Canada Co.) and 5 g sucrose to 500 mL $H_2O$.

For solid media, 4 g agar was added per 500 mL broth, to obtain an agar concentration of 0.8 % (m/v). All media were autoclaved using a 45-minute liquid cycle.

Agar plates were made by adding approximately 20 mL in either sterile polystyrene or glass Petri dishes, and the broths were all cooled and divided in volumes of 100 mL into 250 mL flasks. An agar plug of approximately 0.5 x 0.5 cm in size, taken from the edge of the actively growing mycelia on PDA, was added to each of the media, followed by incubation at room temperature (23 ºC). Agar plates were placed on a stagnant surface while liquid cultures were placed in the incubator on a shaker (100 rpm) at approximately 25 ºC. Growth of the *Pythium* candidate was visually observed daily.

### 3.2.4 Morphological characterization and identification

After testing a variety of media, an optimal medium was chosen based on the morphological structure to be observed. For morphological characterization of the vegetative hyphal structures of the *Pythium* candidate, no specific medium composition was required, but to induce septa formation, colonies were either incubated for a more extended period or were transferred to a nutrient-poor environment consisting of autoclaved MiliQ water. Cornmeal agar in polystyrene Petri dishes (VWR Cat. #470313-352) was selected for the induction and observation of sexual and asexual reproductive structures after seven days of incubation at room temperature. Rice agar in polystyrene Petri dishes was used to simulate a nutrient-rich environment with a hydrophobic substrate for the induction of appressoria formation. Cultures were incubated for a maximum of 5 days at room temperature.

The morphological characteristics were examined with three microscopes: firstly, the fluorescence microscope (Zeiss Axioplan), secondly, the brightfield setting of the LSM 510 meta laser-scanning confocal microscope (Zeiss Confor2, 2005) and thirdly, the DIC setting of the Zeiss apotome microscope (Zeiss Axio Imager Z1, 2009; Carl Zeiss, Gottingen, Germany). All morphological characteristics were studied using two different methods. For the first method, the isolate was grown on an agar medium of which plugs were removed after approximately 5-7 days of incubation at room temperature. The plugs were then transferred to slides for observation under either the fluorescence microscope or confocal microscope at a 20X, 40X or 63X magnification. To ensure successful appressoria observation, agar plugs were inverted 180 degrees, so the appressoria were facing the objective lens. The second method included growing

the isolate in a liquid medium for approximately 10 days on a shaker at 100 rpm and temperature of 25 ºC, followed by detaching hyphae from the edge of the mycelial growth. The hyphae were then transferred to slides for observation under the fluorescence microscope or confocal microscope at a 20, 40 or 63X magnification. The goal was to capture the vegetative hyphae, the appressoria and several different stages of the reproductive structure development. Pictures that were taken with either of the microscopes were analysed using Fiji (ImageJ, 1.52s), and Adobe Photoshop (CS4) as needed.

### 3.2.5 Molecular characterization and identification

#### 3.2.5.1 Genomic DNA extraction

Pure cultures of the *Pythium* candidate and its reference species *P. irregulare* and *P. ultimum* var. *ultimum* were grown on ½ MSA for optimal aerial hyphae formation in 2-3 days incubation at room temperature. Total genomic DNA was extracted for each pathogen by collecting a volume of approximately 0.2 $cm^3$ from the aerial or surface hyphae and transferred to a microcentrifuge tube with 500 mL lysis buffer after which it was manually ground with a sterile micro pestle. After centrifuging for 1 minute at 13,000 rpm, the supernatant was transferred to a new microcentrifuge tube and mixed by inversion with 1/10 volume 3 M sodium acetate and 1 volume chloroform. The samples were then incubated at room temperature for 15 minutes, followed by centrifugation for 10 minutes at 13,000 rpm. After the supernatants were discarded, the pellets were rinsed with 70% ethanol, airdried for 10 minutes and finally dissolved in 50 µL sterile distilled water and stored at -20 ºC.

#### 3.2.5.2 PCR amplification

The ITS1 region (5.8S rRNA gene) and the ITS2 region (26S or 28S rRNA gene) of the *Pythium* candidate and the *Pythium* reference species were amplified using the primers ITS1 (5′-TCCGTAGGTGAACCTGCGG-3′) and ITS4 (5′- TCCTCCGCTTATTGATATGC-3′; White *et al.*, 1990) as described in Moorman *et al.* (2002). Per *Pythium* sample, a 50 µL PCR reaction mix was prepared including the following components: 5 µL 10X Standard Taq Reaction buffer (New England Biolabs), 1 µL 10 mM dNTP's (New England Biolabs), 1 µL 10 µM ITS1 forward primer, 1 µL 10 µM ITS4 reverse primer, 39.25 µL distilled water, 0.25 µL Taq DNA-polymerase (New England Biolabs) and 2.5 µL undiluted template DNA. Internal transcriber spacer regions of the rDNA sequence were amplified with the thermal cycler (Applied

Biosystems™ SimpliAmp™) using an initial denaturation at 98 °C for 3 min, followed by 33 cycles of 30 sec at 95 °C for denaturation, 30 sec at 54 °C for annealing and 90 sec at 72 °C for extension, respectively. The PCR amplification was finalized with an additional elongation phase of 5 min at 72 °C and a final 3 min temperature of 24 °C.

Ten microliters of the PCR products were mixed with 10,000x GelRed® and run on a 1% agarose gel dissolved in 1x TEA (Tris-Acetate EDTA buffer) for resolution. For estimation of the size of these PCR products, the DL2000 DNA marker (Beijing, Zoman Biotechnology Co., Ltd) was also included in the run. Electrophoretic migration was carried out for 1.5 hours at 100V, after which the amplified products were visualized and photographed under UV light. The remaining 40 µL of the PCR products were sent to Eurofins Genomics where they were subjected to Sanger sequencing using the sequence primers ITS1 (5′-TCCGTAGGTGAACCTGCGG-3′) and ITS4 (5′- TCCTCCGCTTATTGATATGC-3′; White *et al.*, 1990).

#### 3.2.5.3 Analysis of amplified ITS sequence

The obtained DNA sequences of the ITS1 and ITS4 regions of all three isolates were assembled into a consensus contig using DNA Baser Assembler v5 (2018, Heracle BioSoft, www.DnaBaser.com). This contig was then subjected to the nucleotide BLAST search (BLASTn) at the National Center for Biotechnology Information (NCBI) website (http://blast.ncbi.nlm.nih.gov/blast.cgi) where the ITS sequences of the *Pythium* isolates were compared with ITS sequences of known *Pythium* species available in the GenBank database. Meanwhile, Clustal X (v.2; Thompson *et al.*, 1997) was used to align the contig of the *Pythium* candidate with the 10 reference sequences, mentioned previously in Table 3.2, for differentiation between *P. irregulare* and *P. cryptoirregulare*. The eleven sequence sites that were defined by Garzón *et al*. (2007) to distinguish between the species were examined to determine the identity of the *Pythium* candidate.

A second alignment was conducted with sequences of *Pythium* strains that were presented in the F-clade by Lévesque and de Cock (2004) and a *P. ultimum* var. *ultimum* species to serve as a clade outgroup. *Phytophthora infestans* was selected to be the genus outgroup due to its close relatedness *Pythium*. Additional *P. cryptoirregulare* isolates, based on the previous alignment and the NCBI BLASTn results, were also included in this alignment to specify the relationship

between the *Pythium* candidate and other close-related *Pythium* species. A list of all used isolates can be found in Table 3.3. The MUSCLE alignment in the MEGA X (v.10.0.5; Kumar *et al.*, 2018) software was used for the initial alignment, after which the 23 sequences were all trimmed to a similar base-pair length and realigned for a more detailed alignment.

#### 3.2.5.4 Phylogenetic tree construction

The neighbour-joining method (Saitou & Nei, 1987) in MEGA X (v.10.0.5; Kumar *et al.*, 2018) was used to construct a phylogenetic tree for the *Pythium irregulare* versus *Pythium cryptoirregulare* differentiation, as well as for defining the evolutionary relationship of the *Pythium* candidate that was collected in this study compared to other related *Pythium* species. For both phylogenetic tree constructions, a bootstrap test (Felsenstein, 1985) with 1000 replicates and all positions with less than 95% site coverage were eliminated, but the partial deletion option was chosen to allow fewer than 5% alignment gaps, missing data, and ambiguous bases at any position. The evolutionary distances were computed using the Maximum Composite Likelihood method (Tamura *et al.*, 2004).

## 3.3 Results

Circular areas of infection were observed in which the majority of the *A. thaliana* transgenic *FH1-YFP* seedlings were showing damping-off symptoms as seedlings had collapsed (Figure 3.1). Seedlings in this zone that had not collapsed were showing poor seedling establishment characterized by delayed growth that resulted in a visibly shorter hypocotyl and smaller leaves compared to the uninfected seedlings. Also, death of seedlings and lack of germination was observed closer to the centre of the infected area. After the infected seedlings were removed, surface sterilized and transferred to a growth medium, a pure culture of the *Pythium* candidate was obtained by subculturing hyphal tips repeatedly.

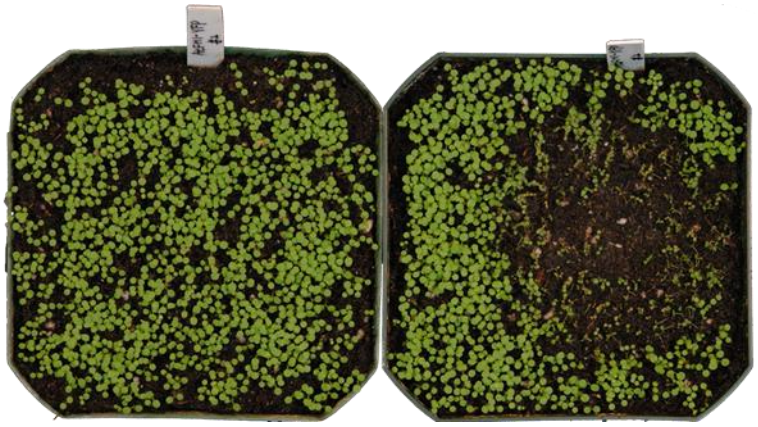

**Figure 3.1 *Arabidopsis thaliana* transgenic line *FH1-YFP* showing damping-off symptoms upon infection by the *Pythium* candidate. Left**. Non-infected *A. thaliana* transgenic *FH1-YFP* seedlings. **Right**. A circular area of infected *Arabidopsis thaliana* transgenic *FH1-YFP* seedlings.

### 3.3.1 Optimized media for the structure development of *Pythium* species

After testing the six different liquid media, the components of the PDB, MYPB and CMGPB seemed very favourable for bacterial growth. It was also observed that this bacterial growth had an antagonistic or competitive effect on the growth of the isolate that was collected in this study. Overall, using these media posed a high risk of contamination, causing inconsistent metabolite secretion; a reason not to use these liquid cultures in the following experiments. However, RB, CMB and MSB remained good options for follow-up experiments. Although the isolates grown in these broths developed an abundance of vegetative hyphae and a few oospores, zoospores were not detected.

Extracting hyphae from the mycelia grown in the broth appeared to be difficult without disturbing or damaging the hyphae. Excessive loss of cytoplasm was observed during this

procedure, which made it difficult to distinguish between contamination by spherical bacteria and cytoplasmic droplets. The cytoplasmic streaming was also altered as it changed direction towards the damaged tissue where it was released. As a consequence, liquid cultures were not used for the morphological characterization and identification but were only used for experiments that involved the assessment of metabolic activities where the mycelia did not need to be partially extracted.

The remaining media candidates CMA, RA, PDA and MSA were all used to optimize *P. cryptoirregulare* growth on agar plates for maintaining a viable culture, morphological characterization and identification, and for inoculum preparation. Potato dextrose agar was included as the starting medium, on which mycelia would spread to the edges of a Petri dish in approximately five days. Growth on CMA and RBA progressed at a slightly faster rate by spreading to the edge of the plate in three to four days. Moreover, a difference in mycelial development was also observed. Hyphae in PDA seemed to exhibit an organized growth pattern, whereas they did not on CMA and RA. Also, hyphae grown on CMA branched more frequently than hyphae on RA. The most rapid growth of hyphae was observed on MSA, where only approximately 1.5 days were needed for the mycelium to spread and reach the edge. This medium also induced the highest development of aerial hyphae, which, combined with the rapid growth, resulted in a high hyphal density above and inside the agar. This high hyphal density obstructed the ability to characterize *P. cryptoirregulare* based on morphology using light microscopy due to the lack of light that was passed through the sample. Therefore, this medium was considered unsuitable for this purpose. Instead, CMA and RA were used for this purpose despite the slower growth rate.

After the optimal media were selected, the brightfield settings of the Axioplan fluorescence microscope and the LSM 510 meta confocal microscope, and the DIC setting of the apotome microscope were used to observe and capture the characteristics of the isolate that was obtained in this study. Vegetative growth of the isolate was observed in all media, but based on previously mentioned reasons, PDA was selected for presenting the vegetative hyphae structures which were found in great abundance and geometrical patterns throughout the medium (Figure 3.2A). Even five days post-inoculation, this medium did not induce any reproductive structure formation and was therefore used, exclusively, to examine vegetative growth. Seven days post-

inoculation, the formation of oospores and zoosporangia were carefully observed in CMA throughout the medium (Figure 3.2B). Moreover, oospores were frequently observed, whereas zoosporangia were barely detected at all. In contrast, appressoria formation was observed abundantly in RA at five days post-inoculation, but only where the medium was in contact with the polystyrene Petri dish, suggesting that it was used as a replacement for the interaction with the hydrophobic surface of a host (Figure 3.2C).

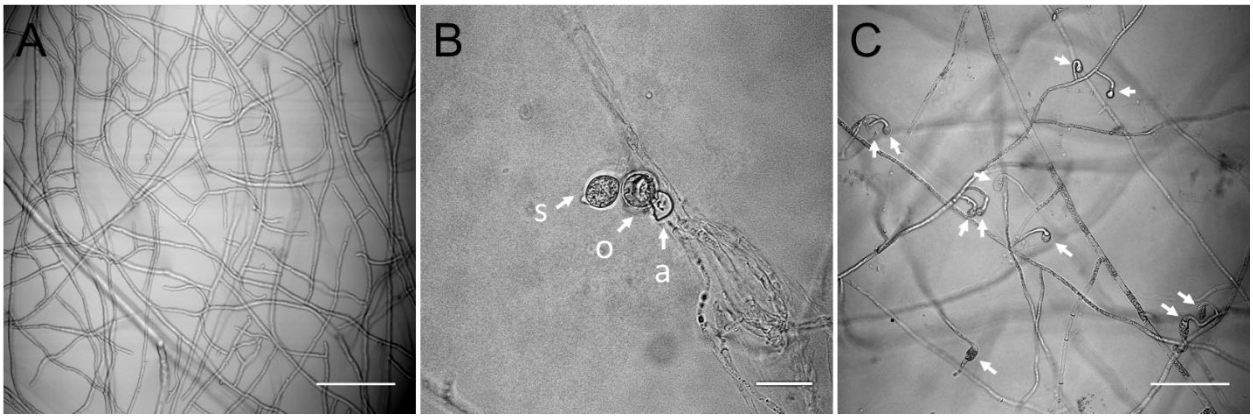


**Figure 3.2 Structure induction of *Pythium cryptoirregulare* through media composition.** Photos were taken using the brightfield setting of the Zeiss LSM 510 meta confocal microscope, five (**A** and **C**) or seven (**B**) days post-inoculation at room temperature (23 ºC). Reproductive structures and appressoria are indicated with arrows. **A**. Induction of vegetative hyphae formation on PDA throughout the medium. **B**. Induction of oospore and sporangia formation on CMA throughout the medium where s = sporangium, o = oogonium and a = antheridium. **C**. Induction of appressoria formation in RA where the medium is in contact with the polystyrene Petri dish. Appressoria are indicated by arrows. Scale bars = 100 µm (**A** and **C**) and 50 µm (**B**).

Moreover, the latter observation led to the question whether the formation of appressoria indeed depended on the material of the Petri dish. When *P. cryptoirregulare* was grown in the RA in polystyrene Petri dishes, the formation of appressoria was observed as soon as the hyphae came into contact with the material (Figure 3.3A), whereas the hyphae coming into contact with a glass Petri dish did not form any appressoria (Figure 3.3B). This result presents the effect of the material of the Petri dish on the formation of appressoria. The explanation for this phenomenon is the difference in hydrophobicity, considering that glass Petri dishes are more hydrophilic, and therefore negatively charged, than polystyrene Petri dishes. The charge of the Petri dish material could thus influence the adhesion of the hyphae to the surface, or another possibility could be a difference in the pre-treatment or sterilization methods of the Petri dishes.

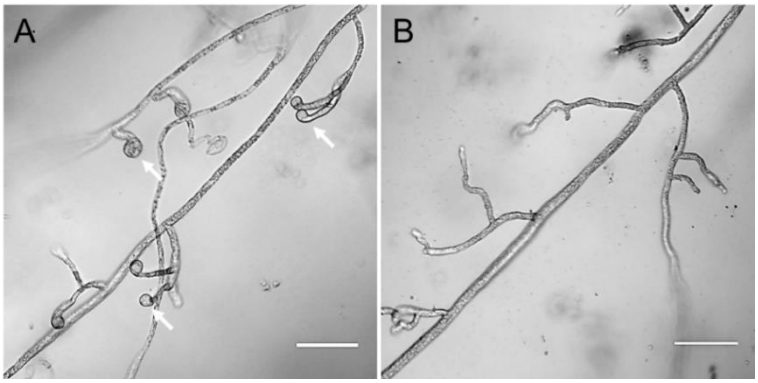


**Figure 3.3 The influence of surface contact on the appressoria formation of *Pythium cryptoirregulare*.** Photos were taken using the brightfield setting of the Zeiss LSM 510 meta confocal microscope, five days post-inoculation on RA at room temperature (23 ºC). Appressoria are indicated by arrows. **A**. Appressoria formation where hyphae meet the polystyrene Petri dish. **B**. Absence of appressoria formation where hyphae meet the glass Petri dish. Scale bars = 50µm.

### 3.3.2 Hyphal characteristics of *Pythium* species

The vegetative state of *Pythium* is known to consist of mycelia with coenocytic hyphae (van der Plaats-Niterink, 1981). These coenocytic hyphae were indeed observed in the new viable growing mycelia (Figure 3.4A). However, septa formation was observed when mycelia from RA cultures were placed in sterile water (Figure 3.4B) and during oospore development. Cultures older than three weeks, especially in CMA, consisted of almost only septate hyphae (Figure 3.4C). These findings suggest that the formation of septa is part of the sexual reproduction mechanism and a survival mechanism during unfavourable nutrition conditions.

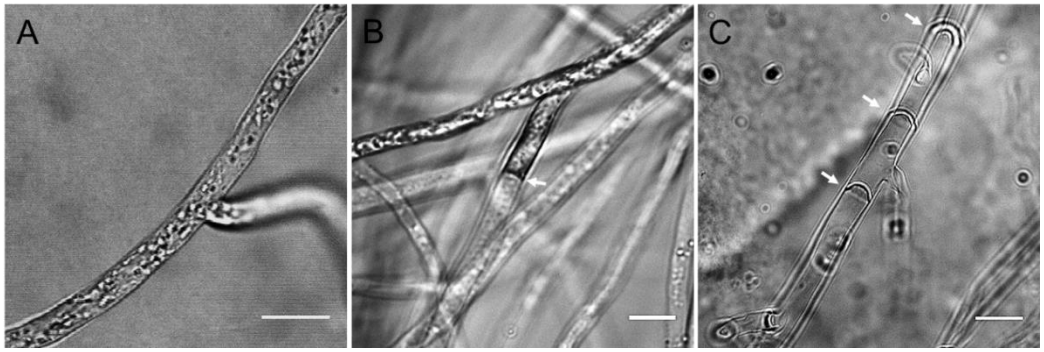


**Figure 3.4 Hyphae characteristics of *Pythium cryptoirregulare*.** Photos were taken using the fluorescence microscope or the brightfield setting of the Zeiss LSM 510 meta confocal microscope, after 5-14 days of incubation at room temperature (23 ºC). Septa are indicated with arrows. **A**. Coenocytic hypha in RA after five days of incubation. **B**. Septa formation in hyphae, after one day of incubation in sterile water after growth on RA for five days. C. Septate hyphae after 14 days of incubation in CMA. Scale bars = 10 µm.

Humidity also played an essential role in vegetative hyphae development. This was confirmed by the increased branching that was observed after the aerial hyphae reached the condensation droplets on the lid of the Petri dish (Figure 3.5), which also suggests that this pathogen is capable of growth in nutrient-poor environments.

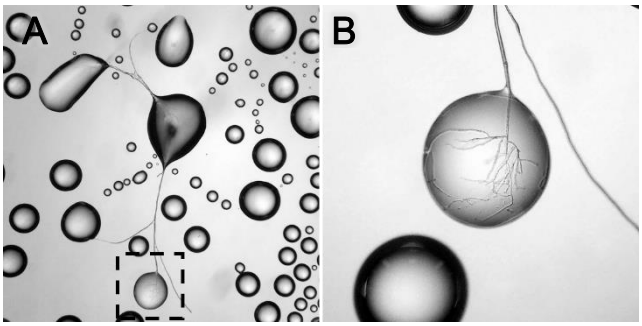


**Figure 3.5 Mycelial growth of *Pythium cryptoirregulare* in water droplets.** Photos were taken after 5 days of incubation in ½ MSA at room temperature (23ºC) when aerial hyphae had reached the lid of the Petri dish. **A**. Aerial hyphae growing from water droplet to water droplet of the condensation on the lid of the Petri dish. **B**. An approximate 20 times enlargement of the boxed area seen in **A**, presenting the increased branch development of a single hypha in a water droplet.

### 3.3.3 Characteristics of the reproductive structures of *Pythium* species

#### 3.3.3.1 Characteristics of the sexual reproductive structures

The sexual reproduction was induced on CMA and observed three weeks post-inoculation when several stages of oospore development were observed. This event was initiated by the formation of two septa on a hyphal branch, blocking the cytoplasmic transport, and capturing cell organelles. Swelling and the second cell wall formation followed in this isolated region for the developing oogonium (Figure 3.6).


**Figure 3.6 Oogonium development of *Pythium cryptoirregulare*.** Photos were taken using the brightfield setting of the Zeiss LSM 510 meta confocal microscope after three weeks of incubation on CMA at room temperature (23 ºC). The development was initiated by the formation of two septa (**A**), blocking the cytoplasm transportation and capturing cell organelles, followed by swelling of the hyphae (**B**-**C**) to form the oogonium (**D**). Scale bars = 10 µm.

Next, the sexual exchange occurred after one or multiple paragynous antheridia were mostly formed on the same hyphal branch, which is characteristic for homothallic species (Figure 3.7). Amphigynous antheridia were not detected, but the monoclinous antheridium or antheridia were often formed on the same hyphal stalk to make apical contact with the oogonium. Diclinous antheridia were observed less than 5% of the time but were nonetheless fertilizing oogonia. Fertilization tubes to fertilize the terminal or intercalary oogonia were occasionally observed and captured, contributing to male nuclei exchange, and therefore the finalization of the oospore formation. Finger-like projections were even more rare as these were only observed up to five times during this study.

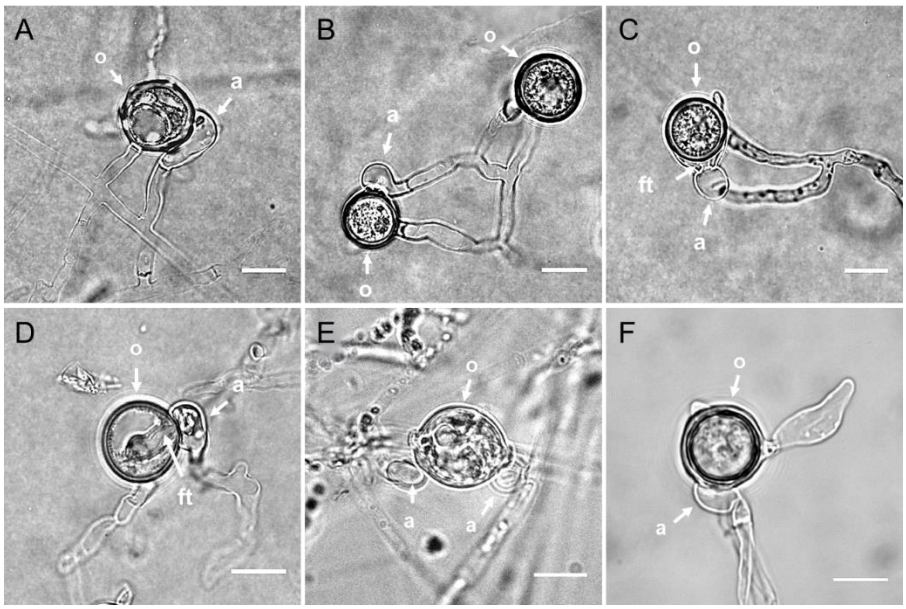


**Figure 3.7 A variety of *Pythium cryptoirregulare* oogonium fertilizations by paragynous antheridium or antheridia.** Photos were taken using the brightfield setting of the Zeiss LSM 510 meta confocal microscope after three weeks of incubation on CMA at room temperature (23 ºC). o = oogonium, a = antheridium, ft = fertilization tube. **A**. Monoclinous antheridium making apical contact to a subterminal oogonium with one clearly visible ooplast body. **B**. Two terminal oogonia, each attached to a monoclinous antheridium. **C**. Fertilization of a terminal oogonium by a diclinous antheridium, showing the fertilization tube in the center of the extended oogonial wall. **D**. Clearly visible transfer of the male nucleus by a diclinous antheridium. **E**. Multiple antheridia fertilizing an intercalary oogonium. **F**. An antheridium in contact with an oogonium that developed a finger-like projection. Scale bars = 10 µm.

The oospores that were formed as a product of this sexual reproduction strategy exhibited a variety of different features. Differences in several important morphological characteristics were observed, including the number of ooplast bodies per oospore (Figure 3.8A) and terminal or intercalary oospores. A less common phenomenon that was seen was a difference in pleroticity,

which is indicated by the distance between the oogonial wall and the oospore (Figure 3.8B). However, aplerotic oospores, where the oogonial wall is located visually distant from the oospore, were observed with an approximate 1:99 ratio compared to the plerotic oospores. More uncommon events (<1%) were the formation of linked or merged oospores within a single oogonial wall (Figure 3.8C) and germinating oospores (Figure 3.8D).

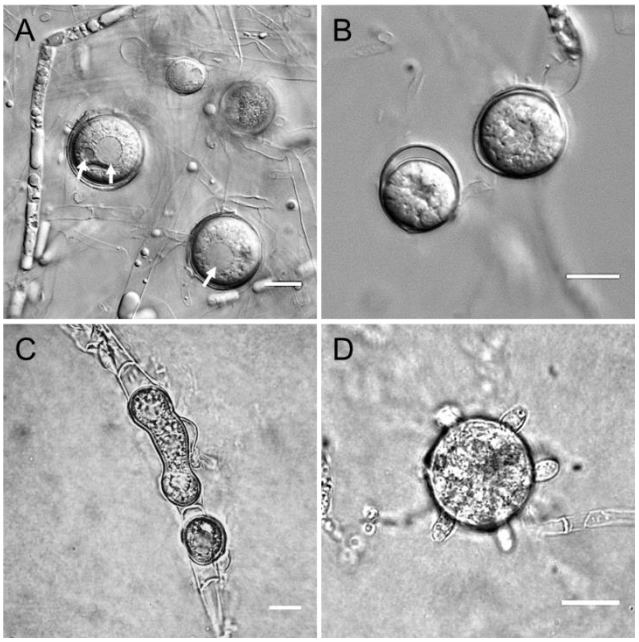


**Figure 3.8 Differences in morphological characteristics of *Pythium cryptoirregulare* oospores.** Photos were taken using the DIC setting of the Zeiss Apotome microscope (**A** & **B**) or brightfield setting of the Zeiss LSM 510 meta confocal microscope (**C** & **D**) after three weeks of incubation on CMA at room temperature (23 ºC). **A**. Two oospores where the difference in ooplast body numbers are indicated by arrows. **B**. Aplerotic oospore (left) and plerotic oospore (right). **C**. Irregular shaped oospore formation. **D**. Oospore with at least 4 germination sites visible. Scale bars = 10µm.

### 3.3.4 Characteristics of the asexual reproductive structures

Zoosporangia were seldomly formed, suggesting that the survival of the species does not depend on it. The assumption that the structures presented in Figure 3.9 were zoosporangia was based on the morphological similarities they shared with the sporangia presented by de Cock *et al.* (2015). Due to the similar appearance compared to terminal oogonia, it was difficult to distinguish these asexual reproductive structures from the sexual reproductive structures. The zoosporangia exhibited a more lemon-like shape compared to the terminal circular-shaped oogonia and occasionally had developed a discharge tube.

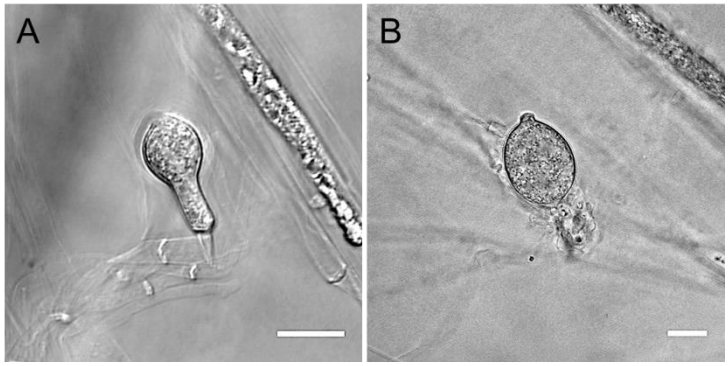


**Figure 3.9 Terminal sporangia of *Pythium cryptoirregulare***. Photos were taken using the brightfield setting of the Zeiss LSM 510 meta confocal microscope after seven days of incubation on CMA at room temperature (23 ºC). **A**. Early stage of sporangium development. **B**. Subglobose papillate sporangium. Scale bars = 10µm.

### 3.3.5 Appressoria characteristics

The formation of appressoria was induced by growing the *Pythium* candidate on RA. In contrast to the development of reproductive structures, appressoria were formed from coenocytic hyphae starting with the formation of a hyphal stalk (Figure 3.10A and B). The formation rate increased when favourable environmental factors were present. In this case, the appressoria only developed in the lowest layer of agar, which was in contact with the hydrophobic polystyrene Petri dish, which served as a substitute for the interaction with the hydrophobic surface of a host. *Pythium cryptoirregulare* also seemed to exhibit an extended appressoria development showing multiple catenulate hyphal swellings, indicating multiple penetration attempts (Figure 3.10C and D).

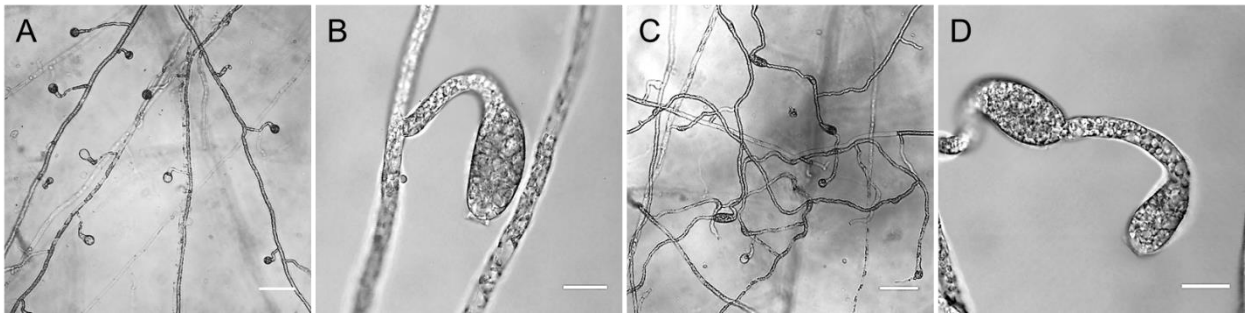


**Figure 3.10 *Pythium cryptoirregulare* appressoria formation upon contact with a hydrophobic surface.** Photos were taken using the light microscope or the brightfield setting of the Zeiss LSM 510 meta confocal microscope after five days of incubation in RA at room temperature (23 ºC). **A**. Overview of appressoria formation along the hyphal branches. **B**. Enlarged view of an appressorium formed from a hyphal stalk, showing the site of germination at the tip of this appressorium. **C**. Overview of extended appressoria formation after failed penetration attempts. **D**. Enlarged view of extended appressorium formation. Scale bars = 50µm (**A** and **C**) and 10µm (**B** and **D**).

### 3.3.6 Morphological similarities and differences of the *Pythium* candidate with the reference species *P. irregulare* and *P. ultimum* var. *ultimum*

To identify the species of the isolate based on morphology, its characteristics were compared to the two reference species *Pythium irregulare* (DOAMC 870 BR) and *Pythium ultimum* var. *ultimum* (DAOMC 628 BR; Figure 3.12). Regarding the hyphae, it was difficult to capture any differences due to the high variation in diameters among all branches, and all species exhibited 90 degrees branching angles. The only discernible difference was within the growth pattern of aerial hyphae. Aerial hyphae of the *Pythium* candidate and reference species *P. irregulare* were equally distributed over the medium whereas aerial hyphae of *P. ultimum* var. *ultimum* were characterized by clustering at random locations. The oogonia, antheridia and oospores also shared very similar characteristics among the species. For example, all oogonia had an approximate diameter of 20 µm. However, they occasionally differed in how often a specific characteristic, e.g. intercalary vs. terminal development, occurred compared to the other. One differentiating observation was the distance of the antheridia to the oogonia. Antheridia of *P. irregulare* were often developed at a distance from the oogonia, whereas antheridia from *P. ultimum* var. *ultimum* were often formed close to the oogonia. Both types of development are presented in Figure 3.11. Also, finger-like projections were observed on the oogonia of *P. irregulare*, but not of *P. ultimum* var. *ultimum*. This was observed in oogonia of the *Pythium* candidate of this study as well (Figure 3.7F). Another difference was seen in the abundance (Figure 3.11) and size of the appressoria. The appressoria of *P. ultimum* var. *ultimum* were visually more abundant and larger in volume. Overall, the isolate from this study shared more similarities with *P. irregulare* than with *P. ultimum* var. *ultimum*.

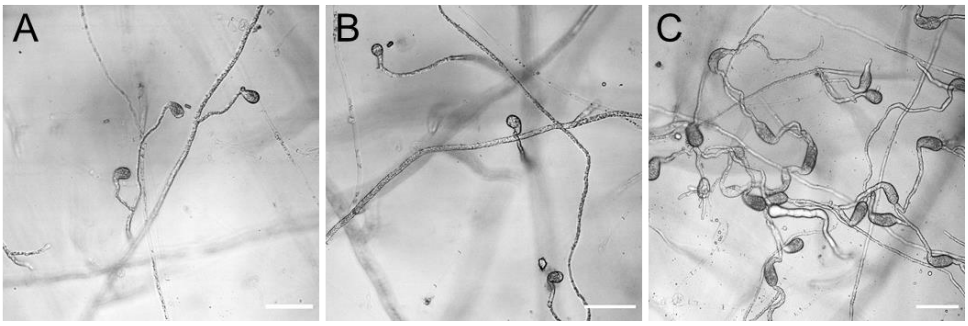


**Figure 3.11 Differences in appressoria abundance between the *Pythium* species of this study.** Photos were taken using the light microscope or the brightfield setting of the Zeiss LSM 510 meta confocal microscope after five days of incubation in RA at room temperature (20 ºC). **A**. Appressoria formation of *P. cryptoirregulare*. **B**. Appressoria formation of *P. irregulare*. **C**. Appressoria formation of *P. ultimum* var. *ultimum*. Scale bars = 50 µm.

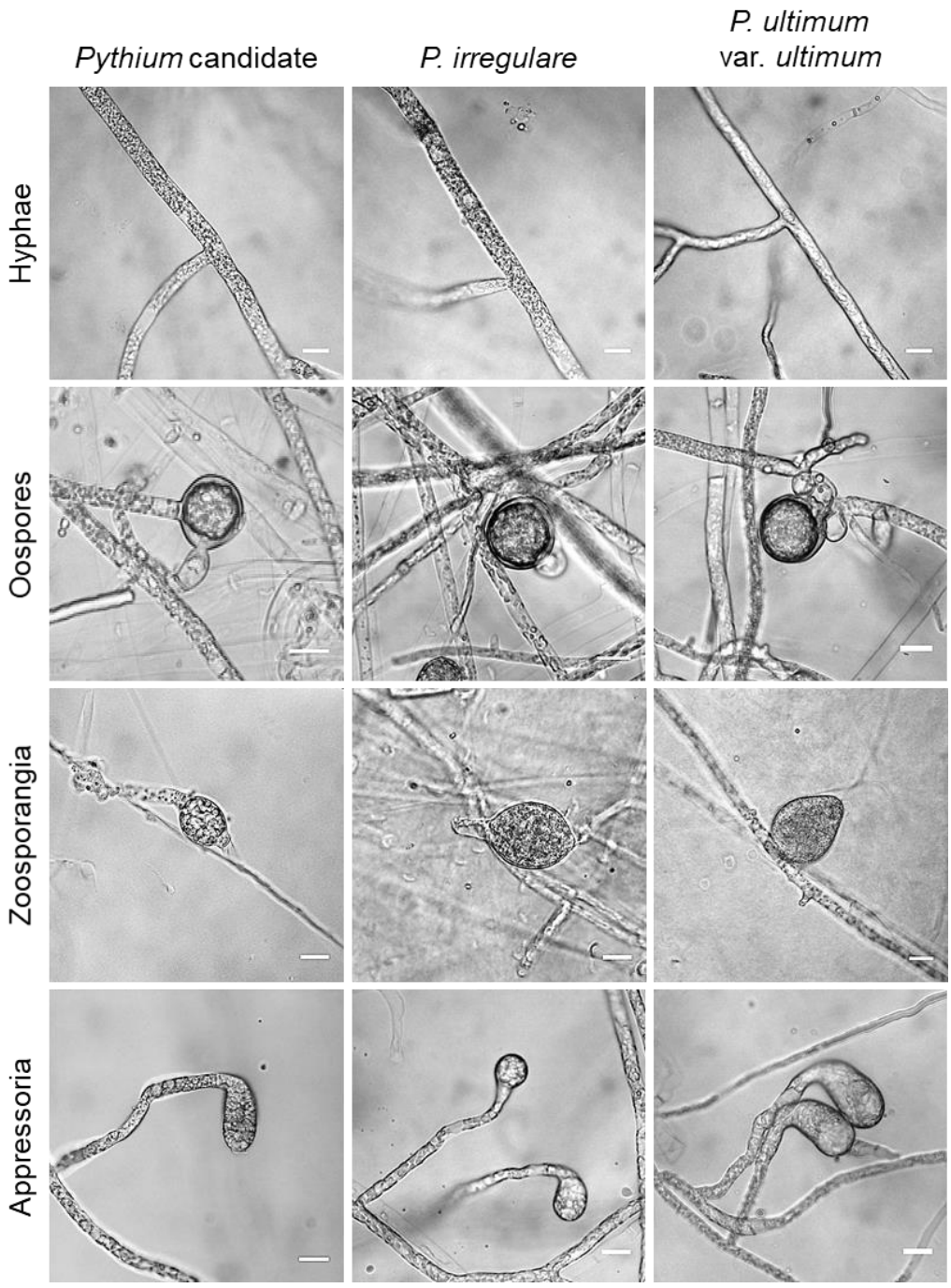


**Figure 3.12 Comparison of morphological characteristics of *Pythium cryptoirregulare*, *Pythium irregulare* and *Pythium ultimum* var. *ultimum*.** Photos were taken using the brightfield setting of the Zeiss confocal 510 microscope either after five days of incubation on RA (**hyphae** and **appressoria**) or seven days of incubation on CMA (**oospores** & **zoosporangia**) at room temperature (23 ºC). All hyphae have a 5-10 µm diameter and branch at a 90 degrees angle. Oospore development from left to right: fertilization of terminal oogonium by a diclinous and paragynous antheridium, fertilization of an intercalary oogonium by a monoclinous and paragynous antheridium, fertilization of an intercalary oogonium by multiple monoclinous and paragynous antheridia. Zoosporangia from left to right: subglobose papillate sporangium with a visible discharge tube, subglobose papillate sporangium, non-papillate ovoid sporangium. All appressoria were formed on a stalk from a hyphal branch, but the appressoria of *Pythium ultimum* var. *ultimum* were larger than the appressoria of other isolates. Scale bars = 10 µm.

### 3.3.7 Molecular characteristics and phylogeny of the *Pythium* candidate compared to *Pythium* reference species

PCR products (using primers ITS1 and ITS4) were shown as bright gel red-stained bands for *P. cryptoirregulare*, *P. irregulare* and *P. ultimum* var. *ultimum* at approximately 1400kb, 1400kb and 1100kb, respectively, indicating that the DNA extraction and amplification were successful (Figure 3.13).

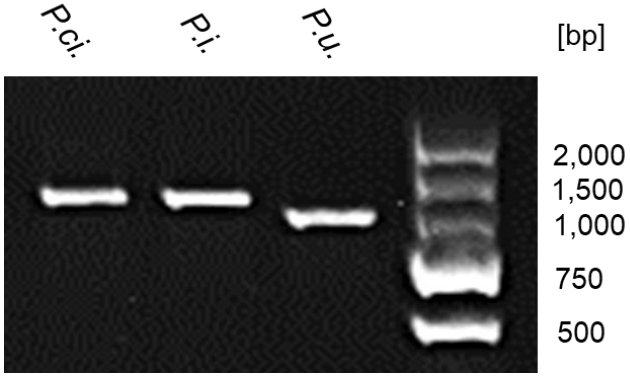


**Figure 3.13 PCR amplification products from the *Pythium* candidate (*P.ci.*), *Pythium irregulare* (*P.i.*, DOAMC 870 BR) and *Pythium ultimum* var. *ultimum* (*P.u.*, DAOMC 628 BR).** DNA extracted from mycelia grown on ½ MSA was used for the amplification with primer pair ITS1/ITS4. DNA marker = DL2000 (Beijing, Zoman Biotechnology Co., Ltd.)

After the sequence consensus contig of the *Pythium* candidate was assembled, the BLASTn alignment in NCBI showed the highest identical alignment score (98.05%) with clone 10 of the *Pythium cryptoirregulare* strain "CBS118731" (Accession: GQ410367.1).

For a more detailed confirmation of its identity, the consensus contig (*P.ci*._Wei2017) was aligned with the 10 reference sequences that were used for differentiation between *P. irregulare* and *P. cryptoirregulare* by Garzón *et al.*; Appendix A-Table A1). The isolate showed resemblance with *P. cryptoirregulare* at sites 55, 84, 100, 102, 106, 109, 160, 187, 777, 880 and 884-887. The sites are summarized in Table 3.4, including sites 821 and 896 that present additional differentiation sites that were not recorded by Garzón *et al.* (2007). Overall, *P. cryptoirregulare* isolate 13-32 showed the highest similarity with the *Pythium* candidate isolate that was introduced in this study.

**Table 3.4 Alignment with reference sequences for differentiation between *Pythium irregulare* (*P.i.*) and *Pythium cryptoirregulare* (*P.ci.*),where the differences in sequence are highlighted in grey**

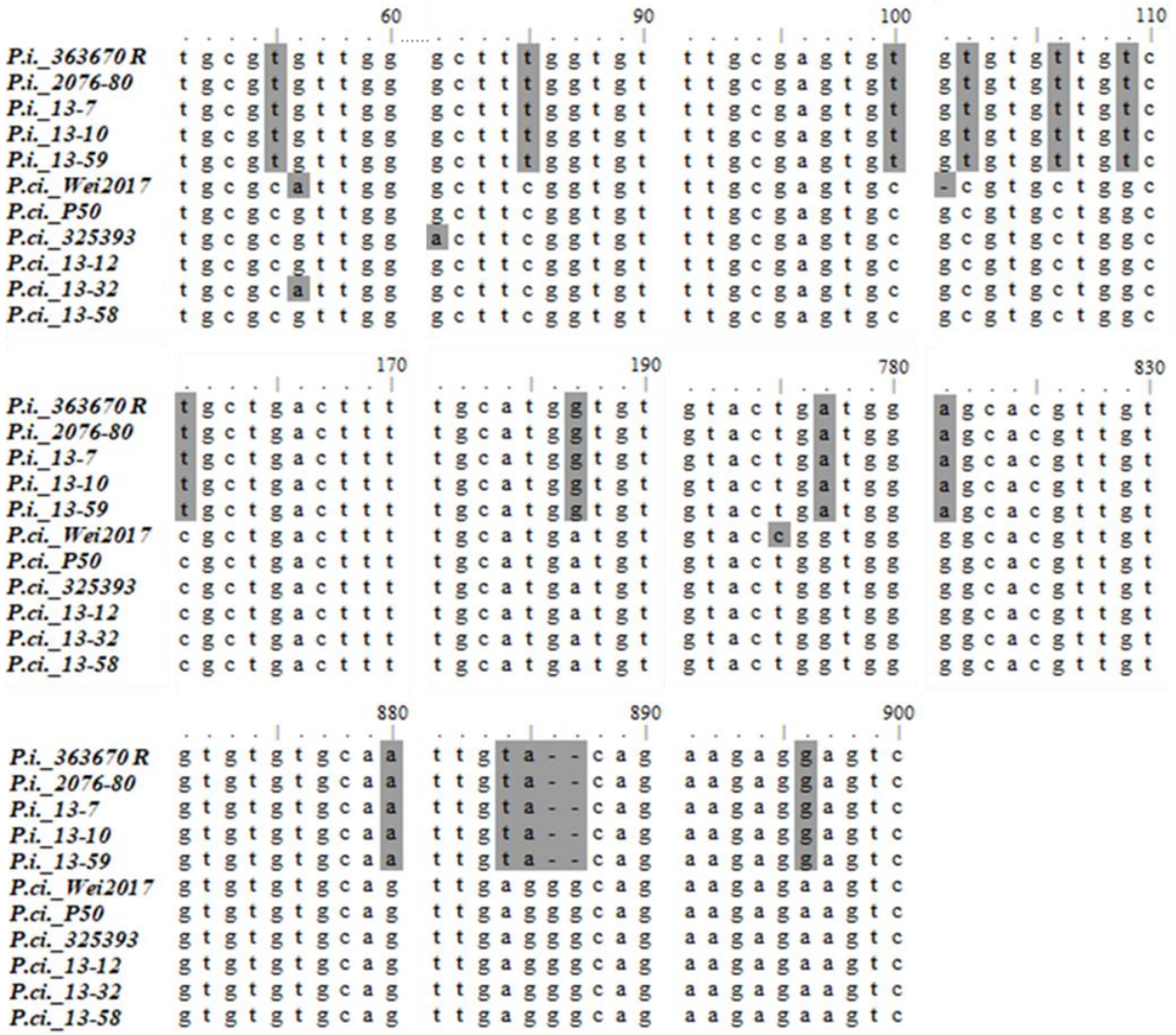


A phylogenetic tree was constructed with Mega X to visualize the relationships of the *Pythium* candidate isolate with the reference isolates (Figure 3.14). Both the alignment and the phylogenetic tree construction share the differentiation between *P. cryptoirregulare* and *P. irregulare*, and the *Pythium* candidate isolate was grouped with the species *P. cryptoirregulare*. The close relatedness of *Pythium cryptoirregulare* isolate 13-32 was also confirmed once more.

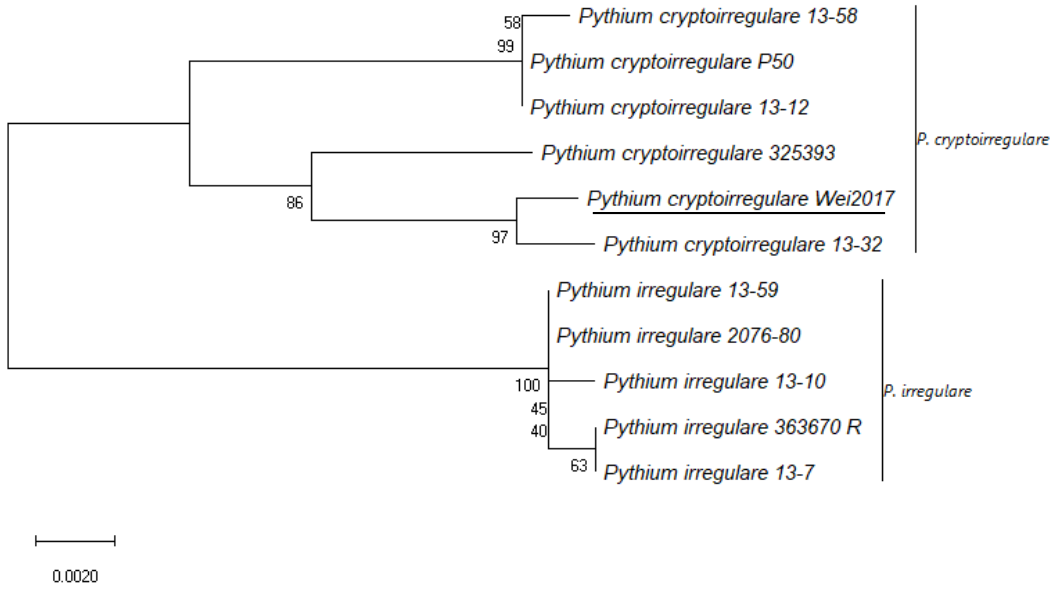


**Figure 3.14 Evolutionary relationships between the *Pythium irregulare* and *Pythium cryptoirregulare* taxa.** The evolutionary history was inferred using the Neighbor-Joining method (Saitou and Nei, 1987). The optimal tree with the sum of branch length = 0.04773988 is shown. The percentage of replicate trees in which the associated taxa clustered together in the bootstrap test (1000 replicates) are shown next to the branches (Felsenstein, 1985). The tree is drawn to scale, with branch lengths in the same units as those of the evolutionary distances used to infer the phylogenetic tree. The evolutionary distances were computed using the Maximum Composite Likelihood method (Tamura *et al*., 2004) and are in the units of the number of base substitutions per site. This analysis involved 11 nucleotide sequences. Codon positions included were 1st+2nd+3rd+Noncoding. All positions with less than 95% site coverage were eliminated, i.e., fewer than 5% alignment gaps, missing data, and ambiguous bases were allowed at any position (partial deletion option). There was a total of 844 positions in the final dataset. Evolutionary analyses were conducted in MEGA X (Kumar *et al.*, 2018). The *Pythium* isolate that was identified and examined in this study is underlined.

The phylogenetic tree in Figure 3.15 presents an indication of the potential evolutionary relationships of the *Pythium* candidate isolate with other isolates and species. Isolates that showed close relatedness in previous results and the strains of the F clade were included, as well as isolates from a different clade and different genus. The phylogenetic tree visualized the separation between taxa of the genera *Pythium* and *Phytophthora*. Also, the two separate branches leading towards the *Pythium ultimum* species and the remaining *Pythium* species indicated the relatively distant relationship between the F clade and the I clade. Moreover, besides other *P. cryptoirregulare* isolates in the F clade, *P. irregulare*, *P. cylindrosporum* and *P. regulare* are closest related according to the evolutionary relationship to the isolate.

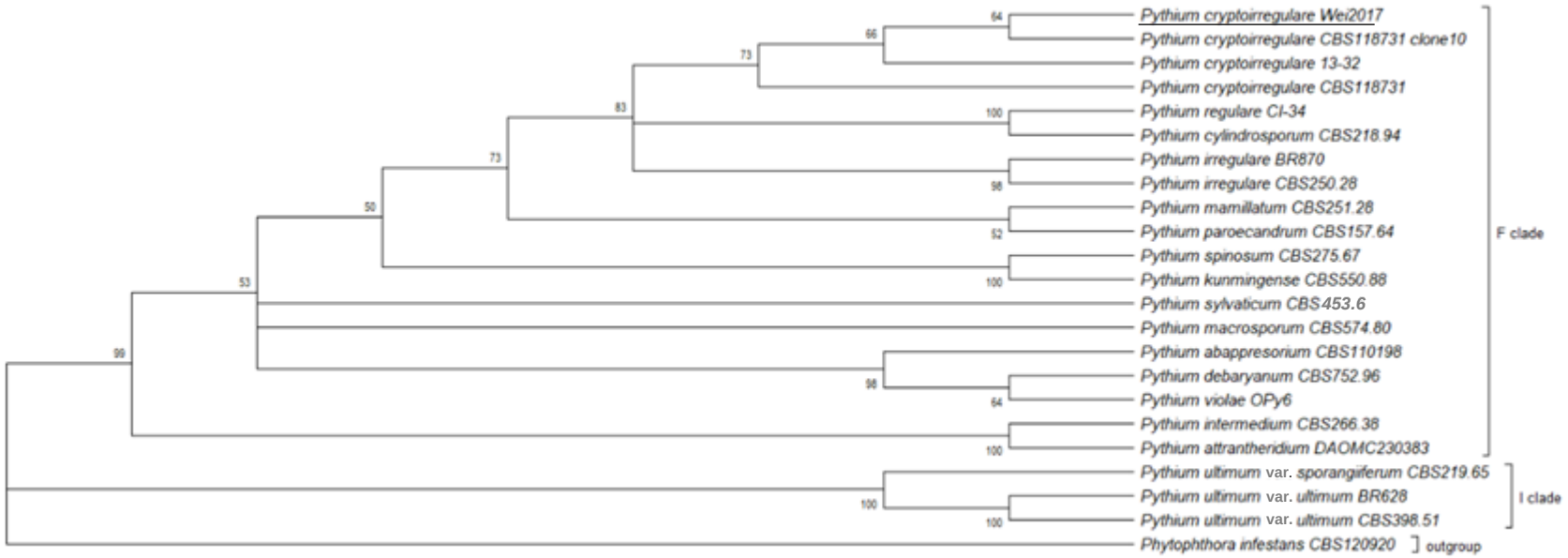


**Figure 3.15 Evolutionary relationships of *Pythium* taxa.** The evolutionary history was inferred using the Neighbor-Joining method (Saitou and Nei, 1987). The optimal tree with the sum of branch length = 0.72899411 is shown. The percentage of replicate trees in which the associated taxa clustered together in the bootstrap test (1000 replicates) are shown next to the branches (Felsenstein, 1985). The tree is drawn to scale, with branch lengths in the same units as those of the evolutionary distances used to infer the phylogenetic tree. The evolutionary distances were computed using the Maximum Composite Likelihood method (Tamura *et al*., 2004) and are in the units of the number of base substitutions per site. This analysis involved 23 nucleotide sequences. Codon positions included were 1st+2nd+3rd+Noncoding. All positions with less than 95% site coverage were eliminated, i.e., fewer than 5% alignment gaps, missing data, and ambiguous bases were allowed at any position (partial deletion option). There was a total of 701 positions in the final dataset. Evolutionary analyses were conducted in MEGA X (Kumar *et al*., 2018). The *Pythium* isolate that was identified and examined in this study is underlined.

## 3.4 Discussion

During the morphological characterization, PDA, CMA and RA were found to be most useful for structure induction, as seen in Figure 3.2. Potato dextrose agar was used in the interest of observing vegetative growth. On this medium, hyphal growth was slowly generated in a somewhat organized growth pattern with a lower mycelial density compared to the other media. The *Pythium* candidate exhibited coenocytic hyphal growth until septa were formed during hyphal degradation or when sexual reproduction was initiated (Figure 3.4). However, the latter and asexual reproduction were observed more abundantly on CMA medium. Either the CMA components or the lack of required nutrition in CMA induced the development of oospores and sporangia. The formation of oogonia and antheridia, the fertilization of these structures as well as oospore development were carefully captured, whereas sporangia were rarely detected. Therefore, spore release was not detected and thus not characterized. In his monography, van der Plaats-Niterink (1981) states that sporangia production itself is also species-specific and that *P. irregulare* rarely or never produces sporangia. Even though spores could not be characterized, appressoria formation was found in great abundance at the bottom of the RA where the hyphae came in contact with the polystyrene Petri dish. No appressoria were formed in glass Petri dishes, which suggests that the hydrophobic surface of the polystyrene Petri dish provided cues to act as a host substrate for infection. This surface substrate was nonetheless not a living host that could be infected, which resulted in extended appressoria formation after failed penetration attempts, as seen in Figure 3.10.

Moreover, the *Pythium* candidate showed high similarities with the reference species *P. irregulare* and fewer similarities with *P. ultimum* var. *ultimum*. This observation corresponds with the information provided by Lévesque & de Cock (2004), where *P. cryptoirregulare* was initially identified as *P. irregulare*, but later genetically re-identified by Garzón *et al.* (2007) as a new species. Growth patterns on media presented a visually identical development for the *Pythium* candidate and *P. irregulare*, while aerial hyphae development of *P. ultimum* var. *ultimum* deviated from them by forming clusters at random locations on the medium. Differences in reproduction structure development further confirmed that the *Pythium* candidate was closer related to *P. irregulare* than to *P. ultimum* var. *ultimum*. Due to the high variation and almost identical structures among the three species, minimal but crucial differences such as location of

the oospores, antheridia and oogonium characteristics and oospore plerocity were observed. A final clear difference was seen in the appressoria abundance on the polystyrene substrate. Again, the *Pythium* candidate and *P. irregulare* showed a similar number of appressoria, whereas *P. ultimum* var. *ultimum* formed visibly more appressoria, suggesting that this species may exhibit a more aggressive infection.

Molecular analysis confirmed the close relatedness of the *Pythium* candidate to *P. irregulare* once again, but also presented the distinction between the two and identified the candidate as *P. cryptoirregulare*. For all sequence sites that were used by Garzón *et al.* (2007) to differentiate between *P. irregulare* and *P. cryptoirregulare*, the *Pythium* candidate showed great resemblance with the *P. cryptoirregulare* isolates that were included in the alignment of this study. The phylogenetic tree construction with these *P. irregulare* and *P. cryptoirregulare* isolates (Figure 3.14) showed additional evidence as the *Pythium* candidate was grouped among the *P. cryptoirregulare* taxa. The phylogenetic tree shown in Figure 3.15 provides an indication of the candidate's relationships within the F-clade of the *Pythium* taxa. It confirms its identity, indicated by other *P. cryptoirregulare* isolates as its closest evolutionary relationships. This second phylogeny construction also corresponds to the phylogeny by Lévesque and de Cock, (2004) regarding the placement of *P. cryptoirregulare* in a subclade along with *P. regulare* and *P. cylindrosporum*.

In conclusion, the hypothesis of a *Pythium* species being the causal agent of the damping-off in *A. thaliana* was confirmed with morphological and molecular characterization when the pathogen was identified as *Pythium cryptoirregulare*. Morphological characterization and identification were only based on observations by microscope where the candidate could be differentiated from *P. ultimum* var. *ultimum*, but not from *P. irregulare*. The absence of statistical analyses for morphological characterization also limits the reliability of these observations. In contrast, the molecular analysis identified the candidate as a member of the *P. cryptoirregulare* taxa. Overall, the identification of this *Pythium* candidate highlights the importance of using both morphological as well as molecular techniques for the identification of the *Pythium* species.

# CHAPTER 4

## PATHOGENICITY AND INFECTION STRATEGIES OF *PYTHIUM CRYPTOIRREGULARE*

### 4.1 Introduction

*Pythium* is commonly known as the phytopathogen that causes damping-off, which is characterized by the collapse of emerging seedlings. Before these symptoms occur, this soil-borne pathogen infects its host, mostly through the root tissue, either through zoospores, mycelia or oospores (Sutton *et al.*, 2006), which is then followed by hyphal colonization and (a)sexual reproduction within the host to restart its life cycle and infect new hosts.

Chemical fungicides are most commonly used for prevention or control of these losses, even though these applications are limited in many ways. It is, therefore, essential to establish an understanding of the infection strategies of *Pythium* to target or interfere with the development and spread of these oomycete pathogens.

*Pythium* species are mainly described as necrotrophic pathogens (Laluk & Mengiste, 2010; Lévesque *et al.*, 2010; Adhikari *et al.*, 2013; Agrawal, 2018) that do not produce any specialized infection structures such as haustoria (Whisson *et al.*, 2007). On the other hand, Adie *et al.* (2007) showed that *P. irregulare* does develop haustoria-like structures after penetration of the host. Furthermore, specific temperature conditions allowed *P. aphanidermatum* and *P. dissotocum* to exhibit biotrophic characteristics during colonization of the host (Owen-Going *et al.*, 2008). These contradictory observations indicate that it is unclear whether all *Pythium* species follow a necrotrophic lifestyle. This study provides evidence of biotrophic characteristics, which contribute to a better understanding of the infection strategy of *P. cryptoirregulare* on the host *A. thaliana*. Prior to this study, *P. cryptoirregulare* had not been

reported as a natural pathogen of *A. thaliana*. This observation created new opportunities to study its infection mechanism further.

Histological approaches, such as live-cell imaging and fixed cell imaging, were used to illustrate the infection process and to determine whether *P. cryptoirregulare* follows a hemibiotrophic or a necrotrophic infection strategy. Intercellular hyphae were located in cells where the viability was indicated by plasmolysis and neutral red staining. Additionally, hyphal penetration, colonization and reproduction were also observed by fixing the infected tissue and staining it with fluorescent dye to visualize the distinctive phases of *P. cryptoirregulare* infection.

## 4.2 Materials and Methods

### 4.2.1 Plant and pathogen materials

**Host** – To assess the susceptibility to *P. cryptoirregulare* based on age, *A. thaliana* wildtype Col-0 was grown in growth chambers at 22 °C with a 16-h photoperiod and an approximate 55% RH on sterilized Sungro® Sunshine mix #1 soil in 3 ½ inch pots. The same host was used for observation of the primary host penetration and colonization, but due to the difficulty of detecting the exact time point of infection in soil, these *A. thaliana* seeds were germinated, grown and inoculated on ½ MSA at room temperature (23 °C). The primary infection was also observed in the GFP-tagged cell membrane lines "PMA-GFP" and "LTI6b-GFP", mainly to determine the colonization strategy of *P. cryptoirregulare* on a cellular level. Based on literature and observed growth inhibition, the plasmodesmata mutant "*PDLP1α-GFP*" and the three auxin insensitive mutants "*axr1-3*", "*axr4-2*" and "*aux1-7*" were tested for resistance against this pathogen.

**Isolate** – The previously collected isolate that was morphologically and molecularly identified as *Pythium cryptoirregulare* was maintained on either PDA, CMA or ½ MSA for inoculation purposes. The isolate was subcultured every two weeks to maintain a viable culture and was also subcultured on ½ MSA, specifically, 1.5 days before each inoculation time point to create inoculum with strong, actively growing mycelia.

### 4.2.2 Inoculation procedures

Several factors of inoculation were tested. First, seeding was staggered by planting *A. thaliana* Col-0 seeds 0.5, 3 and 7 days prior to inoculation based on establishing three different developmental stages of the seeds or seedlings upon inoculation. Fifty to 100 seeds were placed on sterilized Sungro® Sunshine mix #1 soil in approximately 9 cm pots and vernalized for four days at 4 ºC. After this vernalization, they were transferred to a growth chamber at approximately 22 ºC and an approximate 55% RH and organized according to a completely randomized design. All pots were inoculated in the centre of the pot at the same time with an agar plug of approximately 0.5 x 0.5 cm, containing actively growing mycelium from the edge of the culture where the mycelium was most viable. As a negative control, one pot remained

uninoculated and was placed in a separate dish inside the pot-holding tray to prevent contamination through the water from submerging the pots.

Moreover, to create favourable conditions for *Pythium* infection, the trays were covered with a plastic lid or each pot was separately covered with plastic foil or a plastic container to increase the humidity. Five pots, representing the different seedling stages upon inoculation and the negative control, were assessed per humidity treatment at approximately 10 days post-inoculation when this pathogen initiated no further disease development.

A similar method of inoculation was used for the seedlings that were grown on ½ MSA. However, only an incubation time point of 5 days was used for inoculation, and these seedlings were exclusively used for infection strategy observations. Inoculations of seedlings on ½ MSA were not used for pathogenicity testing due to the optimized growth conditions for *P. cryptoirregulare* by the medium, and therefore guaranteed infection success regardless of the age or stage of the seedling.

Lastly, *A. thaliana* Col-0 seedlings were also grown on ½ MSA for five days to be used as bait to observe the penetration of *P. cryptoirregulare*. The five-day-old seedlings were transferred to a Petri dish containing sterile water. Agar plugs with actively growing mycelia were added to this sterile water and incubated for one day at room temperature until the mycelia growth had reached the *Arabidopsis* bait.

### 4.2.3 Material preparation and microscopy techniques

Infected seedlings from all inoculation methods were removed, washed with sterile water, stained, if required, and observed using microscopy for a more detailed presentation of the individual infection.

#### 4.2.3.1 Live-cell staining and plasmolysis of *Pythium*-infected *Arabidopsis* seedlings

To differentiate between the biotrophic and necrotrophic hyphae of *P. cryptoirregulare*, cells were plasmolyzed by transferring infected *A. thaliana* Col-0 seedlings into a hypertonic solution (0.85 M KCl) for 5-10 min in which it was also mounted and stained with 5 µL 0.05% Neutral red (NR) that was added to the drop of KCl solution. This procedure was performed to collect evidence of the viability of the infected cells, indicated by the stained lysosomes and the cell's ability to undergo plasmolysis, despite the presence of hyphae.

Additionally, plasmolysis was also performed with infected transgenic *A. thaliana* lines expressing GFP-tagged plasma membrane markers “PMA-GFP” and “LTI6b-GFP” to clearly determine the locations of the (intact) plasma membrane and hyphal structures.

#### 4.2.3.2 Fixation and fluorescent staining of *Pythium*-infected *Arabidopsis* seedlings

After *P. cryptoirregulare* infected seedlings were extracted from the infested soil, they were transferred to fixation buffer (30% chloroform, 60% methanol and 10% acidic acid, v/v) for fixation of the sample. After the solution was refreshed twice, rehydration of the sample was conducted by replacing the solution by 95%, 70%, 50%, 30% and 0% ethanol, respectively, residing in each solution for an hour.

Staining procedures that were tested for the observation of the infected seedlings under the LSM 510 confocal microscope included the following: Trypan blue staining as described by Bhadauria *et al.* (2010) where samples were stained by 0.5% trypan blue in $H_2O$ overnight, followed by destaining twice with $H_2O$ for an hour, respectively; an aniline blue staining, also according to Bhadauria *et al.* (2010), staining the samples overnight in aniline blue dissolved in 150 mM $KH_2PO_4$, but in concentrations of 0.01%, 0.05%, 0.5% or 1% as described by Díez-Navajas *et al.* (2007). This procedure was repeated with identical aniline blue concentrations but dissolved in 0.067 M $K_2HPO_4$, as described by Hood & Shew (1996). Either staining method was followed by destaining twice for an hour with its corresponding $KH_2PO_4$ or $K_2HPO_4$ solution; overnight calcofluor white (CFW) staining (1% CFW in 150 mM $KH_2PO_4$) after which the samples were destained for an hour, twice, with $KH_2PO_4$; Alexa Fluor®633 conjugate of wheat germ agglutinin (WGA; Life Technologies) staining, which included staining the sample for 15 minutes with 5.0 µg/mL of Alexa Fluor®633 dissolved in $H_2O$, followed by washing twice with $H_2O$.

All stained seedlings were mounted on glass slides in either 30% glycerol or $H_2O$ and observed under the LSM 510 or LSM 710 confocal microscope, focussing on penetration sites and internal colonization to determine whether *P. cryptoirregulare* follows a necrotrophic or hemibiotrophic infection style.

#### 4.2.3.3 Light microscopy

Firstly, *Arabidopsis thaliana* seedlings that were inoculated in sterile water using the baiting technique were observed under the fluorescence microscope (Zeiss Axioplan) without any fixation or staining treatment. Here, the main focus was the initial penetration of the pathogen into the epidermal layers of the host tissue. Secondly, the primary colonization, as well as the secondary colonization, were observed in the infected plasmolyzed and NR-stained seedlings. These infected *A. thaliana* seedlings were either taken from inoculated soil or ½ MSA. All treated and untreated seedlings were observed under a 10 to 63X magnification. After photos were taken with the Axioplan microscope camera, the photos were processed and analysed using Fiji (ImageJ, 1.52s), and Adobe Photoshop (CS4) if necessary.

#### 4.2.3.4 Confocal microscopy for fluorescence visualization

Trypan Blue staining was visualized using the LSM 510 meta confocal laser-scanning microscope (Zeiss Confor2, 2005) at a 514 nm fluorescence excitation of the Argon laser with a 38.1% intensity and a >650 nm LP emission filter, whereas aniline blue staining was observed with the same microscope, but at a 405 nm fluorescence excitation of the Diode laser with a 38.6% intensity through a 505-530 nm BP emission filter. Magnifications of 25X or 63X were used to observe the samples.

In contrast, the Alexa Fluor® 633-stained tissue was observed at a 488 nm excitation of the Argon laser with a 6.5% light intensity and a 493-598 emission filter under the LSM 710 confocal microscope (AxioObserver Z1) for the detection of the GFP-tagged membranes in the infected PMA-GFP and LTi6b-GFP *A. thaliana* seedlings. A second channel at an excitation of 633 nm with a 3.0% light intensity and 638-747 emission filter was used for the detection of the Alexa Fluor® 633 staining of the hyphae. Only a 40X magnification was used for observations of these infected tissues.

All pictures that were taken with either of the microscopes were processed and analysed using Fiji (ImageJ, 1.52s), and Adobe Photoshop (CS4) if necessary.

### 4.2.4 Mutant and host-specific screening for resistance

A selected collection of *A. thaliana* mutants and the *Brassica napus* cultivar (cv.) “Westar” were screened for resistance in other pathosystems. *PDLP1α-GFP*, an *A. thaliana* plasmodesmata

mutant, was screened for resistance, focussing on the potentially reduced colonization of neighbouring host cells through the plasmodesmata after the primary infection phase. Auxin-insensitive mutants *axr1-3*, *axr4-2*, *aux1-7* were also tested for increased resistance, as the metabolite secretion of *P. cryptoirregulare* might have less effect on these seedlings and can therefore not prolong the seedling stage for a greater infection success. Fifty to 100 seeds of these mutants or up to five *B. napus* "Westar" seeds were placed on autoclaved Sungro® Sunshine mix #1 soil in 3 ½ inch pots and vernalized for four days at 4 ºC after which they were transferred to a growth chamber at approximately 22 ºC and an approximate 55% RH. The seedlings in the pots were then inoculated in the centre at seven days post-seeding and observed and photographed five days later.

## 4.3 Results

### 4.3.1 Sensitivity of *Arabidopsis thaliana* to *Pythium cryptoirregulare*

Covering the pots separately with plastic foil appeared to be the most effective inoculation method. This way, high humidity was retained inside and not lost when another pot was inoculated. Also, inoculating with cubes of agar containing mycelia was the most efficient way to inoculate as it was difficult to detach the pure mycelia from the liquid cultures. The inoculation results confirmed that *Pythium* targets seedlings (Figure 4.1). When inoculated at 0.5 days post seeding (dps), seed germination was partially prevented, and seedlings showed no resistance to the pathogen. When inoculated at 3 dps, partial resistance was observed among the seedlings, and when the seedlings were inoculated 7 dps, seedlings showed increased resistance to the pathogen. According to this inoculation method, *P. cryptoirregulare* has the highest infection success up to 7 dps during the early seedling stage. However, the humidity had a significant influence on the overall infection of this pathogen. An increase in humidity resulted in increased susceptibility to the pathogen, including seedlings of seven days or older.

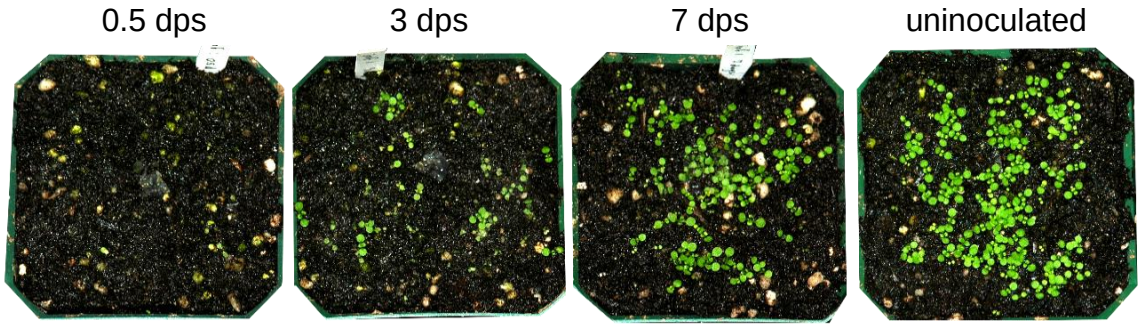


**Figure 4.1 Disease development of *Arabidopsis thaliana* seeds and seedlings after inoculation with *Pythium cryptoirregulare* at time points 0.5, 3 and 7 days post-seeding (dps).** Photos of the pots were taken 10 days post-inoculation when no further disease development was observed.

Interestingly, reduced seedling development, specifically in the roots, was observed over time in the presence of *P. cryptoirregulare* prior to infection and in older, resistant seedlings. This inhibition suggested that *P. cryptoirregulare* secretes metabolites that prevent root growth and possibly seed germination. This discovery created an opportunity to investigate the metabolic activity of this pathogen and related species, which formed an additional research objective.

### 4.3.2 Colonization and reproduction on *Arabidopsis thaliana*

*Pythium cryptoirregulare* is well-known for root infections, which was repeatedly confirmed during this study. However, only hyphal infection was observed. Within one day after *A. thaliana* seedlings were placed as bait in sterile water containing *P. cryptoirregulare* mycelia, several penetration sites were observed under the light microscope (Figure 4.2). This rapid infection lead to the assumption that *P. cryptoirregulare* is a very aggressive pathogen towards *A. thaliana*.

The penetration sites were indicated by the hyphal swellings on the outside of the epidermal cells of the host tissue (Figure 4.2A, left). Moreover, surrounding cells often showed abnormalities in size and shape (Figure 4.2A, right), root hair development was induced, and inhibited growth in the elongation zone was also observed. Figure 4.2B shows infection by the pathogen in the epidermal cells (left) as well as the root hairs (right). Neutral red was only capable of staining the external hyphae outside the host tissue and hyphae development close to the penetration site.

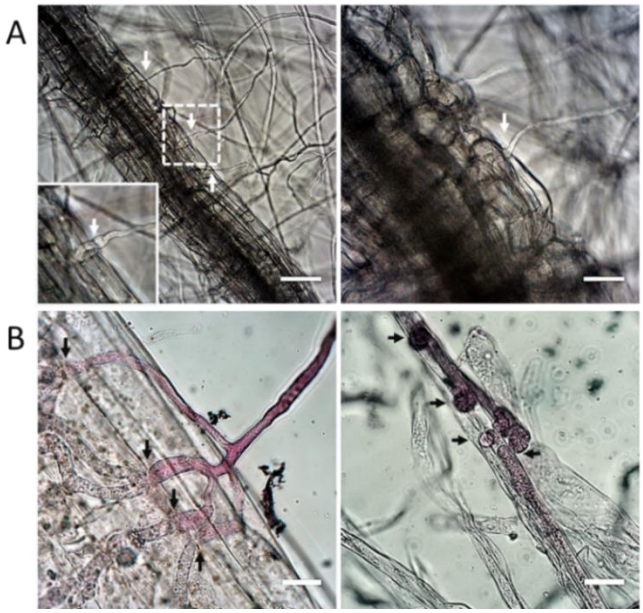


**Figure 4.2 Infection of the root tissue of *Arabidopsis thaliana* seedlings after inoculation with *Pythium cryptoirregulare*.** Photos were taken of living host tissues using the Axioplan fluorescence microscope, 1.5 days post-inoculation in sterile water at room temperature (23 ºC). Penetration sites are indicated by the arrows. **A**. Untreated *A. thaliana* seedlings of which on the **left**, three penetration sites of the epidermal cells are shown, indicated by the hyphal swelling on the outside of the host tissue which is shown in the enlarged boxed area. On the **right**, a single penetration site of an epidermal cell is shown, surrounded by abnormally swollen host cells. **B**. Neutral Red stained *A. thaliana* seedlings of which on the **left**, four penetration sites of the epidermal cells are shown, indicated by the hyphal swelling on the outside of the host tissue and the loss of staining effectiveness of the hyphae inside the host tissue. On the **right**, four penetration sites of the root hair are shown. Scale bars= 100µm (**A**, **left**), 50 µm (**A**, **right**) and 20 µm (**B left**/**right**).

Of the staining methods that were tested, 0.05% aniline blue in 150 mM $K_2HPO_4$ appeared to be the most effective for staining the internal hyphal structures. The staining visualized *P. cryptoirregulare* during in-plant colonization. This colonization initially started with the development of biotrophic primary hyphae that had a large diameter and were either intercellular or intracellular, and often grew parallel to the vascular system (Figure 4.3). This biotrophic development then switched to necrotrophic secondary hyphae that were narrower and entirely intracellular. Boxes in Figure 4.3 highlight a site where a necrotrophic hypha penetrated the cell wall, indicated by a hyphal swelling.

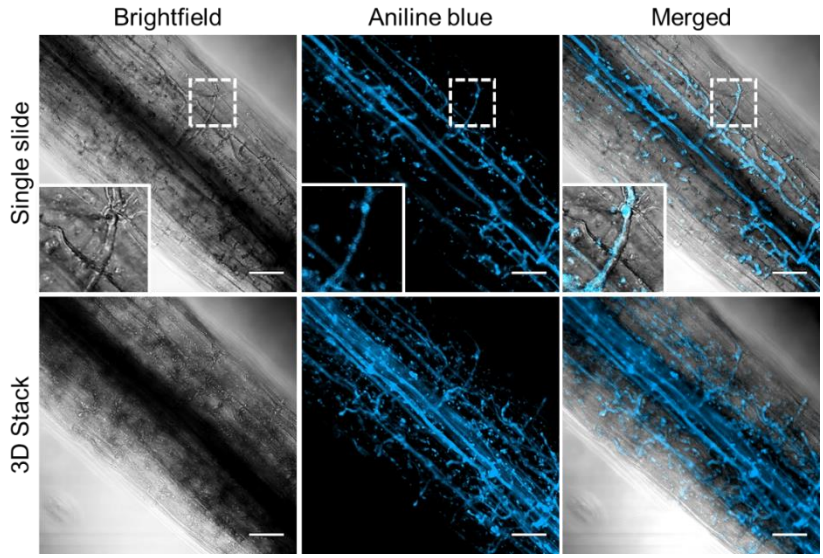


**Figure 4.3 Colonization of *Pythium cryptoirregulare* within *Arabidopsis thaliana* hypocotyl tissue associated with intracellular and intercellular hyphae.** Photos were taken of fixed and aniline blue-stained host tissues using the brightfield setting and the Diode laser (405 nm with a 38.6% intensity through a 505-530 nm BP emission filter) of the LSM 510 meta confocal microscope, five days post-inoculation in soil at approximately 22 ºC and 100% RH. The **top row** presents a 2D image of the interior of colonized hypocotyl tissue, emphasizing on the intracellular hypha which is shown in the enlarged boxed area. The **bottom row** presents a 3D image of the hypocotyl tissue in which several intercellular hyphae can be observed parallel to the vascular system of the host. Scale bars = 50 µm.

One of the rarer observations that were seen after infection were hyphal structures exiting the host and re-entering the host shortly after. Figure 4.4 shows two sites where this rare event occurred, but the reason for this event is yet unknown as there did not seem to be any interaction with environmental factors involved before it re-entered the same cell.

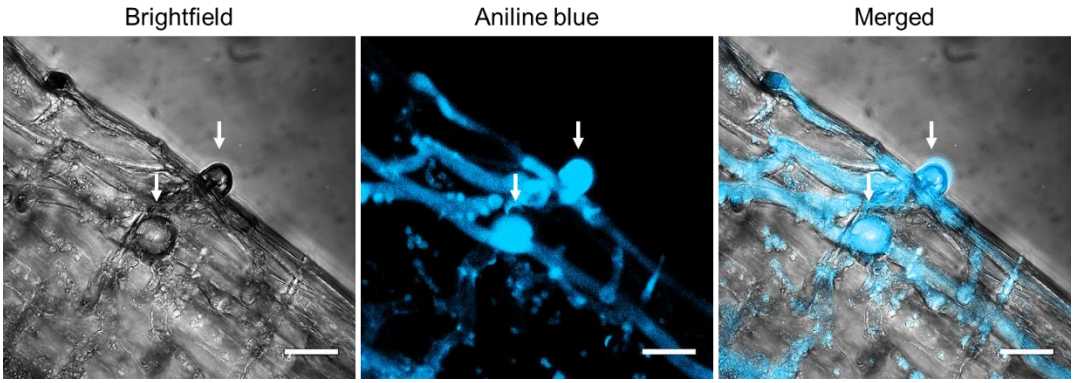


**Figure 4.4 *Pythium cryptoirregulare* hyphae exiting and re-entering *Arabidopsis thaliana* root tissue.** Photos were taken of fixed and aniline blue-stained host tissues using brightfield setting and the Diode laser (405 nm with a 38.6% intensity through a 505-530 nm BP emission filter) of the LSM 510 meta confocal microscope, five days post-inoculation in soil at approximately 22 ºC and 100% RH. The image is a 3D composition based on the maximum pixel intensity and the arrows indicate the sites where the hyphal exit- and immediate re-entrance occurred. Scale bars = 20 µm.

Two to three weeks post-inoculation, oospore development was observed in the hypocotyl of the infected *A. thaliana* seedlings that showed severe damping-off symptoms (Figure 4.5). This reproductive stage can be triggered by nutrient deficiency after a seedling has been severely infected with *P. cryptoirregulare* for several weeks. The pathogen will then develop resting spores for its survival within a dying host.

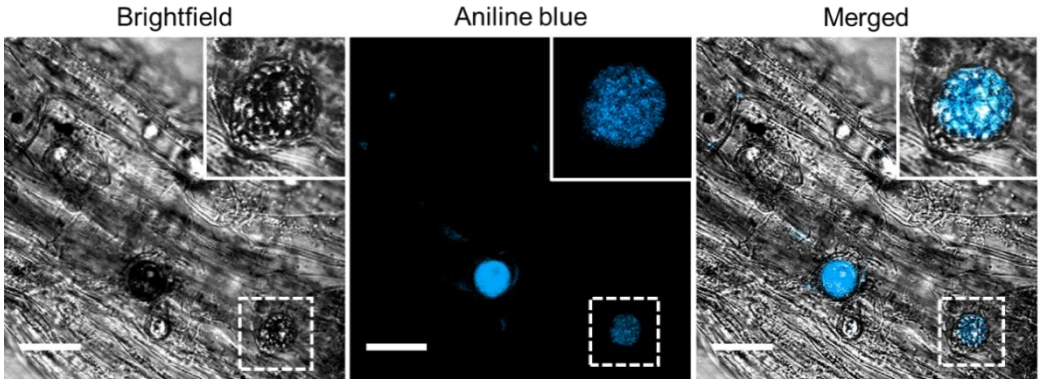


**Figure 4.5 *Pythium cryptoirregulare* oospore development inside *Arabidopsis thaliana* host tissue.** Photos were taken of fixed and aniline blue-stained host tissue using brightfield setting and the Diode laser (405 nm with a 38.6% intensity through a 505-530 nm BP emission filter) of the LSM 510 meta confocal microscope, 2-3 weeks post-inoculation in soil at approximately 22 ºC and 100% RH. The image is a 3D composition of summed slices which emphasizes an oospore in the enlarged boxed area. Scale bars = 20 µm.

Finally, sites where hyphae exit the host tissue without re-entrance were also observed in infected seedlings (Figure 4.6). Whereas the swelling of entering hyphae upon penetration was found on the outside of the host tissue, a swelling of these hyphae was also found on the inside of the epidermal layer, suggesting that these hyphae finalized their internal colonization and were therefore exiting the host to potentially infect neighbouring hosts.

Figure 4.6 shows exiting hyphae through root tissue (A), root hairs (B), and hypocotyl epidermal cells, respectively. The hyphal growth exiting through the root tip is the most interesting of all, as this hypha is clearly able to grow through all cell layers of the root tip, including the pericycle, endodermis, cortex and the epidermis before the saprophytic hypha exits the host. When focusing on the epidermal layers separately, several stages of the penetration become visible from the intercellular hypha in the inner body of the epidermal cell to the penetration site of the epidermal cell, and the surface of the epidermal cell (C). Possibly the pathogen exits the host for infection of neighbour hosts or reproduction outside the host tissue.

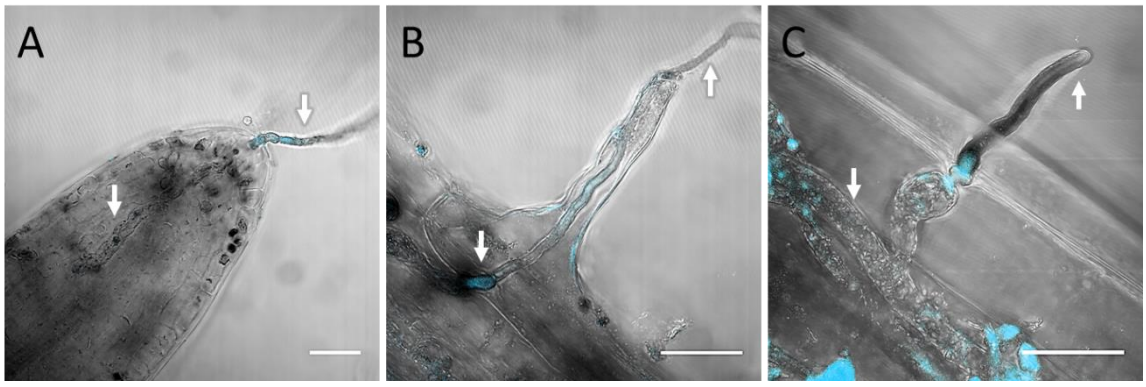


**Figure 4.6 *Pythium cryptoirregulare* hyphae exiting *Arabidopsis thaliana* tissues by penetration of epidermal surface** Photos were taken of fixed and aniline blue-stained host tissues using brightfield setting and the Diode laser (405 nm with a 38.6% intensity through a 505-530 nm BP emission filter) of the LSM 510 meta confocal microscope, five days post-inoculation in soil at approximately 22 ºC and 100% RH. The left arrow in each photo indicates internal hyphal development and the right arrow indicates external hyphal development. Photos were taken by focusing on the root tip (A), the root hair (B) and the epidermal surface of the hypocotyl (C), respectively. Scale bars = 20 µm.

### 4.3.3 Hemibiotrophy versus necrotrophy

During plasmolysis and staining with neutral red of the *P. cryptoirregulare* infected *A. thaliana* seedlings, plasmolysis and staining were most successful in the roots and cotyledons, respectively, whereas hypocotyl cells often remained unplasmolyzed and unstained.

Figure 4.7 shows two colonization sites (A and B) of plasmolyzed and stained mesophyll cells in the cotyledons. In the first site (A), a single hypha was observed entering the cell and dividing the cytoplasm in two, which is emphasized in the two different levels presented in the figure. Interestingly, the cell membrane remained intact during this colonization, indicated by the ability of the cell to undergo plasmolysis after infection. The neutral red uptake also shows that the cell is still viable. These observations suggest that the hypha exhibits a biotrophic interaction with the host cells.

Another biotrophic interaction was seen in the second site (B), where a hypha entered and exited a cell, also leaving the membrane intact. It was observed that a hypha residing inside the host is not capable of taking up neutral red staining, whereas external hyphae stain pink. The site presented in the figure highlights the entrance of the hypha into the cell, and the internal unstained hyphal growth and external stained hyphal growth. Yet again, the cell was able to be plasmolyzed after this colonization, and the cytoplasm was stained by neutral red, providing more evidence for a biotrophic interaction between *P. cryptoirregulare* and *A. thaliana*.

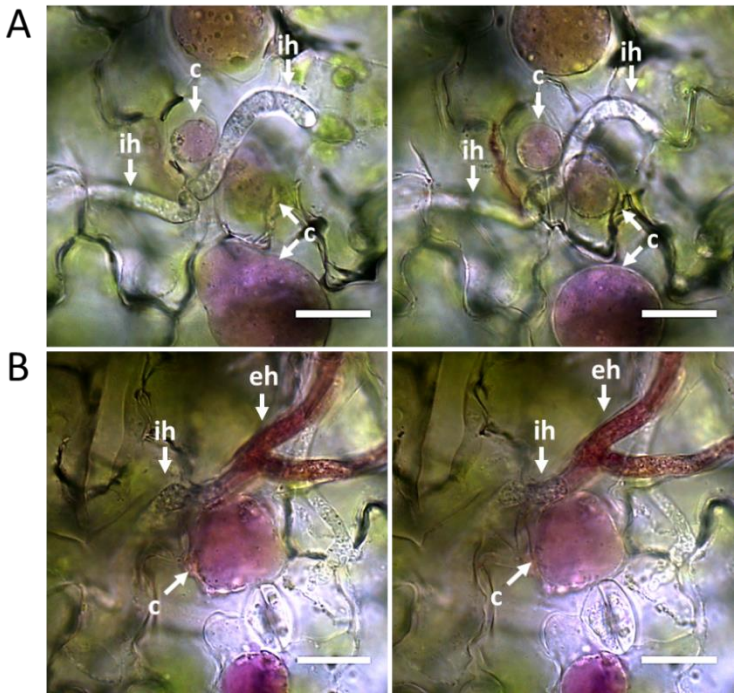


**Figure 4.7 Plasmolyzed and neutral red-stained *Arabidopsis thaliana* cotyledon cells infected by *Pythium cryptoirregulare*.** Photos were taken of living host tissues using the Axioplan fluorescence microscope, approximately seven days post-inoculation in soil at approximately 22 ºC and 100% RH. c = cytoplasm, ih = internal hyphae, eh = external hypha. **Left** and **right** pictures represent different levels inside the host tissue emphasizing on the hypha entering the cell (**left**) and further development (right). **A.** Entirely internal hyphal development causing division of cytoplasm. **B**. A hypha entering a neighboring cell and exiting the host tissue through a plasmolyzed cell. Scale bars = 20 µm.

Further examination of the infected seedlings revealed even more contradictory evidence about the assumed necrotrophic lifestyle of *Pythium*. In the root tissue, many sites were discovered where *P. cryptoirregulare* hyphae were surrounded by viable host tissue (Figure 4.8). The abundant viability of these neighbouring cells implies the absence of lytic enzymes for cell wall- and cell membrane degradation, which is typical for a necrotrophic infection strategy. The colonization sites that are shown in Figure 4.8A and B present plasmolysis and staining next to hyphae in the primary colonization stage, whereas other images show plasmolysis and staining at an infection site in the root hair (C) and during secondary colonization (D). These occurrences increase the likelihood of a biotrophic interaction.

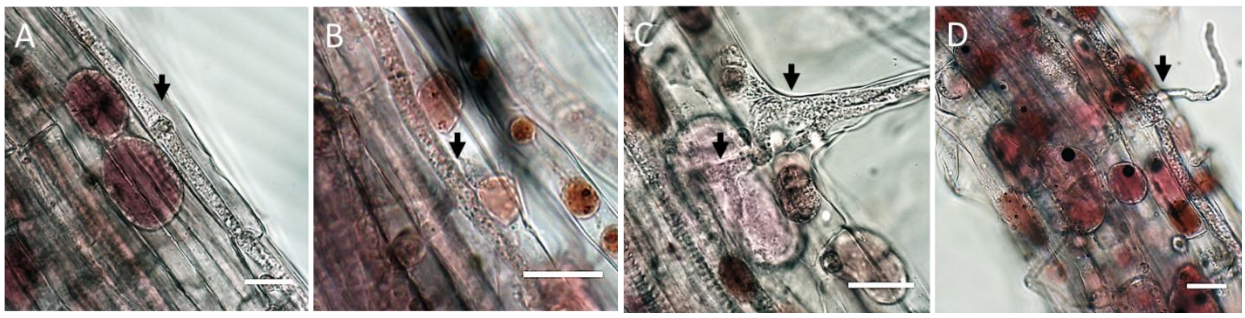


**Figure 4.8 Plasmolyzed and neutral red-stained *Arabidopsis thaliana* root cells surrounded by *Pythium cryptoirregulare* hyphae**. Photos were taken of living host tissues using the Axioplan light microscope, approximately seven days post-inoculation in soil at approximately 22 ºC and 100% RH. The arrows indicate the hyphae inside the host tissue. **A**. Infected epidermal cells with plasmolyzed neighbour cells. **B**. Surface contact between an internal hypha and the cytoplasm of plasmolyzed cells. **C**. Plasmolysis after the initial infection via the root hair. **D**. Plasmolyzed root tissue after colonization by a hypha that developed a branch for exiting the host tissue. Scale bars = 20 µm (**A**, **B** and **C**) and 50 µm (**D**).

More viable infected cells were also visualized by the GFP-tagged plasma membranes in the PMA-GFP and LTI6b-GFP *A. thaliana* marker lines. The clearest GFP expression was found in PMA-GFP, where a combination of the brightfield setting and the Argon laser (488nm) provided an image showing the infecting hyphae as well as the intact GFP-tagged plasma membranes. Figure 4.9 presents both these features. As seen in the brightfield image, after swelling in the neighbour cell, this hypha entered the cell that is shown in the centre of the image. The brightfield also shows the location of the cell wall of this cell, which is not aligned with the plasma membrane that is visualized by green fluorescence, meaning that plasmolysis had occurred and that this cell is also still viable after infection.

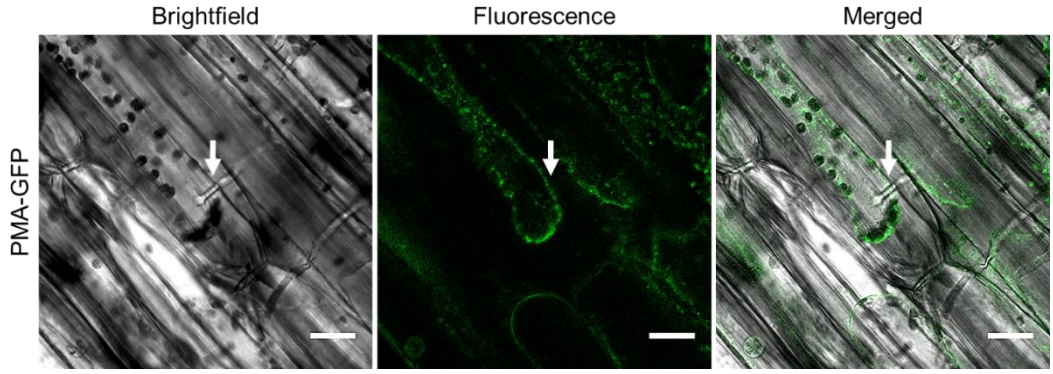


**Figure 4.9 Plasmolysis and GFP expression in the hypocotyl of the *Arabidopsis thaliana* plasma membrane marker line PMA-GFP after hyphal infection by *Pythium cryptoirregulare.*** Photos were taken of living host tissue using the brightfield setting and the Argon laser (488 nm through a 505-530 nm BP emission filter) of the LSM 510 meta confocal microscope, six days post-inoculation in soil at approximately 22 ºC and 100% RH. The arrows indicate the infection site of the hypha into the cell. Scale bars = 20 µm.

The plasma membrane-tagged marker lines were also used in combination with the Alexa Fluor®-633 staining. It was discovered that the staining was only successful in host cells that were heavily colonized (Figure 4.10). Other cells, where no hyphae or a single hypha was present, showed only GFP expression of the plasma membranes and an equal green fluorescence surrounding the hyphae. Potentially, this presents a difference between the characteristics of the hyphae or the viability of the cell in which they are located. The green fluorescence seen in the centre of the viable cells could, therefore, be the intact plasma membrane surrounding the hyphae.

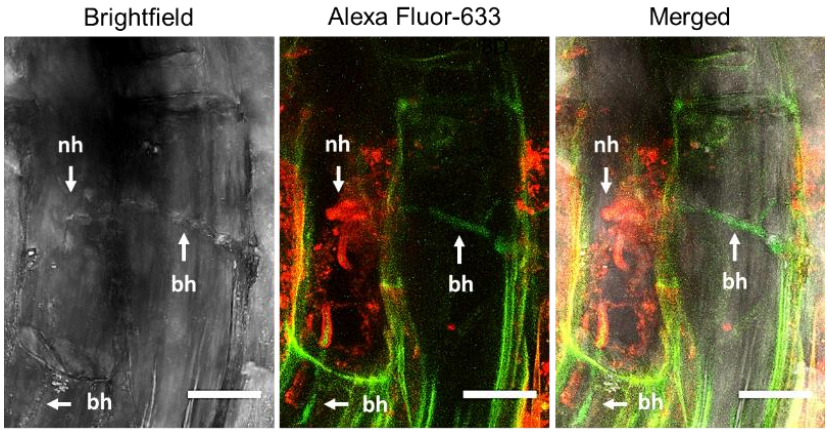


**Figure 4.10 *Arabidopsis thaliana* plasma membrane marker line LTI6b-GFP infected by *Pythium cryptoirregulare* hyphae.** Photos were taken of living hypocotyl host tissues stained by Alexa Fluor-633 and visualized using the using the brightfield setting and Argon laser (488nm excitation with a 6.5% light intensity and a 493-598 emission filter) of the Zeiss LSM 710 confocal microscope, six days post-inoculation in soil at approximately 22 ºC and 100% RH. Necrotrophic hyphae (nh) are indicated by red fluorescence due to Alexa Fluor staining in dead host cells, whereas biotrophic hyphae (bh) are indicated by their green fluorescence due to the inability of Alexa Fluor to stain hyphae in viable cells. Scale bars = 20 µm.

### 4.3.4 Resistance against *Pythium cryptoirregulare*

No resistance was found in either the plasmodesmata mutant *PDLP1α*-GFP or *B. napus* "Westar" variety. Furthermore, the auxin-insensitive mutants also showed no to very little resistance after inoculation (Figure 4.11). Seedlings were either degraded or collapsed (damping-off), while in both situations, the seedlings were covered by an abundance of *P. cryptoirregulare* mycelia. However, two *axr4-2* seedlings were found showing no damping-off symptoms. Whether these seedlings exhibit resistance against infection or were located outside the infected area is unclear. The latter seems unlikely considering the heavily infested soil and seedlings surrounding these "healthy" individuals. These seedlings were also infected at a later seedling age due to the location of the seedlings and the location of inoculation.

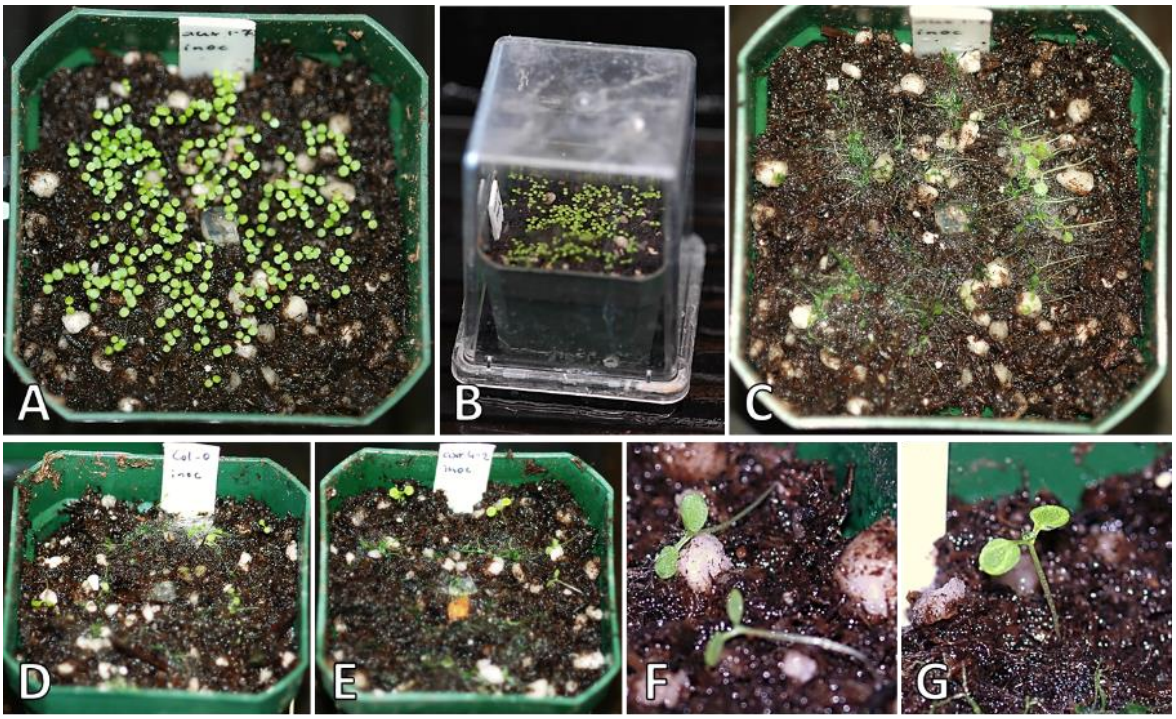


**Figure 4.11 *Arabidopsis thaliana* mutant screening for resistance against *Pythium cryptoirregulare* hyphae.** Photos of the seedlings were taken five days after inoculation of the 7-day-old seedlings. **A**. Fifty to a hundred *aux1-7* seedlings at point of inoculation. **B**. Incubation set-up after inoculation. **C**. *Pythium cryptoirregulare* disease development in *aux1-7*, five days post-inoculation, showing complete seedling death. **D**. *Pythium cryptoirregulare* disease development in Col-0, showing complete seedling death. **E**. *Pythium cryptoirregulare* disease development in *axr4-2* showing seedling death, seedlings with damping-off symptoms, and two seedlings without disease symptoms. **F**. Enlarged image of the *axr4-2* seedlings that are showing damping-off symptoms. **G**. Enlarged image of a seedling showing no signs of disease.

## 4.4 Discussion

This study demonstrates for the first time that *P. cryptoirregulare* is a natural pathogen of *A. thaliana*. The pathogen was discovered when an organism caused obvious damping-off symptoms in *A. thaliana* in the greenhouse, and was identified as *P. cryptoirregulare.* After its identification and characterization, its infection strategy was carefully studied using a histopathological approach.

*Pythium* is known to cause damage mostly to seedlings and less severe damage to adult hosts (Hancock, 1983). This pattern was also observed during the current study because an increase in seedling age coincided with increasing resistance against *Pythium* infection (Figure 4.1). This increase in resistance, most notable in seven-day-old seedlings, suggests that the infection of *P. cryptoirregulare* is most successful during an early seedling stage, likely due to the lack of enzymes to degrade suberized host material (Van Buyten & Höfte, 2013; Kamoun *et al.*, 2015). This finding highlights the importance for virulence of this opportunist to infect before cell wall and cuticle fortifications.

During this study, only hyphal infection was observed due to the inability to inoculate with a spore suspension. When *P. cryptoirregulare* managed to establish infection in the younger seedlings, penetration sites were recognized by the swelling of the hyphae before entering the host tissue. These swellings resembled the appressoria that were observed in contact with the hydrophobic surfaces during the morphological characterization described in Chapter 3. After assessing these penetration sites in the root tip, root hairs, and hypocotyl, the main focus of the infection assessment was the colonization of host cells.

*Pythium* species are mostly described as oomycetes that follow a necrotrophic lifestyle (Laluk & Mengiste, 2010; Lévesque *et al.*, 2010; Adhikari *et al.*, 2013). However, evidence collected in this study contradicts this lifestyle for *P. cryptoirregulare.* Two distinct types of hyphae were observed during the colonization of *P. cryptoirregulare* in the host *A. thaliana*. Visualized through aniline blue staining, this colonization initially started with the development of biotrophic primary hyphae that had a large diameter and were either intercellular or intracellular and often grew parallel to the vascular system. After this biotrophic phase, necrotrophic secondary hyphae were developed that were narrower and entirely intracellular

(Figure 4.3). Colonization of the vascular tissues has been observed in *P. irregulare* in previous studies as well, without clear necrotrophic or biotrophic characteristics (Adie *et al.*, 2007).

Additionally, the ability of the cells to undergo plasmolysis while hyphae colonization was present inside the cells or in surrounding cells (Figure 4.7-4.9) also suggested a biotrophic phase as necrotrophs are known to secrete lytic cell-wall degrading enzymes that kill host cells prior to entering (Walton, 1996). If these infected cells or surrounding cells had been affected by such enzymes, cells would lose their viability. Plasmolysis and cytoplasm staining by neutral red would thus not have been observed.

Lastly, when infected LTI6b-GFP seedlings were stained with Alexa Fluor®-633 staining, only hyphae in host cells that were heavily colonized were stained (Figure 4.10). No Alexa Fluor®-633 staining was detected in the surrounding cells that were colonized by a single hypha, which were visible by the GFP fluorescence, as well. This event could be explained by either the state of the infected host cell or the state of the hyphae. There could be a difference in viability of the cell. The cell in which the Alexa Fluor-stained hyphae reside was heavily colonized, and this cell likely lost its viability. This could have allowed the stain to be absorbed by the host tissue, while the composition of intact viable cells might have prevented staining. Furthermore, Green et al. (1995) and O'Connell & Ride (1990) observed the inability of lectin WGA to bind to the EHM or IFM. *Pythium cryptoirregulare* possibly developed IFM around the primary intracellular hyphae which prevented the Alexa Fluor®633 conjugate of WGA to bind to these hyphae. In contrast, the secondary hyphae, which were not surrounded by an IFM, could be stained. Nevertheless, both these explanations indicate biotrophic colonization.

Unfortunately, no resistance of *A. thaliana* seedlings was found in the lines that were tested in this study. *Arabidopsis thaliana* mutants *PDLP1α*-GFP, *axr1-3*, *axr4-2* and *aux1-7* and the *B. napus* cv. Westar all showed damping-off symptoms followed by seedling death. Only two *axr4-2* seedlings without damping-off symptoms were found and remained viable. However, as these seedlings resided in the outer areas of the infection, it is uncertain if these seedlings were either resistant due to their mutation, or if they were at a later seedling stage upon infection and therefore able to prevent infection by suberization of the host tissue.

# CHAPTER 5

## AUXIN-LIKE METABOLITE EXTRACTION AND CHARACTERIZATION FROM *PYTHIUM CRYPTOIRREGULARE*

### 5.1 Introduction

Metabolite secretion is one of the features that differentiates different lifestyles of a pathogen. While necrotrophs are known for their secretion of toxins and cell-wall degrading enzymes to promote host cell death, biotrophs can secrete metabolites to intervene in the host response to keep their host alive (Centis *et al.*, 1997; Kahmann & Basse, 2001).

During the initial inoculations to study the infection strategy of *P. cryptoirregulare*, a reduction in seedling development was observed among the *A. thaliana* seedlings, prior to infection. Therefore, it was hypothesized that growth-inhibiting metabolites were being secreted into the growth medium before penetration of the host. Especially after observing a reduced root growth, the involvement of auxin was a logical option, because it has been recorded in multiple studies that *Pythium* species can produce IAA (Blok, 1973; Rey *et al.*, 2001; Gravel *et al.*, 2007; Benhamou *et al.*, 2012; Ludwig-Müller, 2015; Mittag *et al.*, 2015). However, there are only a few *Pythium* species known to produce IAA without adding precursors of IAA to the growth medium, and *P. ultimum* has also been reported to secrete toxins, resulting in very similar symptoms to IAA.

To investigate the biological activities of the metabolites, a standard procedure was designed to isolate the filtrate, containing the metabolites, from the liquid cultures. After the media conditions were optimized for these liquid cultures, the culture filtrates (CF) were first tested to determine which effect undiluted filtrate had on *A. thaliana* seeds and seedlings. Culture filtrate dilutions were made to determine if the effect on *A. thaliana* corresponded with the concentration of the CF, and other chemical features and host specificity of the metabolites were

also examined. Furthermore, the transgenic *A. thaliana* GFP-tagged PIN-lines PIN1-GFP, PIN2-GFP, PIN3-GFP and PIN7-GFP, which allow visualization of the auxin efflux, were grown on different concentrations of CF to observe the effect of the filtrate on auxin homeostasis within the root tissue (Feraru & Friml, 2008). DR5::GFP is an auxin responsive reporter and was grown on these media as well to determine the amount of IAA that has accumulated in the *A. thaliana* root tissue (Chen *et al.*, 2013).

Excessive auxin causes root inhibition in plants, but because *A. thaliana* mutants *axr1-3*, *axr4-2* and *aux1-7* have defects in the auxin influx into the cell, they are thus insensitive to excessive auxins (TAIRa; TAIRb; TAIRc). These mutants were therefore grown on CF-containing media to confirm whether IAA was causing the earlier observed root inhibition. Root lengths of wildtype Col-0 and these mutants were measured and used for statistical analyses, to indicate any significant differences between the treatments. The Col-0 values were also used to estimate the concentration of IAA that was produced by *P. cryptoirregulare* and its two references *P. irregulare* and *P. ultimum* var. *ultimum* during this experiment, based on a standard curve that was generated from the root lengths grown on different, known concentrations of IAA. Small amounts of this IAA were also added to the CFs in the media to investigate if the effect of the CFs worsened or improved. If the CFs caused a disturbance in auxin homeostasis, the additional IAA could potentially provide the amounts of auxin that the CFs prevent from being distributed within the host tissue. However, if the metabolites secreted by the tested *Pythium* species already consist of auxins, the additional IAA would increase the already excessive amount of auxin and worsen the effect on the root growth and impaired auxin homeostasis. Even though the auxin-insensitive mutants already exhibit reduced gravitropism (Hopkins, 1995), this experiment was also conducted to investigate a potential change in gravitropism when additional IAA would be added.

Overall, the results of these approaches are expected to contribute to the identity and understanding of the function of the metabolites that are secreted by the three *Pythium* species of this study.

## 5.2 Materials and methods

### 5.2.1 Plant and pathogen materials

**Host** – To assess the susceptibly to *P. cryptoirregulare* filtrate, seeds of *A. thaliana* Col-0 (wildtype), the auxin-insensitive mutants *axr1-3*, *axr4-2*, and *aux1-7*, GFP-tagged PIN1, PIN2, PIN3, and PIN7, and DR5::GFP lines, and *B. napus* cv. Westar were surface-sterilized by first submerging them in 250 µL 70% ethanol for 30 seconds, followed by submersion in 350 µL concentrated liquid bleach for up to 10 minutes after which they were rinsed with sterile water five times to remove bleach residue from the seeds. Per 100 x 15 mm square Petri dish, five to twelve replicates of these surface-sterilized seeds were then individually placed in a horizontal line at the top of the ½ MSA with culture filtrate (CF) or control solutions. One Petri dish per treatment was positioned in the incubator according to a completely randomized design at an approximate 5-10° angle to ensure the roots of growing into the media. The seeds were incubated up to 14 days, depending on the assessment, at 21-22 °C with a 12-h photoperiod.

**Pathogen** – The *P. cryptoirregulare* strain that was isolated in this study and its reference *P. irregulare* (DOAMC 870 BR), and *P. ultimum* var. *ultimum* (DAOMC 628 BR) were maintained on either PDA, CMA or ½ MSA at room temperature for preparation of the liquid cultures used in the filtrate assessments. The strains were subcultured on ½ MSA every two weeks to maintain viability and 1.5 days before each liquid culture preparation to ensure actively growing mycelia.

### 5.2.2 Metabolite extraction and media preparation

Agar plugs of 0.5 x 0.5 cm were taken from *P. cryptoirregulare*, *P. irregulare* and *P. ultimum* var. *ultimum* cultures grown on MSA and carefully added to cooled CMB, RB or MSB broths in 250 mL flasks, which was prepared as described in Section 2.2.3. Six liquid cultures per *Pythium* species were covered with sterilized aluminium foil after which they were incubated and shaken (100 RPM) at approximately 23-24 °C.

After 10 or 20 days of incubation, the mycelia of all six flasks per species were either filtered out with cheesecloth and Miracloth, disposable filtration units with a pore size of 0.45 µm, 0.45 µm syringe filters or metal or glass filter holders containing filter membranes with a 0.45 µm pore size. The mycelia were discarded, and the CF was mixed 1:1 with ½ MSA containing 1.5%

agarose, to obtain MSA with 0.75% agarose for optimal germination and growth of *A. thaliana*. Approximately 30 mL of the CF/MSA mixtures were added per 100 x 15 mm square Petri dish.

After the filtration and media type trials, the method involving filtration of MSB cultures with 0.45 µm membranes in filter holders was used in all subsequent experiments. During these metabolite experiments, several different CF conditions were used to assess the function and the identity of the metabolite(s) secreted by *P. cryptoirregulare*. Additional to the 0.5x CF obtained from mixing the CF 1:1 with MSA, CFs were also diluted with uninoculated ½ MSB prior to mixing it 1:1 with ½ MSA, resulting in 0.25x and 0.05x final CF concentrations in the media. Diffusion of the metabolite(s) was tested by placing separately-prepared ½ MSA with and without 0.5x *P. cryptoirregulare* CF in a single square Petri dish adjoining one another. The undiluted CF was also assessed by adding sterilized agar directly to the CF until a final agar concentration of 0.75% was obtained. Furthermore, the effect of exposure to high temperatures was tested twice by autoclaving the CF before preparing 0.5x *P. cryptoirregulare* CF in ½ MSA. The possibility of inhibition of *A. thaliana* growth as a result of decreasing availability of nutrients during the liquid culture incubation was also investigated. Sterile water was mixed 1:1 with ½ MSA (and 1.5% agar) to simulate a situation where all MS and sucrose nutrients were used up by *P. cryptoirregulare*.

Media containing uninoculated ½ MSB mixed 1:1 with ½ MSA (1.5% agarose) was used as a negative control, providing a comparison with unaltered *A. thaliana* or *B. napus* growth. Additionally, media with 1nM, 10nM, 50nM and 100nM synthetic indole-3-acetic acid (IAA) concentrations were used as positive controls, providing a comparison of *A. thaliana* seedlings with altered auxin homeostasis as a response to excessive auxin. One media plate was prepared for each treatment or control.

### 5.2.3 Seedling development assessment

Three to nine replicates of surface-sterilized *A. thaliana* Col-0 seeds were individually placed on the media in a horizontal line at the top of each square Petri dish. The Petri dishes were positioned in the incubator according to a completely randomized design at an approximate 5-10° angle at 21-22 °C with a 12-h photoperiod. Seeds were incubated either 7 or 10 days in these conditions. To determine whether the secreted metabolites prevent seedling development by potentially causing permanent damage or only inhibit and slow down the process, seedlings were

initially incubated on 0.5x CF for 10 days after which they were transferred to uninoculated ½ MSB and incubated for another seven days.

In addition to the *A. thaliana* assessment, five replicated *B. napus* cv. Westar seeds were also grown in triplicate on 0.5x *P. cryptoirregulare* CF and uninoculated ½ MSB to investigate whether the effect of the metabolites is host-specific. These *B. napus* seeds were incubated for 10 days under the same conditions as the *A. thaliana* seeds.

After the designated days of incubation, each Petri dish was photographed with the Canon EOS camera. *Arabidopsis thaliana* root growth was also more closely observed under the fluorescence microscope (Zeiss Axioplan), focussing specifically on the root tip and the elongation zone using a magnification of 10X or 25X.

Fiji (ImageJ, v.1.52s) and Adobe Photoshop (CS4) were used for image processing and editing while the Simple Neurite Tracer-function of Fiji was used to measure the root length of the *B. napus* seedlings. While descriptive analysis was executed for the treated *A. thaliana* seedlings, statistical analysis of the *B. napus* measurements was executed using R (v. 3.6.0) to apply the analysis of variance (ANOVA) and the Tukey post-hoc test to the data.

### 5.2.4 Visualization of the auxin homeostasis with the use of confocal microscopy

Prior to incubation on media, seeds of *A. thaliana* lines PIN1-GFP, PIN2-GFP, PIN3-GFP, PIN7-GFP and DR5::GFP were surface-sterilized with ethanol and bleach. Twelve seeds of each of these GFP-tagged lines were placed on ½ MSA containing 0.5x, 0.25x, or 0.05x CF concentrations of the *P. cryptoirregulare* isolate and the reference species *P. irregulare* (DOAMC 870 BR) and *P. ultimum* var. *ultimum* (DAOMC 628 BR). As an addition to these CF treatments, water, uninoculated ½ MSB and ½ MSB with IAA concentrations of 1nm, 10nm, 50nm and 100nm, were also mixed with the ½ MSA (1.5% agar, 5% sucrose) to serve as controls for comparison between the effect of these conditions on the auxin homeostasis and the impact of the CF. One Petri dish per treatment or control was placed in an incubator according to a completely randomized design at an 80-85° angle and 21-22 °C with a 12h-photoperiod.

After a six-day incubation, the development of the seedlings was photographed with Canon EOS camera, followed by staining the seedlings with 0.1 mg/mL propidium iodide (PI) to

visualize the cell wall. The internal GFP-tagged auxin efflux was then observed and captured under the LSM 510 meta (Confor2, 2005) and LSM 880 (Zeiss AxioObserver Z1) confocal laser-scanning microscopes (Carl Zeiss, Gottingen, Germany). Excitation and emission wavelengths of 488 nm and 505-530 nm of the Argon laser were used to observe the GFP, while PI was observed under the same excitation wavelength, but with a different emission filter of >650 nm.

Image editing and analyses were done using Fiji (ImageJ, v.1.52s), and while a descriptive analysis followed for the PIN-lines, further analysis was done to measure the amount of auxin present in the root tips of the DR5::GFP seedlings grown on ½ MSA containing 0.5x CFs or uninoculated ½ MSB. Photos of six randomly chosen replicates were chosen for these measurements. The total pixel intensity of the expressed GFP in the root cap and epidermal cells or the columella was measured to resemble the relative quantity of auxin present in these selected areas. To exclude background fluorescence from these areas, four randomly chosen selections next to the fluorescent tissue were measured, and the mean of this background fluorescence was subtracted from the fluorescence measured in the epidermal cells and root cap or the columella.

The analysis of variance (One-way ANOVA) and the Tukey post-hoc test were applied to the data using R (v. 3.6.0) to determine whether the CFs had any significant effect on the distribution of auxins and to detect any potential differences in metabolite secretion or function between the three *Pythium* species.

### 5.2.5 Auxin insensitivity assay

Five *A. thaliana* seeds of Col-0 and five seeds of each auxin insensitive mutant, *axr1-3*, *axr4-2*, and *aux1-7*, were grown for 14 days on MSA without any additional solution (negative control), on MSA containing 0.5x, 0.25x or 0.05x CF from *P. cryptoirregulare, P. irregulare* or *P. ultimum* var. *ultimum*, and on MSA containing 1 nM, 10 nM, 50 nM or 100 nM IAA compositions. The Petri dishes were placed in an incubator at approximately 22 °C on a rack that was placed at an 80-85° angle. One Petri dish per treatment was positioned according to a completely randomized design.

After the 14-day incubation time, each Petri dish was photographed with the Canon EOS camera, after which Fiji (ImageJ, v.1.52s) and Adobe Photoshop (CS4) were used for image

processing and editing. The Simple Neurite Tracer-function of Fiji was used to measure the root length of each of the five replicate seedlings, followed by statistical analysis using R (v. 3.6.0) to apply the analysis of variance (Two-way ANOVA) after generating a linear model of the data. The function "difflsmeans" was used to detect significant differences between the treatments. Tables were created, showing significant differences that were relevant to this study. At the same time, graphs were generated from the IAA data to propose potential linear relationships that could be used as a standard curve for determining the concentration of auxin-like metabolites in the CF.

Additionally, IAA was added to the CF media to investigate whether additional auxin would worsen the growth inhibition as a result of adding more auxin to the auxin that was already secreted by the pathogen, or if this IAA would decrease the growth inhibition by supplying auxin to the host to counteract manipulated auxin uptake caused by the secreted metabolites. Media compositions of MSA with either 0.25x CF of *P. cryptoirregulare*, *P. irregulare* or *P. ultimum* var. *ultimum*, or no CF, received an additional 10nM or 50nM IAA. Per treatment, a Petri dish with 12 Col-0 seeds and a Petri dish with five seeds of each auxin-sensitive mutant were prepared and placed in an incubator according to a completely randomized design at approximately 22 °C, on a rack that was placed at an 80-85° angle. After 14 days of incubation, the seeds were photographed and visually compared, followed by image processing and editing with Adobe Photoshop (CS4) and a descriptive analysis.

The last aspect that was studied with the use of Col-0 and the auxin-insensitive mutants was the ability of gravitropic growth adjustment. Five seeds of Col-0 and each auxin-sensitive mutant were placed on MSA containing either uninoculated ½ MSB, 0.25x CF of either *P. cryptoirregulare*, *P. irregulare* or *P. ultimum* var. *ultimum*, or 10nM IAA. One petri dish per treatment or control was placed in an incubator according to a completely randomized design at approximately 22 °C, on a rack that was placed at an 80-85° angle. The Petri dishes were rotated 90° after seven days of incubation. After another seven days of incubation in this new position, the seedlings were observed and photographed. Adobe Photoshop (CS4) was used for image processing and editing, followed by a descriptive analysis.

Table 5.1 shows a summary of assessments that were conducted in this part of the project.

**Table 5.1 Summary of the metabolite function assessments**

| Assessment | Treatment | Host material | Pathogen culture filtrate |
|---|---|---|---|
| Seedling development assessment | Culture filtrate concentration (0.5x/0.25x/0.05x)<br>0x culture filtrate conc. (½ MSB)<br>Diffusion<br>High temperature (autoclave)<br>Damage assay (transfer from culture filtrate to ½ MSB) | *A. thaliana* Col-0 | *P. cryptoirregulare* |
| | Host specificity | *B. napus* (Westar) | |
| Auxin homeostasis visualization | Culture filtrate concentrations (0.5x/0.25x/0.05x)<br>0x culture filtrate conc. (½ MSB)<br>Sterile water<br>IAA concentrations (1 nM/10 nM/50 nM/100nM) | *A. thaliana* lines<br>◦ PIN1::PIN1-GFP<br>◦ PIN2::PIN2-GFP<br>◦ PIN3::PIN3-GFP<br>◦ PIN7::PIN7-GFP<br>◦ DR5::GFP | *P. cryptoirregulare*<br>*P. irregulare*<br>*P. ultimum* var. *ultimum* |
| Auxin sensitivity assay | Culture filtrate concentrations (0.5x/0.25x/0.05x)<br>0x culture filtrate conc. (½ MSB)<br>IAA concentrations (1 nM/10 nM/50 nM/100nM)<br>Filtrate/IAA combination<br>◦ ½ MSB<br>◦ ½ MSB + 10 nM IAA<br>◦ ½ MSB + 50 nM IAA<br>◦ 0.25x culture filtrate<br>◦ 0.25x filtrate + 10 nM<br>◦ 0.25x filtrate + 50 nM<br>Gravitropism adjustment<br>◦ ½ MSB<br>◦ 0.05x culture filtrate<br>◦ 10 nM IAA | *A. thaliana* Col-0<br>*A. thaliana* mutants<br>◦ *axr4-2*<br>◦ *axr1-3*<br>◦ *aux1-7* | *P. cryptoirregulare*<br>*P. irregulare*<br>*P. ultimum* var. *ultimum* |

## 5.3 Results

During the assessment of the growth inhibition, the negative controls of ½ MSA (1.5% agar) mixed 1:1 with RB, CMB, ½ MSB or sterile $H_2O$ without filtrate revealed that the RB and CMB affected the seedling development. Seedlings grown on media with either of these broths already exhibited a reduced root growth in the absence of any culture filtrate. Therefore, for generating liquid cultures during the metabolite assays, *P. cryptoirregulare* was only grown in MSB, for it contained nutrients optimal for plant growth and did not obstruct seedling growth.

### 5.3.1 Growth inhibition in response to *Pythium* culture filtrates

After *A. thaliana Col-0* seeds were placed and incubated on ½ MSA mixed with undiluted *P. cryptoirregulare* CF obtained from a 20-day-old liquid culture, a visual difference in seed germination was observed after four days of incubation. Based on this observation, it was initially thought that *P. cryptoirregulare* possibly secreted metabolites that prevent seed germination. However, after 10 days of incubation seeds had germinated, when compared to the seedlings grown on inoculated ½ MSB (Figure 5.1A), root development in the seedlings grown on CF was severely impaired, equally affecting the development of hypocotyls and cotyledons (Figure 5.1D). Seedlings exhibited a visible lack of chlorophyll indicated by their almost colourless appearance. Despite the optimal growth conditions, these seedlings were likely not viable as a result of the inability to take up the required nutrients due to the absence of required root system.

Diluting the CFs before mixing with ½ MSA resulted in less root growth inhibition (Figure 5.1B and C). Root growth remained significantly inhibited compared to the uninoculated ½ MSB control, while the hypocotyl and cotyledon development showed improvement. Despite this improvement, seedlings grown on 0.25x CF still showed symptoms of nutrient deficiency, including yellowing of the cotyledons and the absence of true leaf development.

Interestingly, autoclaving the CF prior to mixing it with MSA, resulted in various growth alterations. Initially, seedlings showed a comparable leaf development to the ½ MSB control, while the root growth remained inhibited significantly (Figure 5.1E). When repeated, less leaf development was observed compared to the previous trial, even though reduced root inhibition was also observed (Figure 5.1F). Another remarkable observation was the development of more

lateral roots with equal lengths as the taproot, which complicated the differentiation between these root types. The inconsistent growth patterns seen in these seedlings suggested an altered or reduced function of the metabolites as a result of autoclaving. Presumably, the secreted metabolites are therefore not heat-stable.

Figure 5.1G shows seedlings of the diffusion assay after seven days of incubation. Notable differences were observed between seedlings that were grown on individual media conditions and seedlings that were grown in ½ MSB/0.5x CF-adjoined media. In comparison to the individual conditions, seedlings grown on the uninoculated ½ MSB side of the plate showed root growth inhibition, whereas the seedlings that were grown on the 0.5x CF showed a reduced inhibition. This result suggested that the secreted metabolites are mobile and capable of diffusion through MSA.

The last assay shown in Figure 5.1H and Figure 5.1I revealed that the metabolites in the filtrate did not cause permanent damage in most of the *A. thaliana* seedlings. Figure 5.1H shows 10-day old seedlings grown on CF media with severely inhibited root growth and overall reduced seedling development. Three seedlings grew inverted, suggesting a disturbed auxin flux within the seedling. Figure 5.1I shows the same seeds in an identical order after being transferred to ½ MSA containing uninoculated ½ MSB. More than half of the seedlings recovered from the inhibition previously caused by CF. Even the first two seedlings which seemed to be in a critical state in the presence of CF mostly recovered. However, the roots of three seedlings remained significantly inhibited. It is unclear whether their root growth would have been permanently damaged or if more time was required to recover from the stress that was caused by the metabolites.

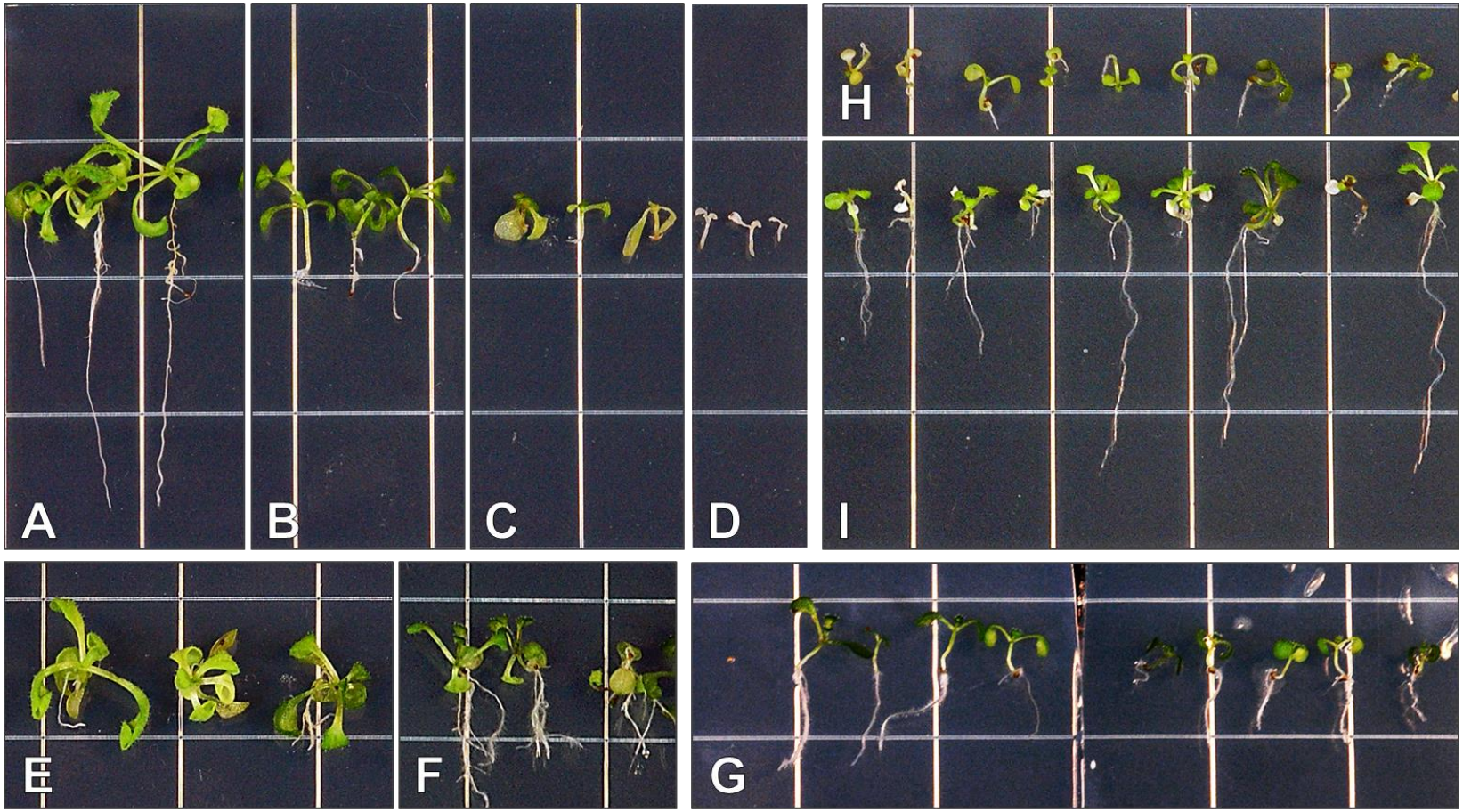


**Figure 5.1 Inhibition of *Arabidopsis thaliana* seedling development caused by unknown metabolites in *Pythium cryptoirregulare* culture filtrate.** Photos were taken after 7 (**E-G**), 10 (**A-D & H**) or 17 (**I**) days of incubation at 22 ºC. **A-D**. From left to right: Seedlings grown on ½ MSA containing uninoculated ½ MSB, 0.05x culture filtrate (CF), 0.25x CF, or 0.5x CF, respectively, showing an increased root growth inhibition. **E**. First trial of seedlings grown on ½ MSA containing autoclaved 0.5x CF, showing typical hypocotyl and leaf development despite the inhibited root growth. **F**. Second trial of seedlings grown on ½ MSA containing autoclaved 0.5x CF, showing a slight alteration of hypocotyl and leaf development, whereas the number of lateral roots is significantly increased during the root development. **G**. Seedlings grown on ½ MSA containing uninoculated ½ MSB (**left**) which is adjoined to ½ MSA containing 0.5x CF (**right**), both showing a difference in development compared to their development on identical media in individual Petri dishes. **H**. Seedlings grown on ½ MSA containing 0.5x CF for transfer purposes, showing severely inhibited seedling development. **I**. Seedlings grown on ½ MSA containing uninoculated ½ MSB after transfer from ½ MSA containing 0.5x CF, showing partial recovery in root growth and overall development of the same seedlings illustrated immediately above (**H**). Gridlines = 13 mm.

Interestingly, *A. thaliana* appeared not to be the only host that could be affected by the metabolites secreted by *P. cryptoirregulare*. *Brassica napus* cv. Westar showed comparable symptoms when grown in the presence of the *P. cryptoirregulare* CF (Figure 5.2). Significant root growth inhibition (Table 5.2), impaired overall seedling development, yellowing of leaves and disturbed gravitropism were observed in the seedlings of this economically important crop as well, similar to the effects seen in *A. thaliana* (Figure 5.1).

**Table 5.2 ANOVA (One-way) results of the linear mixed-effects model based on *Brassica napus* root length upon exposure to ½ MSB or *Pythium cryptoirregulare* CF**

| | numDF | denDF | F-value | p-value | Significance |
|---|---|---|---|---|---|
| (Intercept) | 1 | 21 | 158.5787 | 2.98E-11 | *** |
| Treatment | 1 | 4 | 37.25088 | 0.003647 | ** |

* $p$ <0.05, ** $p$ <0.01, *** $p$ <0.001

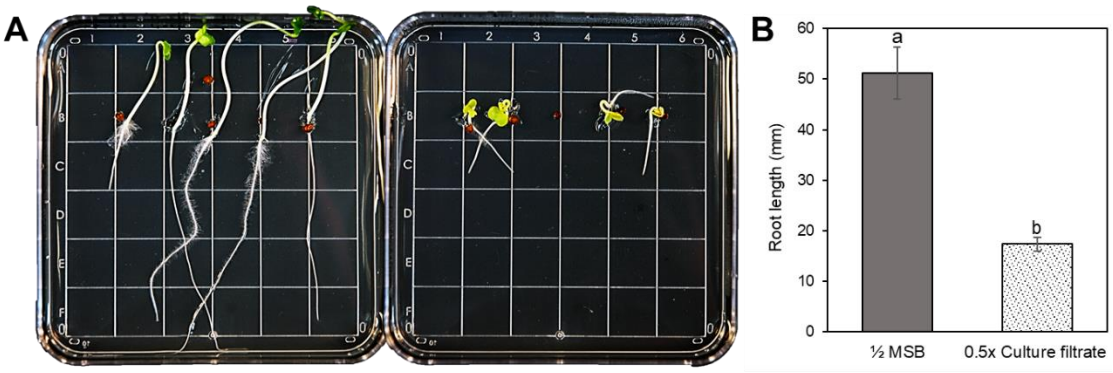


**Figure 5.2 Germination and development of *Brassica napus* cv. Westar seeds and seedlings in the presence of *Pythium cryptoirregulare* culture filtrate.** Photos were taken of the seedlings after 10 days of incubation at 22ºC. The culture filtrate that was used for this experiment was obtained from a 10-day old liquid culture. **A**. Seedlings grown on MSA containing uninoculated ½ MSB (**left**) or 0.5x *P. cryptoirregulare* culture filtrate (**right**). **B.** Mean root lengths in millimeters based on 3 replicated media plates per treatment with each up to five seedlings.

When inoculated *A. thaliana* roots were observed under the microscope, it was notable that cells in the elongation zone were not elongating, thereby inhibiting root growth (Figure 5.3). In seedlings that were grown on uninoculated ½ MSB (Figure 5.3A), the more distant the cells were from the differentiation zone, the more elongated they became. Moreover, this elongated zone also exhibited newly developing root hairs.

Seedlings that were transferred to ½ MSA without CF after initially being grown in the presence of 0.5x CF showed signs of recovery as a whole organism, and also on a cellular level (Figure 5.3B). Elongated cells without abnormal root hair development were observed in these seedlings.

The inconsistent growth seen in the seedlings grown on ½ MSA with autoclaved CF corresponded to the observation under the microscope (Figure 5.3C). Specifically, irregular elongation among the cells in the elongation zone and a small number of root hairs at an atypical location were observed.

The lowest CF concentration (0.05x) resulted in a slightly reduced elongation and cellular extension or displaced root hair development close to the root tip (Figure 5.3D). Meanwhile, concentrations 0.25x and 0.5x show more severe alterations, indicated by short swollen cells in the elongation zone and extensive root hair development close to the root tip (Figure 5.3E & F). Due to the reduced elongation and swollen cells, the roots appeared thicker compared to the seedlings grown on media without CF.

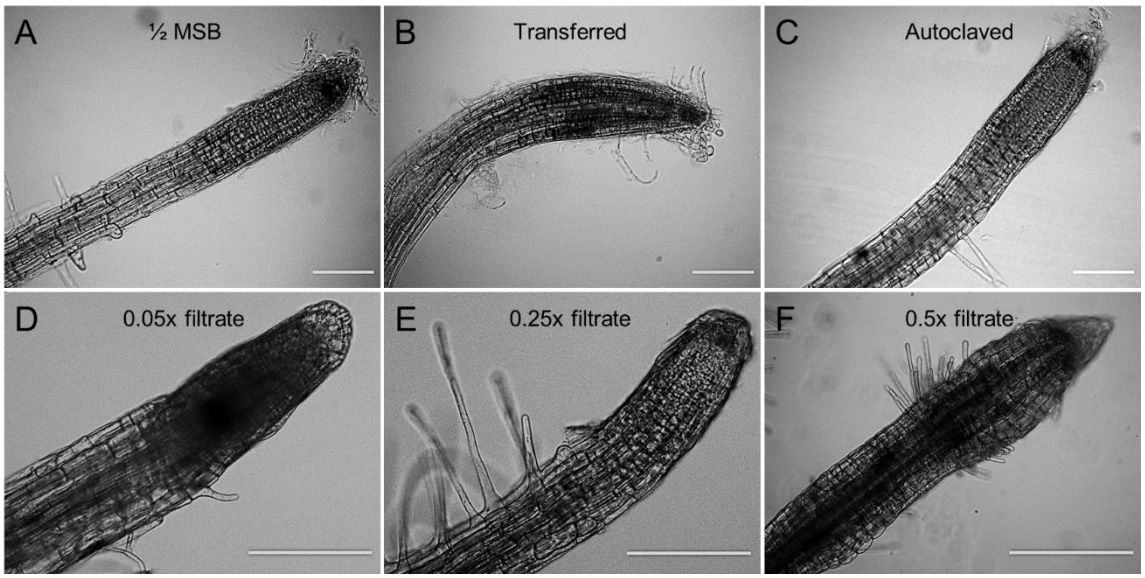


**Figure 5.3 Development of *Arabidopsis thaliana* root tips in the presence of different concentrations and treatments of *Pythium cryptoirregulare* culture filtrate.** Photos were taken of the root tips using the Zeiss Apotome microscope after 10 days of incubation in a mixture of MSA with culture filtrate or ½ MSB at 22ºC. The culture filtrate used for this experiment was obtained from a 20-day old liquid culture. **A**. A root tip of a seedling that was grown on ½ MSB (negative control) showing no abnormal development of the root tip. **B**. A root tip of a seedling that was grown on 0.5x culture filtrate concentration for 10 days and transferred to ½ MSA without *P. cryptoirregulare* for another 7 days, showing no abnormal growth. **C**. Slightly altered cell elongation and root hair formation after incubation on autoclaved 0.5x culture filtrate in ½ MSA. **D**. Mildly altered root development after incubation on 0.05x culture filtrate in MSA, showing a sporadically altered root hair development and a very mildly inhibited elongation in the elongation zone. **E**. Abnormal root development after incubation on 0.25x culture filtrate in ½ MSA, showing swollen cells, increased root hair development and impaired elongation in the elongation zone. **F**. Abnormal root development after incubation on 0.5x culture filtrate in ½ MSA, showing swollen cells, increased root hair development and no elongation in the elongation zone. Scale bars = 100 µm.

### 5.3.2 Altered auxin homeostasis in response to *Pythium* metabolites

Six-day old *A. thaliana* PIN1-GFP seedlings had different root growth depending on whether they were grown in the presence of uninoculated ½ MSB and the CF of the three *Pythium* species (Figure 5.4). Overall, the seedlings grown on ½ MSB had visibly longer hypocotyls and, specifically, longer roots. These roots also exhibited a vertical downwards growth as a result of gravitropism, whereas the majority of the roots grown in the presence of CF showed impaired gravitropism, indicated by roots growing horizontally or even upwards.

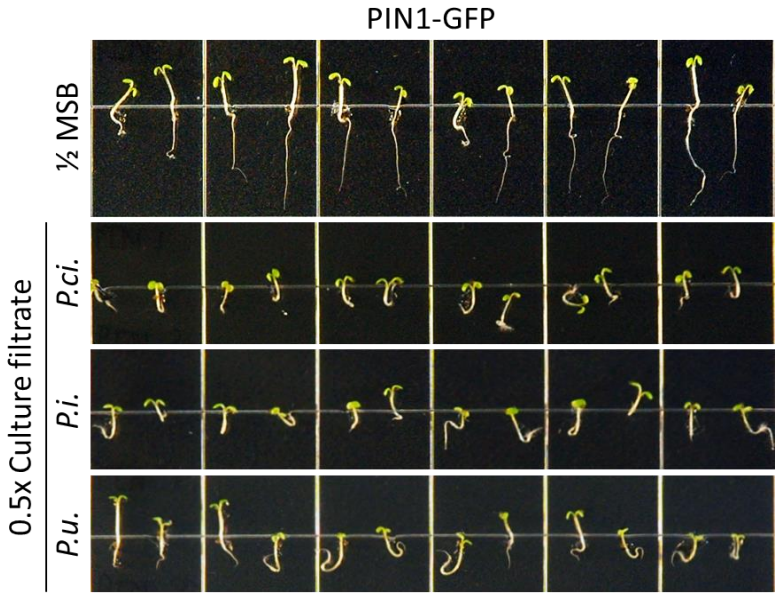


**Figure 5.4 Development of *Arabidopsis thaliana* PIN1-GFP marker line in the presence of uninoculated ½ Murashige and Skoog broth (½ MSB) and *Pythium cryptoirregulare* (*P.ci.*), *Pythium irregulare* (*P.i.*, DOAMC 870 BR) and *Pythium ultimum* var. *ultimum* (*P.u.*, DAOMC 628 BR) culture filtrates.** Photos were taken after 6 days of incubation at 22ºC, and the culture filtrates that were used in this experiment were obtained from 10-day old liquid cultures. Gridlines = 13 mm.

When the GFP-tagged *A. thaliana* lines were observed under the laser-scanning microscope, these PIN-lines revealed several interesting alterations as follows: PIN1-GFP (Figure 5.5A) is involved in the downwards auxin efflux in the stele, as evident by the seedlings growing in the absence of CF. However, seedlings grown in the presence of CF of all three *Pythium* species showed a reduced expression that was mostly localized in only the lower region of the stele. Also, the GFP appears to be expressed in a smaller range of cells close to the root tip when grown in *P. ultimum* var. *ultimum* CF, indicated by the slimmer area of fluorescence. During a more detailed PIN1-GFP assessment, including water and IAA treatments, it was observed that a decrease in CF concentration in the media caused a reduction of the effect on the GFP alteration,

including the range of fluorescent cells *on P. ultimum* var. *ultimum* CF (Appendix B-Figure B1). Moreover, adding water instead of ½ MSB to investigate the effect of reduced nutrition had no noticeable effect on the expression. In contrast, when an IAA concentration of >100 nM was introduced, similar effects were observed as upon exposure to the CFs.

Comparable results were found for PIN2-GFP (Figure 5.5B). Seedlings grown on uninoculated ½ MSB showed expression in up to two epidermal cell layers, whereas seedlings grown on *P. cryptoirregulare* or *P. irregulare* CF showed very little to no expression, again, only in the lower parts closer to the root tip. Interestingly, seedlings that were grown on CF of *P. ultimum* var. *ultimum* seem not to be affected by the CF and occasionally even showed a higher expression. A more detailed PIN2-GFP assessment supported these observations (Appendix B-Figure B2). The higher the concentration of the *P. cryptoirregulare* and *P. irregulare* CFs in the media, the less auxin efflux was found in the epidermal layers in the roots. In contrast, the *P. ultimum* var. *ultimum* CF in the media caused no reduction in auxin efflux, regardless of the concentration. Fewer nutrients by mixing ½ MSA with water did not cause any alterations either, whereas the media containing >50 nm IAA results in a similar declining auxin efflux as seen for *P. cryptoirregulare* and *P. irregulare* CFs.

Whether seedlings were grown in the presence or absence of CF, very little to no differences in expression were observed for the PIN3-GFP line (Figure 5.5C). Compared to the CFs of *P. cryptoirregulare* and *P. irregulare*, the *P. ultimum* var. *ultimum* CF seemed to cause a slightly lower reduction in GFP expression, mostly in the stele of the root. Appendix B-Figure B3 shows additional GFP expressions from seedlings that were grown in the presence of lower CF concentrations. Neither these concentrations nor water or any additional IAA had any effect on the auxin efflux visualized by PIN3-GFP.

PIN7-GFP (Figure 5.5D) followed a similar expression pattern as PIN1-GFP (Figure 5.5A). Culture filtrates of all three *Pythium* species showed a comparable reduction in auxin reflux in the stele and columella compared to the seedlings grown on MSA containing uninoculated ½ MSB. Appendix B-Figure B3 also shows a corresponding decrease in the reduction for lower CF concentrations. Likewise to the effect of CFs, increasing IAA concentrations in the media also resulted in a decrease of GFP expression, whereas, water did not affect the auxin homeostasis.

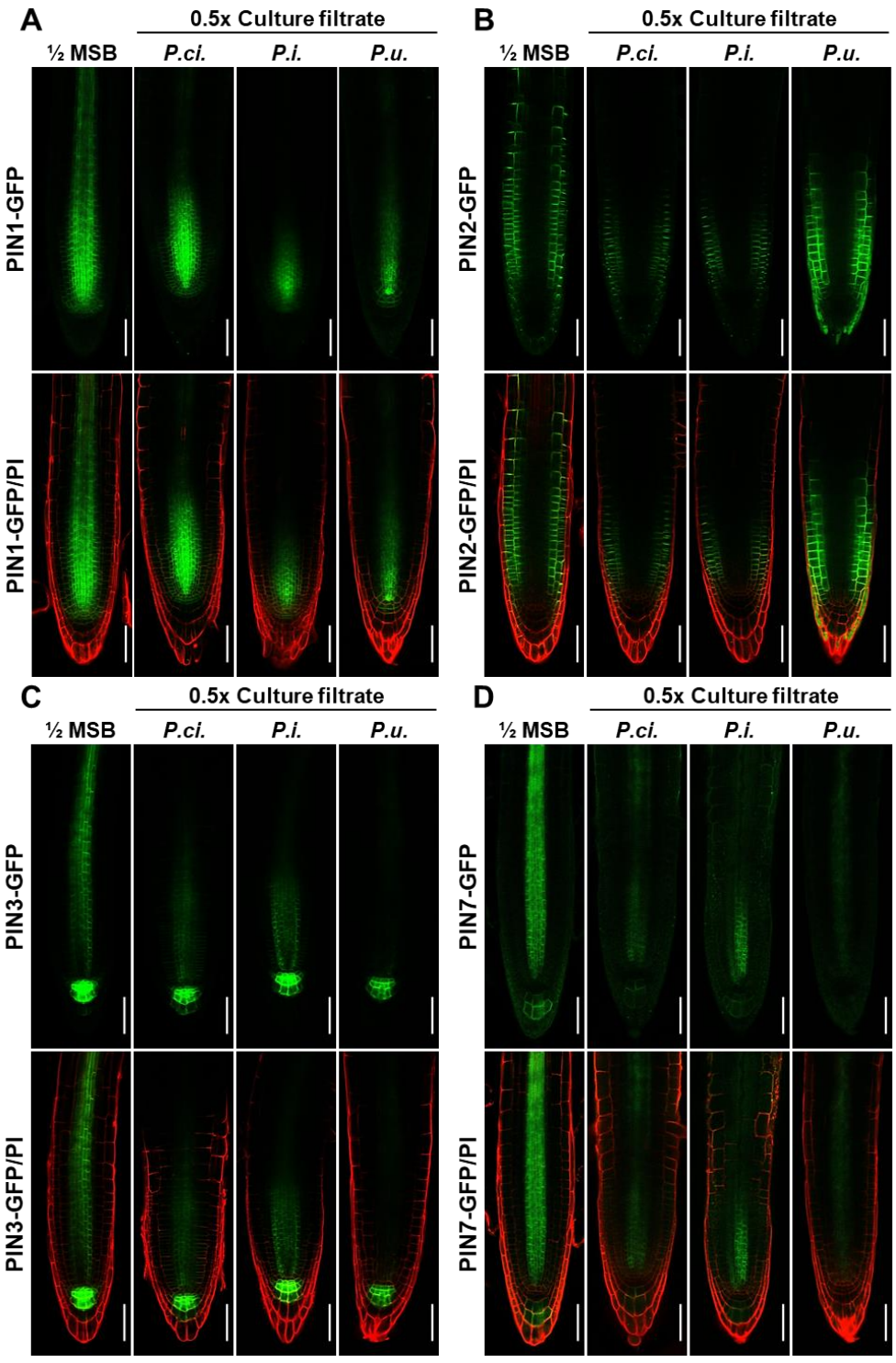


**Figure 5.5 Altered auxin transport in root tissues of *Arabidopsis* seedlings upon exposure to culture filtrates of *Pythium* species.** Photos were taken of propidium iodide(PI)-stained *Arabidopsis* seedlings expressing the auxin reporter constructs PIN1-GFP (A), PIN2-GFP (B), PIN3-GFP (C), or PIN7-GFP (D) after six days of incubation at 22ºC. The seedlings were grown vertically on ½ MSA in the absence (½ MSB) or presence of culture filtrates, extracted from *P. cryptoirregulare* (*P.ci.*), *P. irregulare* (*P.i.*, DOAMC 870 BR) and *P. ultimum* var. *ultimum* (*P.u.*, DAOMC 628 BR) liquid cultures. Confocal images showing GFP signals were captured with the Argon laser using the following excitation/emission settings: 488/505-530 nm for the visualization of GFP while PI was observed with 488/>650 nm wavelengths. Scale bars = 50 μm.

Two distinct regions were selected for observation of DR5::GFP expression: the first two cell layers of the lateral root cap and epidermis, and the columella and quiescent centre. In case of the lateral root cap and epidermis, a significant difference was observed between the expression upon exposure to the ½ MSB treatment and the CFs of *P. cryptoirregulare* and *P. irregulare* (Table 5.3, Table 5.4, and Figure 5.6). Despite there being a low fluorescence detected in these regions for the ½ MSB treatment, the two culture filtrates caused a high GFP-expression, suggesting that a large amount of auxin was present. Another interesting observation upon exposure to these CFs included the auxin efflux of roots that exhibited disturbed gravitropism. Often, the GFP expression in the root cap and epidermal cells was found only on one side of the root. This event explains the altered growth direction of the root against gravity.

Also, as previously seen in the PIN-lines, *P. ultimum* var. *ultimum* CF, did not cause the same response as that of its related *Pythium* species. Its expression was lower, but comparable to the expression of the uninoculated ½ MSB treatment, meaning that this CF has little to no effect on the auxin distribution in this region.

**Table 5.3 Mean fluorescence intensity of the root cap and epidermis region of DR5::GFP**

| Treatment | Mean total fluorescence (per pixel) | Standard error |
|---|---|---|
| ½ MSB | 1.62E+4 | 1.77E+3 |
| *Pythium cryptoirregulare* CF | 6.21E+5 | 1.30E+5 |
| *Pythium irregulare* CF | 5.38E+5 | 7.49E+4 |
| *Pythium ultimum* var. *ultimum* CF | 9.34E+3 | 1.66E+3 |

**Table 5.4 Tukey's HSD post-hoc results of the DR5::GFP root cap and epidermis fluorescence intensity upon exposure to ½ Murashige and Skoog broth (½ MSB) or *Pythium cryptoirregulare* (*P.ci.*), *Pythium irregulare* (*P.i.*, DOAMC 870 BR) or *Pythium ultimum* var. *ultimum* (*P.u.*, DAOMC 628 BR) culture filtrate (CF)**

| Treatment - Treatment | Mean difference | *p*-value | Significance |
|---|---|---|---|
| *P.ci.* CF. - ½ MSB | 6.04E+5 | 7.77E-5 | *** |
| *P.i.* CF - ½ MSB | 5.22E+5 | 4.45E-4 | *** |
| *P.u.* CF - ½ MSB | -6.87E+3 | 1.00E+0 | |
| *P.i.* CF - *P.ci.* CF | -8.26E+4 | 8.63E-1 | |
| *P.u.* CF - *P.ci.* CF | -6.11E+5 | 6.73E-5 | *** |
| *P.u.* CF - *P.i.* CF | -5.29E+5 | 3.84E-4 | *** |

* $p$ <0.05, ** $p$ <0.01, *** $p$ <0.001

Appendix B-Figure B5 shows further expression levels, including lower CF concentrations and uninoculated ½ MSB with additional molarities of IAA. The IAA treatment follows an expression pattern resembling that of *P. cryptoirregulare* and *P. irregulare* CFs. The expression in the CFs even seems to be visibly higher, which implies that the auxin concentration of the 2x

diluted filtrates used for this experiment is higher than 100nM. The figure also confirms that a low to no expression is caused by any concentration of *P. ultimum* var. *ultimum* CF.

The columella and quiescent centre of *A. thaliana* showed less drastic differences between the *P. cryptoirregulare* and *P. irregulare* CFs, and the uninoculated ½ MSB. Even though a visual difference can be spotted (Figure 5.6), no significant difference was detected using the ANOVA analysis of variance (Table 5.5 and Table 5.6). However, the expression in this region strongly confirms the previous observation regarding the effect of CF originating from *P. ultimum* var. *ultimum*. While no significant difference was found between the uninoculated ½ MSB and the *P. cryptoirregulare* CF, the expression caused by *P. ultimum* var. *ultimum* CF showed a significant difference with all the treatments. Interestingly, it showed even lower expression than for the ½ MSB treatment, suggesting that it potentially secretes different metabolites or creates unfavourable conditions that might be antagonistic to auxin distribution.

**Table 5.5 Mean fluorescence intensity of the columella region of DR5::GFP**

| Treatment | Total fluorescence (per pixel) | Standard error |
|---|---|---|
| ½ MSB | 8.50E+5 | 3.53E+4 |
| *Pythium cryptoirregulare* CF | 1.10E+6 | 1.58E+5 |
| *Pythium irregulare* CF | 1.07E+6 | 5.88E+4 |
| *Pythium ultimum* var. *ultimum* CF | 3.43E+5 | 2.70E+4 |

**Table 5.6 Tukey's HSD post-hoc results of the DR5::GFP columella fluorescence intensity upon exposure to ½ Murashige and Skoog broth (½ MSB) or *Pythium cryptoirregulare* (*P.ci.*), *Pythium irregulare* (*P.i.*, DOAMC 870 BR) or *Pythium ultimum* var. *ultimum* (*P.u.*, DAOMC 628 BR) culture filtrates (CF)**

| Treatment - Treatment | Mean difference | *p*-value | Significance |
|---|---|---|---|
| *P.ci.* CF. - ½ MSB | 2.52E+5 | 2.041E-1 | |
| *P.i.* CF - ½ MSB | 2.21E+5 | 3.058E-1 | |
| *P.u.* CF - ½ MSB | -5.07E+5 | 2.776E-3 | ** |
| *P.i.* CF - *P.ci.* CF | -3.15E+4 | 9.939E-1 | |
| *P.u.* CF - *P.ci.* CF | -7.59E+5 | 2.804E-5 | *** |
| *P.u.* CF - *P.i.* CF | -7.28E+5 | 4.890E-5 | *** |

* $p$ <0.05, ** $p$ <0.01, *** $p$ <0.001

Adding IAA or any dilution of *P. cryptoirregulare* or *P. irregulare* CF had little effect on the GFP expression of DR5::GFP in the quiescent centre and columella regions of the root tip (Appendix B-Figure B5). In contrast, reduced expression in these regions was visible relative to the increase of *P. ultimum* var. *ultimum* CF. Little to no expression was observed in the lowest cells upon exposure to 0.5x *P. ultimum* var. *ultimum* CF.

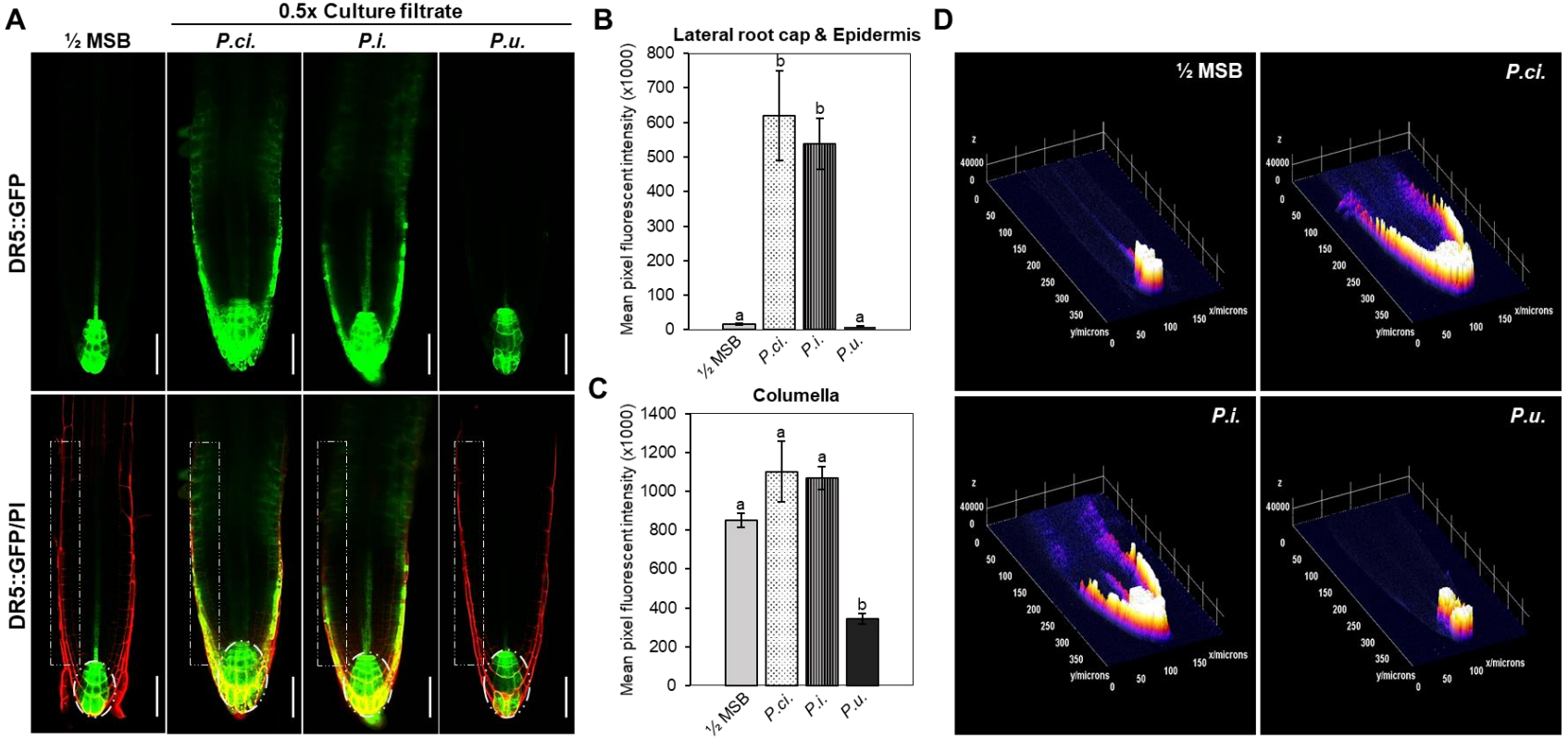


**Figure 5.6 Altered auxin concentrations in the root tips of *Arabidopsis* DR5::GFP seedlings upon exposure to culture filtrates of *Pythium* species. A.** Propidium iodide(PI)-stained *Arabidopsis* seedlings expressing the auxin reporter construct DR5::GFP, grown vertically on ½ MS media in the absence (½ Murashige and Skoog broth/½ MSB) or presence of *Pythium cryptoirregulare* (*P.ci.*), *Pythium irregulare* (*P.i.*, DOAMC 870 BR) and *Pythium ultimum* var. *ultimum* (*P.u.*, DAOMC 628 BR) culture filtrates. Images showing GFP signals were captured after 6 days of incubation at 22 °C, with the Argon laser of the LSM 880 confocal laser-scanning microscope using the following excitation/emission settings: 488/505-530 nm for the visualization of GFP while PI was observed with 488/>650 nm wavelengths. Scale bars = 50 µm. **B** and **C**. Signal intensity of GFP in the lateral root cap and epidermis (**B**) and quiescent center and columella (**C**). The mean fluorescence intensity (per pixel) of the selected areas, as emphasized in **A**, was measured in 6 roots per genotype, followed by subtraction of the background fluorescence (16-bit images). Mean ± SD, $P < 0.05$, One-way ANOVA. **D**. Intensity quantification of the GFP signals of the root tips using a three-dimensional plot and a color scale of blue-red-white, where blue indicates a low intensity and white a high intensity.

### 5.3.3 Reduced root growth inhibition in auxin insensitive mutants in the presence of metabolites secreted by *Pythium* species

During the auxin sensitivity assay, several important events were observed that contributed to the suspicion of auxin-involvement. First, the previously observed root growth inhibition of wildtype Col-0 upon exposure to *Pythium* CF or IAA was present in seedlings during this assay. Figure 5.7 shows *A. thaliana* Col-0 seedlings and the *axr1-3*, *axr4-2* and *aux1-7* mutants grown on ½ MSA containing either MSB, 0.25x CF or MSB with 100 nM IAA, 14 days after incubation. Focussing exclusively on the Col-0, a clear difference can be seen in root length between the long roots after the ½ MSB treatment (negative control) and the shorter roots caused by the 0.25x and 0.5x *Pythium* CF treatments, which was confirmed statistically (Table 5.7). Moreover, the additional 0.05x CF concentrations that were tested in this assay proved that low CF concentrations do not inhibit root growth significantly compared to the root development on ½ MSA with uninoculated MSB (Appendix C-Table C1).

In case of the auxin treatments, the 100 nM IAA caused the most significant root inhibition and showed great similarities in root inhibition to the 0.25x and 0.5x CF treatments. Meanwhile, 50 nM caused a low significant inhibition, while the molarities 1 nM and 10 nM caused no significant inhibition.

**Table 5.7 List of differences according to R using the difflsmeans function for pairwise comparison between the root length of *Arabidopsis thaliana* Col-0 seedlings grown on media containing uninoculated ½ Murashige and Skoog broth, and media containing *Pythium* culture filtrates or IAA, all after 14 days of incubation**

| Treatment | Concentration | *p*-value | Level of significance* |
|---|---|---|---|
| *P. cryptoirregulare* | 0.05x | 9.30E-01 | |
| | 0.25x | 2.76E-03 | ** |
| | 0.5x | 4.19E-07 | *** |
| *P. irregulare* | 0.05x | 4.09E-01 | |
| | 0.25x | 2.20E-05 | *** |
| | 0.5x | 2.78E-07 | *** |
| *P. ultimum* var. *ultimum* | 0.05x | 8.69E-01 | |
| | 0.25x | 4.48E-06 | *** |
| | 0.5x | 5.44E-07 | *** |
| IAA | 1 nM | 7.71E-02 | |
| | 10 nM | 7.91E-01 | |
| | 50 nM | 1.52E-02 | * |
| | 100 nM | 5.96E-04 | *** |

* p <0.05, ** p <0.01, *** p <0.001

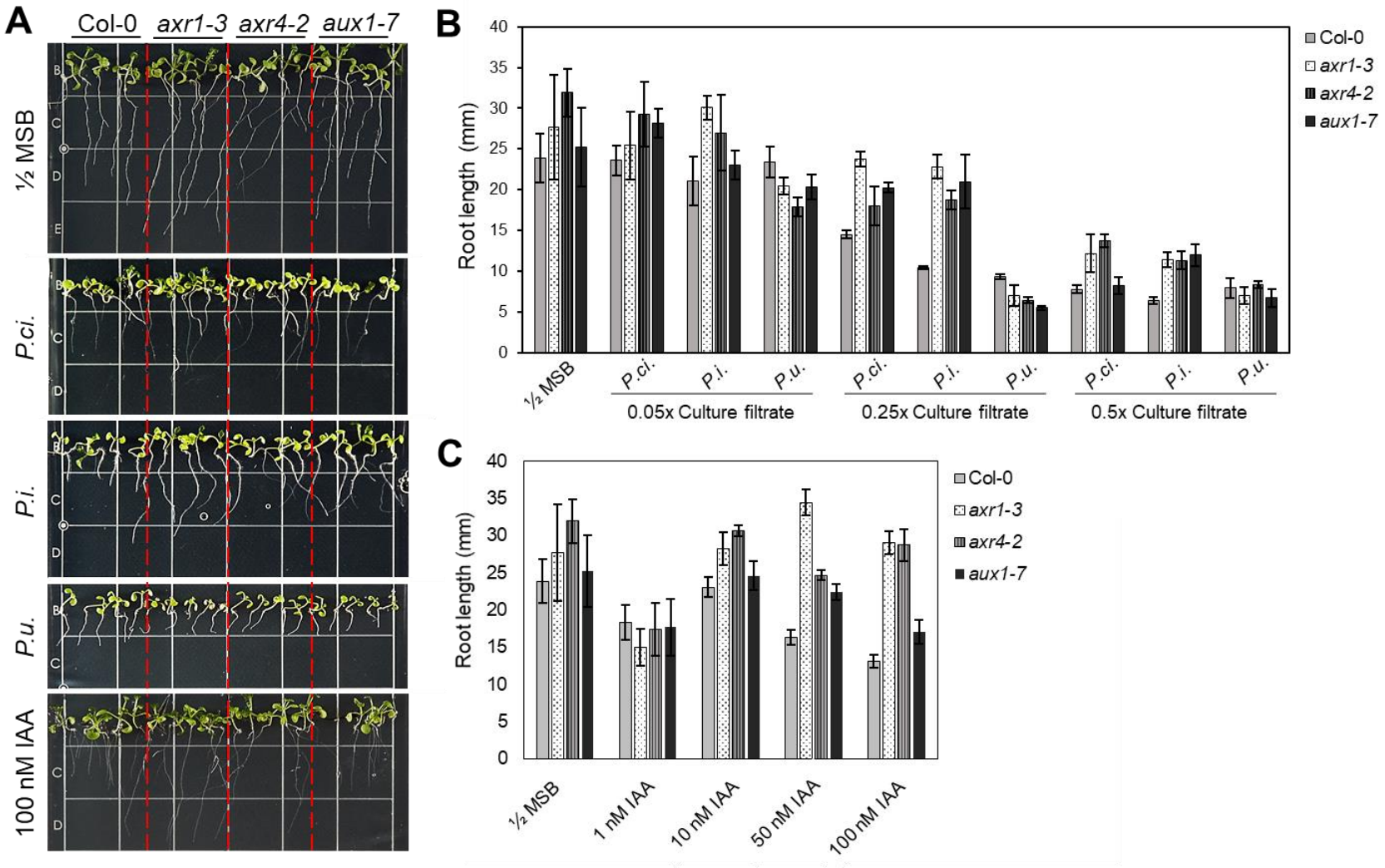


**Figure 5.7 Auxin sensitivity assay presenting the difference in root growth inhibition between *Arabidopsis thaliana* Col-0 roots and roots from the auxin insensitive mutants *axr3-1*, *axr4-2* and *aux1-7*, all grown in the presence of *Pythium cryptoirregulare* (*P.ci.*), *Pythium irregulare* (*P.i.*, DOAMC 870 BR) and *Pythium ultimum* var. *ultimum* (*P.u.*, DAOMC 628 BR) culture filtrates or IAA.** Photos were taken after 14 days of incubation at 22°C. **A.** Photos of the *A. thaliana* seedlings grown in the presence of either Murashige and Skoog broth (½ MSB), 0.25x *Pythium* culture filtrates, or 100 nM IAA. **B.** Visualization of the mean root lengths of *A. thaliana* Col-0 seedlings and auxin insensitive mutants upon exposure to ½ MSB or *Pythium* culture filtrates. **C**. Visualization of the mean root lengths of *A. thaliana* Col-0 seedlings and auxin insensitive mutants upon exposure to ½ MSB or IAA.

When comparing the inhibition caused by the IAA treatments with the inhibition caused by CF treatments, it seems that the presence of 0.5x CF caused an even greater inhibition than 100 nM IAA. This suggested that if the secreted metabolites identify as auxins, the undiluted *Pythium* species would have secreted over 200 nM IAA after 10 days of growth in ½ MSB.

Furthermore, to better estimate the secreted concentration of the auxin-like metabolites, a standard curve was generated from the mean root lengths of seedlings that were grown in the presence of 1, 10, 50, or 100 nM IAA (Figure 5.8). Both a linear (1) and an exponential (2) regression were fitted to the graph, presenting two different potential relations between IAA concentrations and *Arabidopsis* root lengths. These regressions lead to the equations

(1) Mean root length (mm) = -0.09104 × IAA concentration (nM) + 21.8616

(2) Mean root length (mm) = $e^{3.046580} \times (e^{-0.004846})^{\text{IAA concentration (nM)}}$

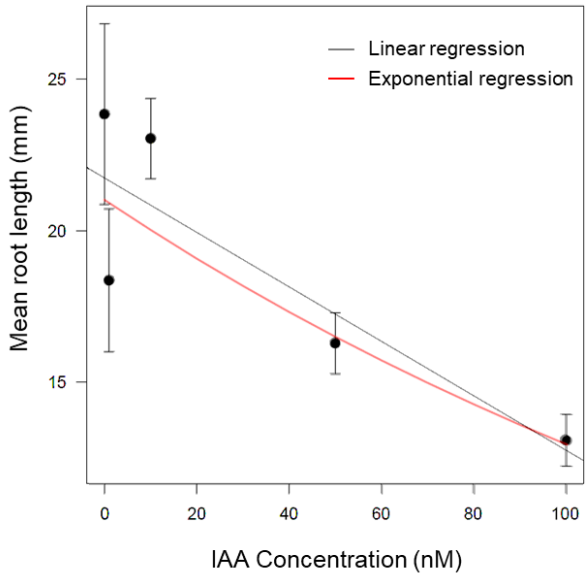


**Figure 5.8 Standard curve, generated from mean root lengths (mm) after incubation in the presence of different IAA concentrations.** The data points are based on 5 *Arabidopsis thaliana* Col-0 seedlings that were grown for 14 days on ½ MSA containing 1, 10, 50, or 100 nM IAA. A linear (**black**) and a exponential (**red**) regression line were generated using the R software, resulting in the following equations: "Mean root length (mm) = -0.09104 * IAA concentration (nM) + 21.86166" for the linear regression, and "Mean length (mm) = e^ 3.046580 * (e^-0.004846 ) ^ IAA concentration (nM)" for the exponential regression.

Estimating auxin concentration based on the linear and exponential regressions resulted in auxin concentrations of approximately 245 nM to 459 nM for the three tested *Pythium* species (Table 5.8). Of these species, *P. irregulare* secreted the highest concentration of auxin, followed by *P. ultimum* var. *ultimum* and *P. cryptoirregulare*, respectively. However, the auxin estimation for *P. ultimum* var. *ultimum* is in this case irrelevant, as this species is likely secreting metabolites other than auxin.

**Table 5.8 Estimated concentrations (nM) of auxin-like metabolites secreted by *Pythium* spp. after 10 days of incubation in ½ MSB**

| | Mean root | Linear | | Exponential | |
|---|---|---|---|---|---|
| **Treatment** | **length (mm)** | **Diluted (0.25x)** | **Undiluted (0.5x)** | **Diluted (0.25x)** | **Undiluted (0.5x)** |
| *P. cryptoirregulare* | 10.71 | 122.44 | 244.89 | 139.29 | 278.58 |
| *P. irregulare* | 6.92 | 164.09 | 328.18 | 229.42 | 458.84 |
| *P. ultimum* var. *ultimum* | 7.89 | 153.50 | 307.00 | 202.52 | 405.03 |

The difference in susceptibility to excessive auxin between the Col-0 wildtype and auxin-insensitive mutants was tested first by growing seedlings on ½ MSA containing different concentrations of IAA. In contrast to the little to no difference in root growth for the mutants grown in the presence of 1 or 10 nM IAA, all mutants showed a significant difference for 50 or 100 nM IAA (Table 5.9). This suggested that 1 nM and 10 nM IAA do not cause enough inhibition for the Col-0 wildtype initially, leading to no significant difference compared to the auxin insensitive mutants.

**Table 5.9 List of differences according to R using the difflsmeans function for pairwise comparison between the root length of *Arabidopsis thaliana* Col-0 seedlings and auxin insensitive mutants grown on media containing IAA, all after 14 days of incubation**

| **IAA concentration (nM)** | **Mutant line** | ***p*-value** | **Level of significance*** |
|---|---|---|---|
| 1 | *aux1-7* | 8.28E-1 | |
| | *axr1-3* | 2.81E-1 | |
| | *axr2-4* | 7.55E-1 | |
| 10 | *aux1-7* | 6.24E-1 | |
| | *axr1-3* | 1.09E-1 | |
| | *axr2-4* | 2.09E-2 | * |
| 50 | *aux1-7* | 4.99E-2 | * |
| | *axr1-3* | 1.63E-8 | *** |
| | *axr2-4* | 7.41E-3 | ** |
| 100 | *aux1-7* | 2.24E-1 | |
| | *axr1-3* | 5.67E-7 | *** |
| | *axr2-4* | 8.81E-7 | *** |

* p <0.05, ** p <0.01, *** p <0.001

More importantly, the auxin-insensitive mutants confirmed the suspected auxin-like activity of the metabolites produced by the majority of the tested *Pythium* species (Table 5.10). Due to the variability in initial inoculum for the liquid cultures, two trials were set up to assess the response of the auxin-insensitive mutants to the CFs. When grown in media containing *P. cryptoirregulare* and *P. irregulare* CF, the mutants showed a decreased root growth inhibition on the CFs compared to Col-0 wildtype. As shown in Figure 5.7, the mutant lines were not capable of overcoming higher concentrations of CF or IAA and therefore cause less obvious differences in root length compared to the Col-0 wildtype. Therefore, after the two trials, statistical tests were performed, focussing on the 0.25x CF treatments in which all mutant lines had shown a significantly reduced inhibition towards the *P. cryptoirregulare* and *P. irregulare*. However, once again, the mutants also confirmed the distinct metabolic activity of *P. ultimum* var. *ultimum*, as no significant difference was found between the mutants and Col-0 grown on *P.u.* CF during either of the trials.

**Table 5.10 List of differences according to R using the difflsmeans function for pairwise comparison between the root length of *Arabidopsis thaliana* Col-0 seedlings and auxin insensitive mutants grown on media containing 0.25x CFs, all after 14 days of incubation**

| | | Trial 1 | | Trial 2 | |
|---|---|---|---|---|---|
| **Treatment** | **Mutant line** | ***p*-value** | **Level of significance*** | **p-value** | **Level of significance*** |
| *P. cryptoirregulare* | *aux1-7* | 2.63E-2 | * | 8.11E-2 | |
| | *axr1-3* | 1.04E-1 | | 3.12E-3 | ** |
| | *axr2-4* | 7.13E-3 | ** | 2.56E-1 | |
| *P. irregulare* | *aux1-7* | 1.11E-2 | * | 8.00E-4 | *** |
| | *axr1-3* | 6.27E-3 | * | 8.88E-5 | *** |
| | *axr2-4* | 3.12E-3 | ** | 7.79E-3 | ** |
| *P. ultimum* var. *ultimum* | *aux1-7* | 3.31E-1 | | 2.15E-1 | |
| | *axr1-3* | 8.62E-1 | | 4.55E-1 | |
| | *axr2-4* | 5.68E-1 | | 3.46E-1 | |

* p <0.05, ** p <0.01, *** p <0.001

Another host response assessment to analyse the effect of *Pythium* CF on *A. thaliana* was established by combining the CFs and IAA in the growth media. This assessment was initiated to find out whether (additional) IAA would worsen the inhibition by increasing the excessive IAA even more, or restore the seedling development by providing IAA during a potentially impaired auxin efflux. This impairment could have caused inadequate amounts of auxin in the root system where it is needed for proper growth. *Arabidopsis thaliana* Col-0 wildtype seedlings responded similarly to additional IAA, whether there was CF present or not (Figure 5.9A). In both cases

additional IAA caused an increase in inhibition and a decrease in gravitropism. However, since seedlings grown in media with CF were already inhibited, the increase in inhibition by the additional IAA was not as pronounced as for seedlings grown in media without CF. Overall, the seedlings did not visually recover from the conditions caused by *Pythium* CF.

The auxin insensitive mutants also showed a similar pattern compared to the seedlings that were grown in the absence of CF (Figure 5.9B). With the exception of the ½ MSB control treatment and the *P. ultimum* var. *ultimum* CF treatment with little or no additional IAA, all the auxin insensitive seedlings seemed to have a similar root length and a longer root when compared to Col-0 wildtype seedlings grown in identical media conditions. The mutant seedlings that were grown in the *P. ultimum* var. *ultimum* CF treatment showed a decreased susceptibility only when an adequate amount of IAA was added to the growth media. No visible differences were observed for its CF alone or with only a small amount of additional IAA. Finally, only *axr1-3* exhibits impaired seedling development upon exposure to 0.25x *P. cryptoirregulare* CF, which was restored by the addition of 10 nM IAA. However, the reason for these responses is yet unknown.

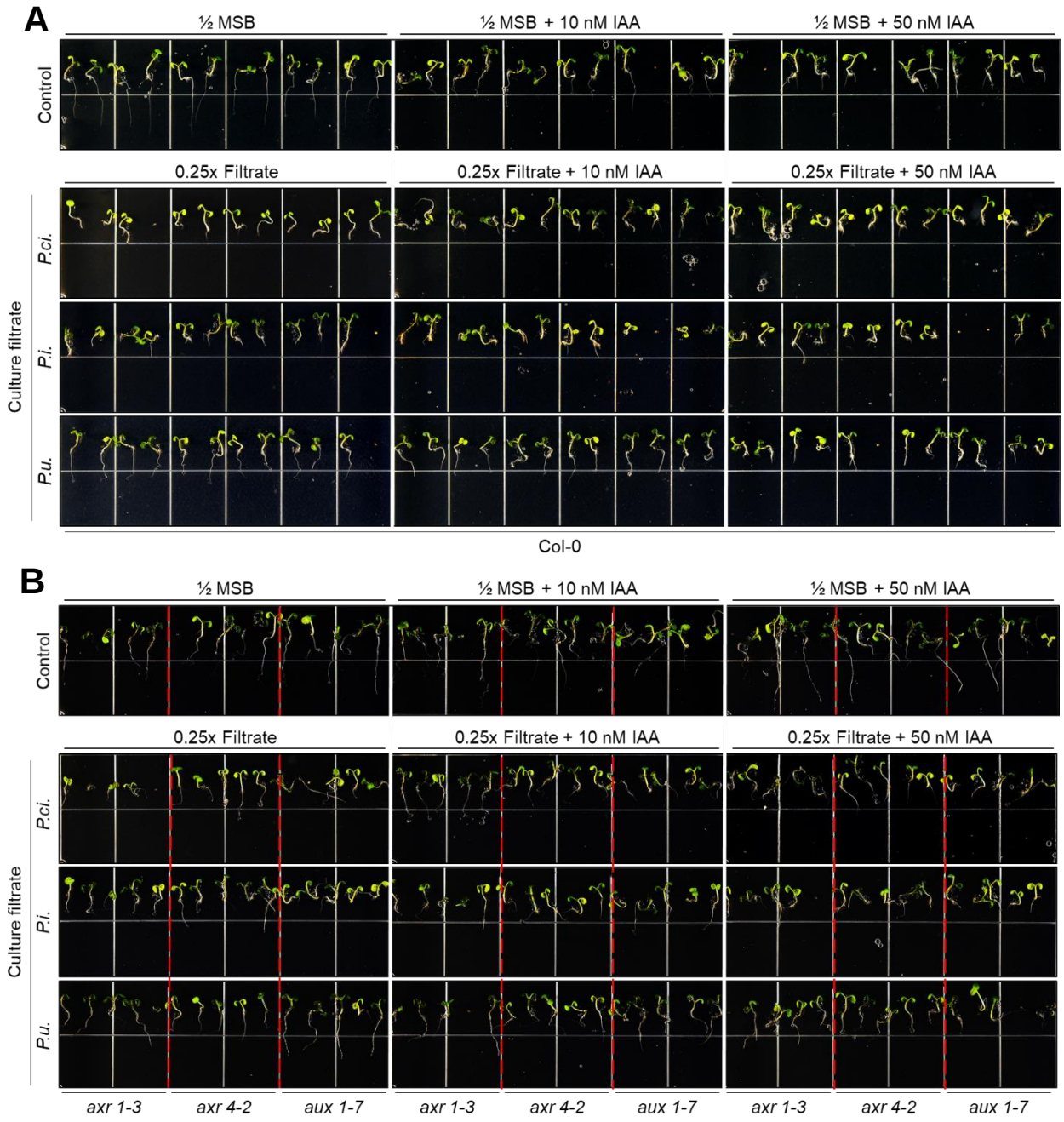


**Figure 5.9 Assessment of the effect of additional IAA on the inhibition of *Arabidopsis thaliana* root growth caused by *Pythium cryptoirregulare* (*P.ci.*), *Pythium irregulare* (*P.i.*, DOAMC 870 BR) and *Pythium ultimum* var. *ultimum* (*P.u.*, DAOMC 628 BR) culture filtrate.** Photos were taken after 14 days of incubation at 22°C. **A**. *Arabidopsis thaliana* Col-0 wildtype seedlings showing an increasing inhibition due to additional CF or IAA. **B**. *Arabidopsis thaliana* auxin-insensitive mutant seedlings showing a mostly consistent decrease in inhibition upon exposure to CF or IAA.

Lastly, a final experiment involved the assessment of adaptive gravitropism upon exposure to IAA or CF, which revealed additional support for earlier findings. Despite their inhibiting properties, additional IAA and *P. cryptoirregulare* and *P. irregulare* CFs did not cause a disturbance in gravitropism, whereas *P. ultimum* var. *ultimum* CF seemed to slightly impair this event (Figure 5.10). A similar observation included the auxin-insensitive mutants which appeared to exhibit a somewhat lower capability of adjusting to gravitropic changes. Once again, the effects of *P. cryptoirregulare* and *P. irregulare* correspond to the effects of IAA while seedlings that were grown on *P. ultimum* var. *ultimum* CF follow a different growth pattern.

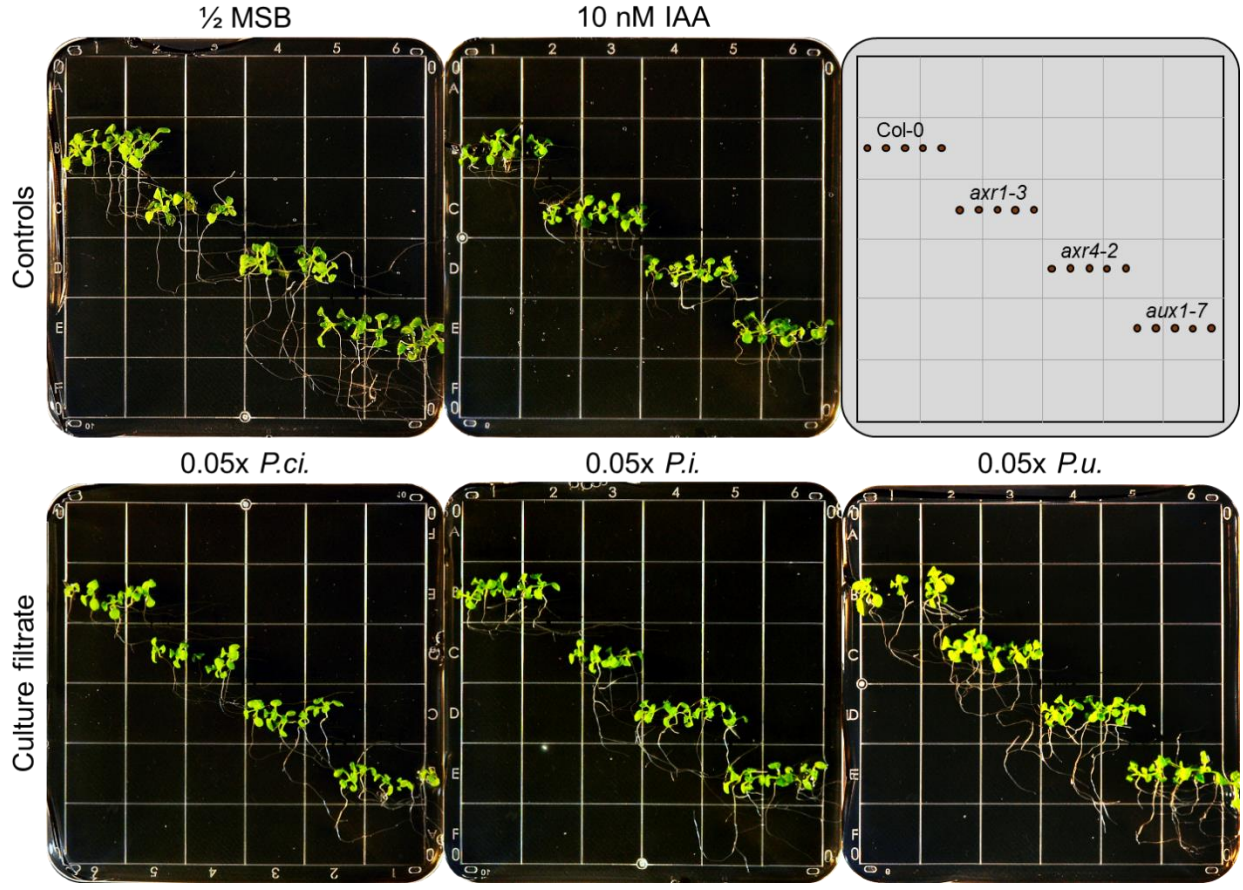


**Figure 5.10 *Arabidopsis thaliana* Col-0 wildtype and auxin-insensitive mutant seedlings showing differences in gravitropism adjustments upon exposure to IAA or *Pythium cryptoirregulare* (*P.ci.*), *Pythium irregulare* (*P.i.*, DOAMC 870 BR) and *Pythium ultimum* var. *ultimum* (*P.u.*, DAOMC 628 BR) culture filtrate.** Photos were taken after 14 days of incubation in 22°C in which seedlings were placed in an upright position for seven days, followed by a 90° direction change for the remaining seven days.

## 5.4 Discussion

The main goal of this research was to assess the metabolic activity of the three *Pythium* species *P. cryptoirregulare, P. irregulare* and *P. ultimum* var. *ultimum*. Initially, after observing a reduced *A. thaliana* seedling development prior to infection, it was hypothesized that *P. cryptoirregulare* secretes auxins or auxin-like metabolites. The additional auxins or auxin-like metabolites would cause a disproportionate amount of auxin, resulting in a hormone imbalance, and therefore growth inhibition. After a standardized filtration procedure was established to isolate the metabolites from the *Pythium* cultures, the metabolite filtrates were integrated into MS media for assessment.

The first assessment included the analysis of the physical and chemical properties of the metabolites, which revealed multiple important observations (Figure 5.1). First, inhibition severity correlated with the CF concentration, meaning that the effect is quantitative and not a matter of presence or absence. Secondly, a reduced inhibition in seedling development and an increase in formation of lateral roots when the filtrate pre-treatment included autoclaving indicated that the molecular structure of the metabolites is not heat-resistant and can be disrupted. Moreover, the metabolites were also observed to be mobile in media after media with and without CF were adjoined and seedlings grown on media without CF showed inhibition, while seedlings grown on media with CF showed a decreased inhibition. Finally, the last assessment led to the conclusion that the filtrate does not have a permanent effect on the seedlings and that the majority of the seedlings can recover after being transferred to media without excessive auxin. All of these observations agree with the molecular structural features and effects of auxin. It is known that the effect of auxin on root growth is concentration-dependent following a bell-curve pattern. Small amounts can induce root formation while higher concentrations cause a hormone imbalance resulting in inhibited root growth (Guan *et al.*, 1997). Moreover, IAA is also known to be unstable after storage under various environmental conditions, but Nissen & Sutter (1988) also observed a 40% loss of IAA after autoclaving, indicating that this plant hormone is temperature-sensitive. Additionally, the metabolites did not seem to be host-specific as the metabolite had an inhibiting effect on *B. napus* cv. Westar as well (Figure 5.2). These metabolites may have a general effect on multiple hosts. Taken together, these findings indicate a strong possibility for the metabolites to be identified as auxins.

At microscopic the level, the most notable effect of the CFs on the seedlings was the lack of elongation in the elongation zone of the roots (Figure 5.3). As auxin is responsible for elongation, these short and swollen cells indicate that the secreted metabolites are auxin-related or at least disturb the auxin transport inside the host.

Furthermore, the GFP-tagged PIN lines provided additional clarification on the effect of the CFs on the auxin distribution and transport. Overall, a reduced auxin efflux was observed in PIN1-GFP, PIN2-GFP, PIN3-GFP and PIN7-GFP when seedlings were grown in the presence of *P. cryptoirregulare* and *P. irregulare* filtrates (Figure 5.5). Most important is the reduced expression that was seen in PIN2-GFP, because a low expression in the PIN2-region, indicating an impaired auxin transport, explains the lack of elongation and polarity and therefore short roots and lack of gravitropism.

The increased expression intensity of DR5::GFP grown on culture filtrates of *P. cryptoirregulare* and *P. irregulare* (Figure 5.6) suggests that auxin(-like) metabolites either accumulated in the columella due to the blocked internal auxin transport into the PIN2 region, entered the host from its surrounding media, or both, where the absorbance of excessive auxins resulted in the impaired auxin transport. Regardless of the exact origin of the higher concentration, both CFs and synthetic IAA resulted in increased GFP expressions in the same regions, again confirming the likeliness of auxin metabolites being secreted by these pathogens.

However, since growth in *P. ultimum* var. *ultimum* CF did not result in a reduced GFP-expression in the auxin efflux or a decreased concentration of auxin in the columella compared to the other two species, it is likely that this species secretes different metabolites and therefore follows a different infection mechanism. The absence of any expression in the root cap and a reduced expression in columella of DR5::GFP grown in culture filtrate of *P. ultimum* var. *ultimum* also confirms the possibility of this species exhibiting a different metabolic activity, potentially antagonistic to auxin uptake and/or distribution.

Root growth inhibition upon exposure to *Pythium* CFs also reoccurred during the auxin sensitivity assay (Figure 5.7). Meanwhile, the significant insensitivity of the auxin-insensitive mutants (*axr1-3*, *axr4-2* & *aux1-7*) to the culture filtrates of *P. cryptoirregulare* and *P. irregulare* evidently suggests that these species secrete auxin(-like) metabolites. The remaining

root inhibition of the mutants grown on the culture filtrate of *P. ultimum* var. *ultimum* suggests, yet again, that this species exhibits a different metabolic activity, possibly unrelated to auxin.

When IAA was added to the CFs, no growth or development recovery was seen in the Col-0 wildtype or auxin-insensitive seedlings. Adding IAA only increased the effects caused by the CF even more. It is thus likely that by adding IAA to the CFs, the causal agent of the inhibition was increased instead of providing the IAA that was unavailable due to impairment caused by the secreted metabolites. In case of the latter, either an improved seedling growth or no change in growth would have been observed.

In the polarity assessment, growth of the Col-0 wildtype and mutant seedlings in the presence of *P. cryptoirregulare* and *P. irregulare* CF was comparable to the IAA treatment. Both the CFs and the IAA treatment showed a 90° angle in the roots, suggesting that the auxin efflux that is responsible for gravitropism was not impaired and that auxin, therefore, could still be distributed to other regions in the root. The root growth was inhibited while the roots were still capable of adjusting the direction of growth. However, low concentrations of CF and IAA were used to observe the ability to adapt to a change in polarity, which reduced the effects of the CFs. It is unclear if higher concentrations will disrupt auxin polarity. At low concentrations, there were already multiple mutant seedlings that showed reduced gravitropism, but this seemed to occur in any treatment, including the uninoculated control. It is therefore likely that this could be a feature of the mutants as described by Hobbie & Estelle (1995), Dharmasiri *et al.* (2006) and Tiryaki & Staswick (2013), rather than the effect of the CF and IAA. In case of *P. ultimum* var. *ultimum*, many seedlings, including the Col-0 wildtype, showed impaired gravitropism. This inability to adapt to gravity changes could be related to the infection mechanism of this pathogen. According to the previous assessments, this mechanism seems to differ from the infection strategy that is followed by *P. cryptoirregulare* and *P. irregulare*.

Overall, several challenges and complications were encountered during these metabolite assessments. The first variable factor was introduced during the inoculation of the MS broths to generate liquid cultures. A standardized size of agar plugs was added, but this does not represent the actual amount of mycelia that was used for inoculation. Therefore, the effect of the CFs could only be compared in relative terms. Despite the approximate concentration of IAA for these CFs that was calculated based on the inhibition severity, the corresponding amount of mycelia that

produces these concentrations are unknown, and therefore, an estimation of metabolite secretion per mycelia weight cannot be estimated.

As mentioned earlier, according to the bell-curve-like effect of auxin on root formation, low amounts of auxin can also induce root formation (Guan *et al.*, 1997). Low CF concentrations (0.05x) and low IAA concentrations (1nM and 10nM) had therefore caused a high variability of expressions in the GFP-tagged PIN-lines and high inhibition variability in the Col-0 wildtype and mutant seedlings. Effects caused by the culture filtrate from *P. cryptoirregulare* were most at risk for causing variability because it appeared to have the lowest IAA concentration. Also, the low concentrations did not cause a significant root length difference of the Col-0; thus, these concentrations did not differ significantly from the auxin-insensitive mutants either. On the other hand, the highest CF and IAA concentrations resulted in inhibitions too severe, which also caused complications. A concentration too high resulted in no root growth and therefore, no root to assess for any purpose. Dilutions were made to resolve this complication, but as a result, the effects of the CFs on *Arabidopsis* seedlings were also diluted. Despite the dilutions, the roots remained to have a swollen appearance which interfered in the imaging process due to a lack of a flatter surface to capture the GFP-expression at the same level throughout the root. The reduced expression closer to the root was therefore only reliable when PI-staining was also observed in the epidermal layer of the same region.

# CHAPTER 6

## GENERAL DISCUSSION AND CONCLUSION

After establishing induced growth of mycelia in RA, oospores and sporangia formation in CMA and appressoria formation in RA, these structures of the *Pythium* candidate were carefully observed. Comparison of these structures between the *Pythium* candidate and the reference species *P. irregulare* and *P. ultimum* var. *ultimum* showed great similarities with *P. irregulare* but fewer similarities with *P. ultimum* var. *ultimum*. However, molecular methods were applied to identify the candidate as morphological features were practically identical to *P. irregulare*. In the end, the *Pythium* candidate was identified as *P. cryptoirregulare* and was presented in a phylogenetic tree among other *Pythium* taxa. The difficulty of identifying the *Pythium* candidate based on morphology was not unexpected as *P. cryptoirregulare* is closely related to *P. irregulare* and was previously even identified as *P. irregulare* (Lévesque & de Cock, 2004; Garzón *et al.*, 2007). In contrast, the distinction between the candidate and *P. ultimum* var. *ultimum* was less challenging due to their more distant relationship.

This pathogen belongs to the genus *Pythium*, which is known to follow a necrotrophic lifestyle (Laluk & Mengiste, 2010; Lévesque *et al.*, 2010; Adhikari *et al.*, 2013). During this study, evidence was collected that contradicts this statement. Plasmolysis and neutral red staining were observed in infected *Arabidopsis* host cells, indicating that these cells did not lose viability upon colonization by *P. cryptoirregulare*. Additionally, cells that were surrounding (heavily) infected cells also showed viability, which is not likely when a necrotrophic lifestyle is being pursued because cell wall-degrading enzymes secreted by the necrotroph would then kill these cells prior to infection (Walton, 1996). Furthermore, the inability of Alexa Fluor®633 to stain the hyphae also contributed to the hypothesis of a biotrophic phase. This could potentially be explained by the movement of the hyphae in the apoplastic space that prevented the destruction of the cell, or the formation of an IFM to which the Alexa Fluor®633 cannot bind. Regardless,

all these findings indicate a biotrophic phase and/or interaction as part of the infection mechanism of *P. cryptoirregulare*. This finding can be supported by other Pythium species including the closely related *P. irregulare*, that were observed to exhibit biotrophic structures (Adie *et al.*, 2007; Owen-Going *et al.*, 2008).

Unfortunately, a more detailed understanding and extensive testing of its infection strategy was required to find or create resistance against this pathogen.

Besides the biotrophic phase, another important feature of the infection mechanism was observed in this study. Inhibition of seedling growth and development was observed prior to infection by *P. cryptoirregulare*. Therefore, the liquid culture of this pathogen and its reference species *P. irregulare* and *P. ultimum* var *ultimum* were filtered to isolate the secreted metabolites for assessment. The metabolites were found to be temperature-sensitive and mobile, and the effect caused to the host was concentration-dependant. Furthermore, *Arabidopsis* auxin-insensitive lines *axr1-3*, *axr4-2* and *aux1-7* showed insensitivity to the CFs, indicated by the significantly reduced inhibition compared to the Col-0 wildtype. During all assessments, the effects caused by *P. cryptoirregulare* and *P. irregulare* CFs on the *Arabidopsis* seedlings were similar to identical to effects caused by excessive IAA, and when the CFs were combined with IAA, the CF-caused symptoms worsened. Overall, the chemical features and effect of the metabolites resembled the features and effect of auxin, strongly suggesting that *P. cryptoirregulare* secretes auxin.

Similar disease symptoms, including the growth inhibition, swelling of the root tip and increased root hair development, were observed as a result of *P. aohanidermatum*, *P. sylvaticum* and *P. oligandrum* presence (Blok, 1973; Shimada *et al.*, 1999; Le Floch *et al.*, 2003). The study by Blok (1973) also suggested that *P. paroecandrum* and *P. irregulare* also produce IAA, of which the latter pathogen is closely related to the *P. cryptoirregulare* isolate of this study. That a closely related species is known to produce auxins, could increase the probability of *P. cryptoirregulare* to exhibit this feature as well.

The difference in PIN expression, auxin measurements and auxin sensitivity for *P. ultimum* var. *ultimum* has been detected before. Earlier studies also have recorded these findings which raised the question if this species excretes toxins that cause similar symptoms (Blok, 1973; Rey *et al.*, 2001; Gravel *et al.*, 2007).

In conclusion, inhibition of root development by secreting excessive auxins would affect the overall seedling development and therefore temporarily prevent suberization. This strategy will make the host susceptible for an extended period by prolonging the early seedling stage that is targeted by this pathogen. This strategy is therefore very effective in increasing infection success and could play a crucial role in the infection mechanism of *P. cryptoirregulare*.

# CHAPTER 7

## FUTURE PERSPECTIVE

In this study, only *P. cryptoirregulare* was studied focussing on the physical infection strategy. Future studies could include inoculation with related species, *P. irregulare* and *P. ultimum* var. *ultimum*, to determine whether these species follow a different physical infection strategy under the conditions of this study. Additionally to the phenotypic differences in infection strategy, molecular methods could also be included to provide genetic differentiation in effectors or infection-related genes.

Furthermore, as the initial penetration sites observed in this study are the result of infection by using *A. thaliana* seedlings as bait in sterile water, the experiment can also be repeated under natural conditions in the soil. A method has to be developed where mycelial spread and infection can be monitored closely to determine when the host is infected which can then be observed using microscopy after carefully removing the infected tissue from the soil, without detaching the mycelia from the host tissue. Especially the latter would pose a challenge due to the fragility of the mycelia.

In this study, a standardized procedure was established for the assessment of the metabolites produced by the *Pythium* species. Despite the standardized procedure, due to the absence of zoospore production by these species, the MS broths were inoculated with agar plugs instead of a spore suspension, resulting in slight variabilities between the exact amount of mycelia that was added as inoculum. This was also the case during the inoculations of the physical infection assessment, but irrelevant as the infection severity was not focussed on quantity, but more so on quality and individual infection sites.

In contrast to the infection assessment, the metabolite assessment was quantified and compared among *Pythium* CFs and IAA treatments. Detection, identification and measurement of the metabolites would therefore be an extensive addition to the results. Culture filtrate samples

were sent out to the National Research Council (NRC) Canada to provide this identification and quantification through the use of high-performance liquid chromatography (HPLC). These results can then be incorporated into the data to increase the accuracy of the measurements taken during this study.

# LITERATURE CITED

**Adhikari BN, Hamilton JP, Zerillo MM, Tisserat N, Lévesque CA, Buell CR**. **2013**. Comparative genomics reveals insight into virulence strategies of plant pathogenic oomycetes. *PLoS ONE* **8**: e75072.

**Adie BAT, Pérez-Pérez J, Pérez-Pérez MM, Godoy M, Sánchez-Serrano JJ, Schmelz EA, Solano R**. **2007**. ABA is an essential signal for plant resistance to pathogens affecting JA biosynthesis and the activation of defenses in *Arabidopsis*. *Plant Cell* **19**: 1665–1681.

**Agrawal S**. **2018**. *Arabidopsis thaliana* as a model organism to study plant-pathogen interactions. In: Singh A, Singh IK, eds. Molecular Aspects of Plant-Pathogen Interaction. Singapore: Springer Singapore, 1–20.

**Agricultural Research Service - ARS**. **2015**. Solid media.

**Anderson RG, Deb D, Fedkenheuer K, McDowell JM**. **2015**. Recent progress in RXLR effector research. *Molecular Plant-Microbe Interactions* **28**: 1063–1072.

**Bailey JA, O'Connell RJ, Pring RJ, Nash C**. **1992**. Infection strategies of *Colletotrichum* species. In: Bailey, J.A. and Jeger MJ, ed. *Colletotrichum*: Biology, Pathology and Control. Wallingford: CAB International, 88–120.

**Bala K, Robideau GP, Désaulniers N, de Cock ADAM, Lévesque CA**. **2010**. Taxonomy, DNA barcoding and phylogeny of three new species of *Pythium* from Canada. *Persoonia: Molecular Phylogeny and Evolution of Fungi* **25**: 22–31.

**Baldauf SL, Roger AJ, Wenk-Siefert I, Doolittle WF**. **2000**. A kingdom-level phylogeny of eukaryotes based on combined protein data. *Science* **290**: 972–977.

**Barr SDJ**. **1983**. The zoosporic grouping of plant pathogens - entity or non-entity? *Zoosporic Plant Pathogen*: 43–83.

**de Bary A**. **1866**. Morphologie und physiologie der pilze, flechten und myxomyceten. In: W. Engelmann, Leipzig. 1–338.

**Begum MM, Sariah M, Puteh AB, Zainal Abidin MA, Rahman MA, Siddiqui Y**. **2010**. Field performance of bio-primed seeds to suppress *Colletotrichum truncatum* causing damping-off and seedling stand of soybean. *Biological Control* **53**: 18–23.

**Benhamou N, le Floch G, Vallance J, Gerbore J, Grizard D, Rey P**. **2012**. *Pythium oligandrum*: An example of opportunistic success. *Microbiology (United Kingdom)* **158**: 2679–2694.

**Bennett R**. **2015**. Global challenges in plant pathology. *Journal of General Plant Pathology* **81**: 487–489.

**Bent AF, Mackey D**. **2007**. Elicitors, effectors, and R genes: The new paradigm and a lifetime supply of questions. *Annual Review of Phytopathology* **45**: 399–436.

**Berg LE, Miller SS, Dornbusch MR, Samac DA**. **2017**. Seed rot and damping-off of alfalfa in Minnesota caused by *Pythium* and *Fusarium* species. *Plant Disease* **101**: 1860–1867.

**Bhadauria V, Banniza S, Wei Y, Peng YL**. **2009**. Reverse genetics for functional genomics of phytopathogenic fungi and oomycetes. *Comparative and Functional Genomics* **2009**: 380719.

**Bhadauria V, Miraz P, Kennedy R, Banniza S, Wei Y**. **2010**. Dual trypan-aniline blue fluorescence staining methods for studying fungus-plant interactions. *Biotechnic and Histochemistry* **85**: 99–105.

**Biemelt S, Tschiersch H, Sonnewald U**. **2004**. Impact of altered gibberellin metabolism on biomass accumulation, lignin biosynthesis, and photosynthesis in transgenic tobacco plants. *Plant physiology* **135**: 254–265.

**Blake SN, Barry KM, Gill WM, Reid JB, Foo E**. **2016**. The role of strigolactones and ethylene in disease caused by *Pythium irregulare*. *Molecular Plant Pathology* **17**: 680–690.

**Blok I**. **1973**. A growth-regulating substance produced by *Pythium sylvaticum*. *Netherlands Journal of Plant Pathology* **79**: 266–276.

**Brodhun F, Cristobal-Sarramian A, Zabel S, Newie J, Hamberg M, Feussner I**. **2013**. An iron 13S-lipoxygenase with an α-linolenic acid specific hydroperoxidase activity from *Fusarium oxysporum*. *PloS one* **8**: e64919–e64919.

**Van Buyten E, Höfte M**. **2013**. *Pythium* species from rice roots differ in virulence, host colonization and nutritional profile. *BMC Plant Biology* **13**.

**Castro A, Vidal S, Ponce de León I**. **2016**. Moss pathogenesis-related-10 protein enhances resistance to *Pythium irregulare* in *Physcomitrella patens* and *Arabidopsis thaliana*. *Frontiers in Plant Science* **7**: 1–17.

**Centis S, Guillas I, Séjalon N, Esquerré-Tugayé MT, Dumas B**. **1997**. Endopolygalacturonase genes from *Colletotrichum lindemuthianum*: Cloning of CLPG2 and comparison of its expression to that of CLPG1 during saprophytic and parasitic growth of the fungus. *Molecular Plant-Microbe Interactions* **10**: 769–775.

**Chanclud E, Morel JB**. **2016**. Plant hormones: A fungal point of view. *Molecular plant pathology* **17**: 1289–1297.

**Chen HY, Huh JH, Yu YC, Ho LH, Chen LQ, Tholl D, Frommer WB, Guo WJ**. **2015**. The *Arabidopsis* vacuolar sugar transporter SWEET2 limits carbon sequestration from roots and restricts *Pythium* infection. *Plant Journal* **83**: 1046–1058.

**Chen Y, Yordanov Y, Ma C, Strauss S, Busov V**. **2013**. DR5 as a reporter system to study auxin response in Populus. *Plant cell reports* **32**: 453–463.

**Chun SC, Schneider RW**. **1998**. Sites of infection by *Pythium* species in rice seedlings and effects of plant age and water depth on disease development. *Phytopathology* **88**: 1255–1261.

**Clark LH, Harris WH**. **1981**. Observations on the root anatoma or rice (*Oryza sativa* L.). *American Journal of Botany* **68**: 154–161.

**Cline ET, Farr DF, Rossman AY**. **2008**. A synopsis of *Phytophthora* with accurate scientific names, host range, and geographic distribution. *Plant Health Progress* **9**: 32.

**Cosgrove DJ, Li LC, Cho H-T, Hoffmann-Benning S, Moore RC, Blecker D**. **2002**. The growing world of expansins. *Plant and Cell Physiology* **43**: 1436–1444.

**Daughtrey ML, Benson DM**. **2005**. Principles of plant health management for ornamental plants. *Annual Review of Phytopathology* **43**: 141–169.

**Dean R, Van Kan JAL, Pretorius ZA, Hammond-Kosack KE, Di Pietro A, Spanu PD, Rudd JJ, Dickman M, Kahmann R, Ellis J, *et al.* 2012**. The Top 10 fungal pathogens in molecular plant pathology. *Molecular Plant Pathology* **13**: 414–430.

**Denancé N, Sánchez-Vallet A, Goffner D, Molina A**. **2013**. Disease resistance or growth: The role of plant hormones in balancing immune responses and fitness costs. *Frontiers in Plant Science* **4**: 155.

**Dharmasiri S, Swarup R, Mockaitis K, Dharmasiri N, Singh SK, Kowalchyk M, Marchant A, Mills S, Sandberg G, Bennett MJ, *et al.* 2006**. AXR4 is required for localization of the auxin influx facilitator AUX1. *Science* **312**: 1218 LP – 1220.

**Dick MW**. **1991**. Keys to Pythium. *Mycologia* **83**: 386.

**Díez-Navajas AM, Greif C, Poutaraud A, Merdinoglu D**. **2007**. Two simplified fluorescent staining techniques to observe infection structures of the oomycete *Plasmopara viticola* in grapevine leaf tissues. *Micron* **38**: 680–683.

**Erwin DC, Ribeiro OK**. **1996**. *Phytophthora* diseases worldwide. In: Experimental Agriculture. St Paul, Minnesota: The American Phytopathological Society, 125–130.

**Felsenstein J**. **1985**. Confidence limits on phylogenies: An approach using the bootstrap. *Evolution* **39**: 783–791.

**Feraru E, Friml J**. **2008**. PIN polar targeting. *Plant Physiology* **147**: 1553–1559.

**Fisher A**. **1892**. Rabenhorst's Kryptogamen-flora. *Pilze-Phycomycetes* **1**: 1–505.

**Fisher MC, Henk DA, Briggs CJ, Brownstein JS, Madoff LC, McCraw SL, Gurr SJ**. **2012**. Emerging fungal threats to animal, plant and ecosystem health. *Nature* **484**: 186–194.

**Le Floch G, Rey P, Benizri E, Benhamou N, Tirilly Y**. **2003**. Impact of auxin-compounds produced by the antagonistic fungus *Pythium oligandrum* or the minor pathogen *Pythium* group F on plant growth. *Plant and Soil* **257**: 459–470.

**Garrido Haro P, Garzón C**. **2016**. Molecular characterization of *Pythium* populations in ornamental greenhouse and nursery crops. Oklahoma State University. Oklahoma. : 1–103.

**Garzón CD, Geiser DM, Moorman GW**. **2005**. Diagnosis and population analysis of *Pythium* species using AFLP fingerprinting. *Plant Disease* **89**: 81–89.

**Garzón CD, Molineros JE, Yánez JM, Flores FJ, del Mar Jiménez-Gasco M, Moorman GW**. **2011**. Sublethal doses of mefenoxam enhance *Pythium* damping-off of geranium. *Plant Disease* **95**: 1233–1238.

**Garzón CD, Yánez JM, Moorman GW**. **2007**. *Pythium cryptoirregulare*, a new species within the *P. irregulare* complex. *Mycologia* **99**: 291–301.

**George E, Hall M, De Klerk G-J**. **2008**. Plant growth regulators I: Introduction; Auxins, their analogues and inhibitors. *Plant Propagation by Tissue Culture 3rd Edition* **1**: 175–204.

**Geraats BPJ, Bakker PAHM, van Loon LC**. **2002**. Ethylene insensitivity impairs resistance to soilborne pathogens in tobacco and *Arabidopsis thaliana*. *Molecular Plant-Microbe Interactions*® **15**: 1078–1085.

**Govrin EM, Levine A**. **2000**. The hypersensitive response facilitates plant infection by the necrotrophic pathogen *Botrytis cinerea*. *Current Biology* **10**: 751–757.

**Gravel V, Antoun H, Tweddell RJ**. **2007**. Effect of indole-acetic acid (IAA) on the development of symptoms caused by *Pythium ultimum* on tomato plants. *European Journal of Plant Pathology* **119**: 457–462.

**Green JR, Pain NA, Cannell ME, Leckie CP, McCready S, Mitchell AJ, Callow JA, Jones GL, O'Connell RJ, Mendgen K**. **1995**. Analysis of differentiation and development of the specialized infection structures formed by biotrophic fungal plant pathogens using monoclonal antibodies. *Canadian Journal of Botany* **73**: 408–417.

**Guan H, Huisman P, Klerk G-J de**. **1997**. Die bewurzelung von apfelsprossscheiben in vitro wird durch eine indol-3-essigsaeure-verarmung des naehrmediums beeinflusst. *Angewandte Botanik (Germany)* **71**: 80–84.

**Hahn M, Mendgen K**. **2001**. Signal and nutrient exchange at biotrophic plant-fungus interfaces. *Current Opinion in Plant Biology* **4**: 322–327.

**Hancock JG**. **1983**. Seedling diseases of alfalfa in California. *Plant Disease* **67**: 1203–1208.

**Hardison SE, Brown GD**. **2012**. C-type lectin receptors orchestrate antifungal immunity. *Nature Immunology* **13**: 817–822.

**Hausbeck MK, Lamour KH**. **2004**. *Phytophthora capsici* on vegetable crops: Research progress and management challenges. *Plant Disease* **88**: 1292–1303.

**Heath MC**. **1976**. Ultrastructural and functional similarity of the haustorial neckband of rust fungi and the Casparian strip of vascular plants. *Canadian Journal of Botany* **54**: 2484–2489.

**Hendrix FF, Campbell WA**. **1973**. *Pythium*s as plant pathogens. *Annual Review of Phytopathology* **11**: 77–98.

**Hobbie L, Estelle M**. **1995**. The *axr4* auxin-resistant mutants of *Arabidopsis thaliana* define a gene important for root gravitropism and lateral root initiation. **7**: 211–220.

**Hood ME, Shew HD**. **1996**. Applications of KOH-aniline blue fluorescence in the study of plant- fungal interactions. *Phytopathology* **86**: 704–708.

**Hopkins WG**. **1995**. Hormones I: Auxins. In: Introduction to Plant Physiology. John Wiley & sons, New York, 305–321.

**Hückelhoven R**. **2007**. Cell wall–associated mechanisms of disease resistance and susceptibility. *Annual Review of Phytopathology* **45**: 101–127.

**Van Iersel MW, Bugbee B**. **1996**. Phytotoxic effects of benzimidazole fungicides on bedding plants. *Journal of the American Society for Horticultural Science* **121**: 1095–1102.

**Innes R**. **1995**. *Arabidopsis* as a model host in molecular plant pathology. In: Singh RP, Singh US, eds. Molecular Methods in Plant Pathology. CRC Press, Inc., 61–87.

**Inomata M, Hirai N, Yoshida R, Ohigashi H**. **2004**. The biosynthetic pathway to abscisic acid via ionylideneethane in the fungus *Botrytis cinerea*. *Phytochemistry* **65**: 2667–2678.

**Janardhanan KK, Husain A**. **1974**. Production of a toxic metabolite and pectolytic enzyme by *Pythium butleri*. *Mycopathologia et mycologia applicata* **52**: 325–330.

**Jones R. 1985**. Fungicides for bedding plants. *Bedding Plant Inc. News* **4**: 37–44.

**Kahmann R, Basse C**. **2001**. Fungal gene expression during pathogenesis-related development and host plant colonization. *Current Opinion in Microbiology* **4**: 374–380.

**Kamoun S, Furzer O, Jones JDG, Judelson HS, Ali GS, Dalio RJD, Roy SG, Schena L, Zambounis A, Panabières F, *et al.* 2015**. The Top 10 oomycete pathogens in molecular plant pathology. *Molecular Plant Pathology* **16**: 413–434.

**Kamoun S, Huitema E, Vleeshouwers VGAA**. **1999**. Resistance to oomycetes: A general role for the hypersensitive response? *Trends in Plant Science*.

**Koh S, André A, Edwards H, Ehrhardt D, Somerville S**. **2005**. *Arabidopsis thaliana* subcellular responses to compatible *Erysiphe cichoracearum* infections. *Plant Journal* **44**: 516–529.

**Koornneef M, Van Eden J, Hanhart CJ, Stam P, Braaksma FJ, Feenstra WJ**. **1983**. Linkage map of *Arabidopsis thaliana*. *Journal of Heredity* **74**: 265–272.

**Kumar S, Stecher G, Li M, Knyaz C, Tamura K**. **2018**. MEGA X: Molecular evolutionary genetics analysis across computing platforms. *Molecular Biology and Evolution* **35**: 1547–1549.

**Lacomme C**. **2015**. Plant pathology techniques and protocols. In: Methods in Molecular Biology 1302. Humana Press Inc., Springer, 6–7.

**Laluk K, Mengiste T**. **2010**. Necrotroph attacks on plants: Wanton destruction or covert extortion? *The Arabidopsis Book* **8**: e0136.

**Larson R**. **1987**. Growing concerns. Pest control: How much is enough? *Marketletter* **2**: 5.

**Latijnhouwers M, de Wit PJGM, Govers F**. **2003**. Oomycetes and fungi: Similar weaponry to attack plants. *Trends in Microbiology* **11**: 462–469.

**Lévesque CA, Brouwer H, Cano L, Hamilton JP, Holt C, Huitema E, Raffaele S, Robideau GP, Thines M, Win J, *et al.* 2010**. Genome sequence of the necrotrophic plant pathogen *Pythium ultimum* reveals original pathogenicity mechanisms and effector repertoire. *Genome Biology* **11**: R73.

**Lévesque CA, de Cock AWAM**. **2004**. Molecular phylogeny and taxonomy of the genus *Pythium*. *Mycological Research* **108**: 1363–1383.

**Lincoln C, Britton JH, Estelle M**. **1990**. Growth and development of the *axr1* mutants of *Arabidopsis*. *Plant Cell* **2**: 1071–1080.

**Ludwig-Müller J**. **2015**. Bacteria and fungi controlling plant growth by manipulating auxin : Balance between development and defense. *Journal of Plant Physiology* **172**: 4–12.

**Lumsden RD, Locke JC**. **1989**. Biological control of damping-off caused by *Pythium ultimum* and *Rhizoctonia solani* with *Gliocladium virens* in soilless mix. *Disease Control and Pest Management Biological* **79**: 361–366.

**Mao W, Lewis JA, Hebbar PK, Lumsden RD**. **1997**. Seed treatment with a fungal or a bacterial antagonist for reducing corn damping-off caused by species of *Pythium* and *Fusarium*. *Plant Disease* **81**: 450–454.

**Martin FN**. **1995**. *Pythium*. Pathogenesis and host specificity in plant diseases : histopathological, biochemical, genetic, and molecular bases. In: Singh US, Singh RP, Kohmoto K, eds. Oxford, U.K.; Tarrytown, N.Y.: Pergamon, 17–36.

**Martin FN, Loper JE**. **1999**. Soilborne plant diseases caused by *Pythium* spp.: Ecology, epidemiology, and prospects for biological control. *Critical Reviews in Plant Sciences* **18**: 111–181.

**Matsumoto C, Kageyama K, Suga H, Hyakumachi M**. **1999**. Phylogenetic relationships of *Pythium* species based on ITS and 5.8S sequences of the ribosomal DNA. *Mycoscience* **40**: 321–331.

**Matteoni J**. **1987**. No controlling root rot complexes. *Bedding Plant Inc. News* **18**: 6–7.

**Meinke DW, Cherry JM, Dean C, Rounsley SD, Koornneef M**. **1998**. *Arabidopsis thaliana*: A model plant for genome analysis. *Science* **282**: 662–682.

**Mendgen K, Hahn M**. **2002**. Plant infection and the establishment of fungal biotrophy. *Trends in Plant Science* **7**: 352–356.

**Mittag J, Šola I, Rusak G, Ludwig-Müller J**. **2015**. *Physcomitrella patens* auxin conjugate synthetase (GH3) double knockout mutants are more resistant to *Pythium* infection than wild type. *Journal of Plant Physiology* **183**: 75–83.

**Möbius N, Hertweck C**. **2009**. Fungal phytotoxins as mediators of virulence. *Current Opinion in Plant Biology* **12**: 390–398.

**Money NP, Davis CM, Ravishankar JP**. **2004**. Biomechanical evidence for convergent evolution of the invasive growth process among fungi and oomycete water molds. *Fungal Genetics and Biology* **41**: 872–876.

**Moore LD, Couch HB**. **1968**. Influence of calcium nutrition on pectolytic and cellulolytic enzyme activity of extract of highland bent grass foliage blight by *Pythium ultimum.* *Phytopathology* **58**: 833–838.

**Moorman GW, Kang S, Geiser DM, Kim SH**. **2002**. Identification and characterization of *Pythium* species associated with greenhouse floral crops in Pennsylvania. *Plant Disease* **86**: 1227–1231.

**Moorman GW, Kim SH**. **2004**. Species of *Pythium* from greenhouses in Pennsylvania exhibit resistance to propamocarb and mefenoxam. *Plant Disease* **88**: 630–632.

**Morrissey JP, Osbourn AE**. **1999**. Fungal resistance to plant antibiotics as a mechanism of pathogenesis. **63**: 708–724.

**Münch S, Lingner U, Floss DS, Ludwig N, Sauer N, Deising HB**. **2008**. The hemibiotrophic lifestyle of *Colletotrichum* species. *Journal of Plant Physiology* **165**: 41–51.

**Nissen SJ, Sutter EG**. **1988**. Stability of IAA and IBA in nutrient medium after autoclaving and after storage under various environmental conditions. *HortSci* **23**: 758.

**Nowicki B**. **1997**. Etiology of root parsley damping-off. *Acta Agrobotanica* **50**: 35–40.

**O'Connell RJ, Panstruga R**. **2006**. Tête à tête inside a plant cell: Establishing compatibility between plants and biotrophic fungi and oomycetes. *New Phytologist* **171**: 699–718.

**O'Connell RJ, Ride JP**. **1990**. Chemical detection and ultrastructural localization of chitin in cell walls of *Colletotrichum lindemuthianum*. *Physiological and Molecular Plant Pathology* **37**: 39–53.

**Oliver J, Castro A, Gaggero C, Cascón T, Schmelz E, Castresana C**. **2009**. *Pythium* infection activates conserved plant defense responses in mosses. *Planta* **230**: 569–579.

**Oliver RP, Ipcho SVS**. **2004**. *Arabidopsis* pathology breathes new life into the necrotrophs-vs.-biotrophs classification of fungal pathogens. *Molecular Plant Pathology* **5**: 347–352.

**Owen-Going TN, Beninger CW, Sutton JC, Hall JC**. **2008**. Accumulation of phenolic compounds in plants and nutrient solution of hydroponically grown peppers inoculated with *Pythium aphanidermatum*. *Canadian Journal of Plant Pathology* **30**: 214–225.

**Pais M, Win J, Yoshida K, Etherington GJ, Cano LM, Raffaele S, Banfield MJ, Jones A, Kamoun S, Saunders DGO**. **2013**. From pathogen genomes to host plant processes: The power of plant parasitic oomycetes. *Genome Biology* **14**: 1–10.

**Paulitz T, Belanger R**. **2001**. Biological control in greenhouse systems. *Annual Review of Phytopathology* **39**: 103–133.

**Pemberton CL, Salmond GPC**. **2004**. The Nep1-like proteins - A growing family of microbial elicitors of plant necrosis. *Molecular Plant Pathology* **5**: 353–359.

**Perfect SE, Green JR**. **2001**. Infection structures of biotrophic and hemibiotrophic fungal plant pathogens. *Molecular Plant Pathology* **2**: 101–108.

**van der Plaats-Niterink A**. **1981**. Monograph of the genus *Pythium*. *Studies in Mycology* **21**: 1–242.

**Prins TW, Tudzynski P, von Tiedemann A, Tudzynski B, Ten Have A, Hansen ME, Tenberge K, van Kan JAL**. **2000**. Infection strategies of *Botrytis cinerea* and related necrotrophic pathogens. In: Fungal Pathology. Springer Netherlands, 33–64.

**Punja ZK, Yip R**. **2003**. Biological control of damping-off and root rot caused by P*ythium aphanidermatum* on greenhouse cucumbers. *Canadian Journal of Plant Pathology* **25**: 411–417.

**Raven JA**. **1975**. Transport of indoleacetic acid in plant cells in relation to pH and electrical potential gradients, and its significance for polar IAA transport. *New Phytologist* **74**: 163–172.

**Rey P, Leucart S, Désilets H, Bélanger RR, Larue JP, Tirilly Y**. **2001**. Production of indole-3-acetic acid and tryptophol by *Pythium ultimum* and *Pythium* group F: Possible role in pathogenesis. *European Journal of Plant Pathology* **107**: 895–904.

**Rubery PH, Sheldrake AR**. **1974**. Carrier-mediated auxin transport. *Planta* **118**: 101–121.

**Saitou N, Nei M**. **1987**. The neighbor-joining method: A new method for reconstructing phylogenetic trees. *Molecular Biology and Evolution* **4**: 406–425.

**Sánchez-Vallet A, López G, Ramos B, Delgado-Cerezo M, Riviere M-P, Llorente F, Fernández PV, Miedes E, Estevez JM, Grant M, *et al.* 2012**. Disruption of abscisic acid signaling constitutively activates *Arabidopsis* resistance to the necrotrophic fungus *Plectosphaerella cucumerina*. *Plant physiology* **160**: 2109–2124.

**Schroeder KL, Martin FN, de Cock AWAM, Lévesque CA, Spies CFJ, Okubara PA, Paulitz TC**. **2013**. Molecular detection and quantification of *Pythium* species: Evolving taxonomy, new tools, and challenges. *Plant Disease* **97**: 4–20.

**Schwinn FJ, Urech PA**. **1986**. Progress in the chemical control of diseases caused by oomycetes. In: ACS Symposium Series. Fungicide Chemistry. American Chemical Society, 5–89.

**Shimada A, Takeuchi S, Nakajima A, Tanaka S, Kawano T, Kimura Y**. **1999**. Phytotoxicity of indole-3-acetic acid produced by the fungus, *Pythium aphanidermatum*. *Bioscience, Biotechnology and Biochemistry* **63**: 187–189.

**Sideris CP**. **1932**. Taxonomic studies in the family Phythiaceae. II. *Pythium*. *Mycologia* **24**: 14–61.

**Staswick PE, Yuen GY, Lehman CC**. **1998**. Jasmonate signaling mutants of *Arabidopsis* are susceptible to the soil fungus *Pythium irregulare*. *Plant Journal* **15**: 747–754.

**Stephens CT, Powels CC**. **1982**. *Pythium* species causing damping-off of seedling bedding plants in Ohio greenhouses. *Plant Disease* **66**: 731.

**Stergiopoulos I, Collemare J, Mehrabi R, De Wit PJGM**. **2013**. Phytotoxic secondary metabolites and peptides produced by plant pathogenic Dothideomycete fungi. *FEMS Microbiology Reviews* **37**: 67–93.

**Sutton JC, Sopher CR, Owen-Going TN, Liu W, Grodzinski B, Hall JC, Benchimol RL**. **2006**. Etiology and epidemiology of *Pythium* root rot in hydroponic crops: Current knowledge and perspectives. *Summa Phytopathologica* **32**: 307–321.

**Taiz L, Zeiger E**. **1991**. Auxins: Growth and Tropisms. In: Plant Physiology. Benjamin Cunnings, 398–425.

**Tambong JT, de Cock AWAM, Tinker NA, Lévesque CA**. **2006**. Oligonucleotide array for identification and detection of *Pythium* species. *Applied and Environmental Microbiology* **72**: 2691–2706.

**Tamura K, Nei M, Kumar S**. **2004**. Prospects for inferring very large phylogenies by using the neighbor-joining method. *Proceedings of the National Academy of Sciences of the United States of America* **101**: 11030–11035.

**The *Arabidopsis* Genome Initiative**. **2000**. Analysis of the genome sequence of the flowering plant *Arabidopsis thaliana*. *Nature* **408**: 796–815.

**The *Arabidopsis* Information Recourse (TAIRa)**. **2007**. *axr1-3*_Polymorphism: 4769608.

**The *Arabidopsis* Information Resource (TAIRb)**. **2007**. *aux1-7*_Polymorphism:4769605.

**The *Arabidopsis* Information Resource (TAIRc)**. **2006**. *axr4-2*_Polymorphism:4769611.

**Thines M, Kamoun S**. **2010**. Oomycete–plant coevolution: Recent advances and future prospects. *Current Opinion in Plant Biology* **13**: 427–433.

**Thompson JD, Gibson TJ, Plewniak F, Jeanmougin F, Higgins DG**. **1997**. The CLUSTAL X windows interface: Flexible strategies for multiple sequence alignment aided by quality analysis tools. *Nucleic Acids Research* **25**: 4876–4882.

**Thon MR, Nuckles EM, Takach JE, Vaillancourt LJ**. **2002**. CPR1: A gene encoding a putative signal peptidase that functions in pathogenicity of *Colletotrichum graminicola* to maize. *Molecular Plant-Microbe Interactions* **15**: 120–128.

**Tiryaki I, Staswick PE**. **2002**. An *Arabidopsis* mutant defective in jasmonate response is allelic to the auxin-signaling mutant *axr1*. *Plant Physiology* **130**: 887–894.

**Tiryaki I, Staswick PE**. **2013**. An *axr1* suppressor mutation in *Arabidopsis* that partially restores auxin signaling also reverses defects in jasmonate response. *Turkish Journal of Agriculture and Forestry* **37**: 394–400.

**Uzuhashi S, Kakishima M, Tojo M, Kobayashi S**. **2009**. *Pythium apinafurcum*: Its morphology, molecular phylogeny, and infectivity for plants. *Mycoscience* **50**: 281–290.

**De Vleesschauwer D, Van Buyten E, Satoh K, Balidion J, Mauleon R, Choi I-R, Vera-Cruz C, Kikuchi S, Höfte M**. **2012**. Brassinosteroids antagonize gibberellin- and salicylate-mediated root immunity in rice. *Plant physiology* **158**: 1833–1846.

**Vlot AC, Dempsey DA, Klessig DF**. **2009**. Salicylic acid, a multifaceted hormone to combat disease. *Annual Review of Phytopathology* **47**: 177–206.

**Waller JM, Ritchie BJ, Holderness M**. **1998**. Cornmeal agar (CMA). In: Plant Clinic Handbook. CAB International, 77.

**Walters D, Heil M**. **2007**. Costs and trade-offs associated with induced resistance. *Physiological and Molecular Plant Pathology* **71**: 3–17.

**Walton JD**. **1996**. Host-selective toxins: Agents of compatibility. *Plant Cell* **8**: 1723–1733.

**Van West P, Appiah AA, Gow NAR**. **2003**. Advances in research on oomycete root pathogens. *Physiological and Molecular Plant Pathology* **62**: 99–113.

**Whisson SC, Boevink PC, Moleleki L, Avrova AO, Morales JG, Gilroy EM, Armstrong MR, Grouffaud S, van West P, Chapman S, *et al.* 2007**. A translocation signal for delivery of oomycete effector proteins into host plant cells. *Nature* **450**: 115–118.

**White TJ, Bruns T, Lee S, Taylor J**. **1990**. Amplification and direct sequencing of fungal ribosomal RNA genes for phylogenetics. In: PCR Protocols. Elsevier, 315–322.

**Winstead NN, McCombs CL**. **1961**. Pectinolytic and phytopathology, enzyme production by *Pythium aphanidermatum*. *Phytopathology* **51**: 270–273.

**Yoshida K, Schuenemann VJ, Cano LM, Pais M, Mishra B, Sharma R, Lanz C, Martin FN, Kamoun S, Krause J, *et al.* 2013**. The rise and fall of the *Phytophthora infestans* lineage that triggered the Irish potato famine. *eLife* **2**: e00731.

**Zerillo M, Adhikari B, Hamilton J, Buell C, Lévesque C, Tisserat N**. **2013**. Carbohydrate-active enzymes in *Pythium* and their role in plant cell wall and storage polysaccharide degradation. *PloS one* **8**: e72572.

# APPENDIX A

**Table A1 Full alignment of the consensus contig (*P.ci._Wei2017*) with the 10 reference sequences that were used by Garzón *et al*. (2007) for differentiation between *Pythium irregulare* and *Pythium cryptoirregulare***

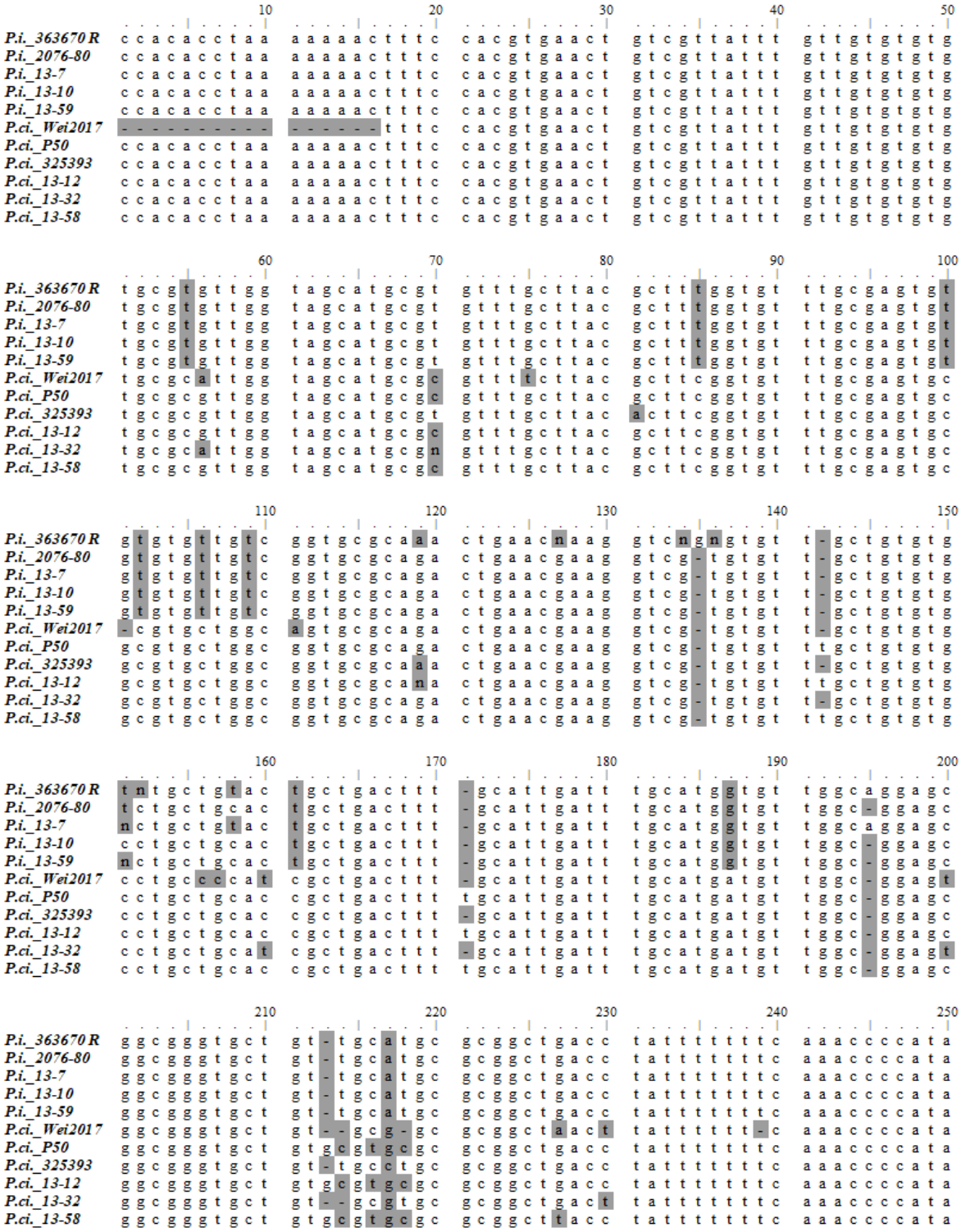

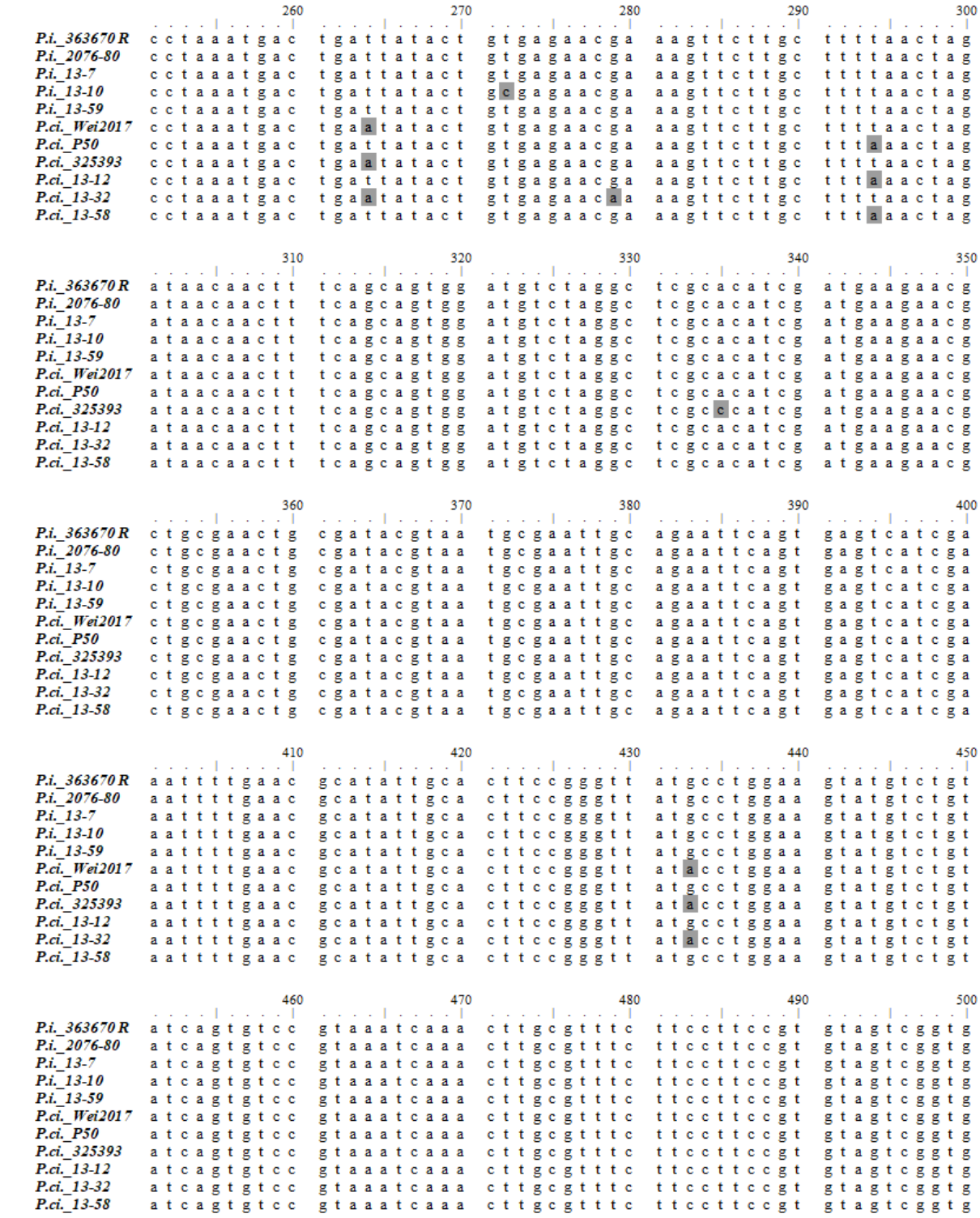
260 270 280 290 300
P.i._363670R c c t a a a t g a c t g a t t a t a c t g t g a g a a a c g a a a g t t c t t g c t t t t a a c t a g
P.i._2076-80 c c t a a a t g a c t g a t t a t a c t g t g a g a a a c g a a a g t t c t t g c t t t t a a c t a g
P.i._13-7 c c t a a a t g a c t g a t t a t a c t g t g a g a a a c g a a a g t t c t t g c t t t t a a c t a g
P.i._13-10 c c t a a a t g a c t g a t t a t a c t g c g a g a a a c g a a a g t t c t t g c t t t t a a c t a g
P.i._13-59 c c t a a a t g a c t g a t t a t a c t g t g a g a a a c g a a a g t t c t t g c t t t t a a c t a g
P.ci._Wei2017 c c t a a a t g a c t g a a t a t a c t g t g a g a a a c g a a a g t t c t t g c t t t t a a c t a g
P.ci._P50 c c t a a a t g a c t g a t t a t a c t g t g a g a a a c g a a a g t t c t t g c t t t a a a c t a g
P.ci._325393 c c t a a a t g a c t g a a t a t a c t g t g a g a a a c g a a a g t t c t t g c t t t t a a c t a g
P.ci._13-12 c c t a a a t g a c t g a t t a t a c t g t g a g a a a c g a a a g t t c t t g c t t t a a a c t a g
P.ci._13-32 c c t a a a t g a c t g a a t a t a c t g t g a g a a a c a a a g t t c t t g c t t t t a a c t a g
P.ci._13-58 c c t a a a t g a c t g a t t a t a c t g t g a g a a a c g a a a g t t c t t g c t t t a a a c t a g
310 320 330 340 350
P.i._363670R a t a a c a a c t t t c a g c a g t g g a t g t c t a g g c t c g c a c a t c g a t g a a g a a c g
P.i._2076-80 a t a a c a a c t t t c a g c a g t g g a t g t c t a g g c t c g c a c a t c g a t g a a g a a c g
P.i._13-7 a t a a c a a c t t t c a g c a g t g g a t g t c t a g g c t c g c a c a t c g a t g a a g a a c g
P.i._13-10 a t a a c a a c t t t c a g c a g t g g a t g t c t a g g c t c g c a c a t c g a t g a a g a a c g
P.i._13-59 a t a a c a a c t t t c a g c a g t g g a t g t c t a g g c t c g c a c a t c g a t g a a g a a c g
P.ci._Wei2017 a t a a c a a c t t t c a g c a g t g g a t g t c t a g g c t c g c a c a t c g a t g a a g a a c g
P.ci._P50 a t a a c a a c t t t c a g c a g t g g a t g t c t a g g c t c g c a c a t c g a t g a a g a a c g
P.ci._325393 a t a a c a a c t t t c a g c a g t g g a t g t c t a g g c t c g c c a t c g a t g a a g a a c g
P.ci._13-12 a t a a c a a c t t t c a g c a g t g g a t g t c t a g g c t c g c a c a t c g a t g a a g a a c g
P.ci._13-32 a t a a c a a c t t t c a g c a g t g g a t g t c t a g g c t c g c a c a t c g a t g a a g a a c g
P.ci._13-58 a t a a c a a c t t t c a g c a g t g g a t g t c t a g g c t c g c a c a t c g a t g a a g a a c g
360 370 380 390 400
P.i._363670R c t g c g a a c t g c g a t a c g t a a t g c g a a t t g c a g a a t t c a g t g a g t c a t c g a
P.i._2076-80 c t g c g a a c t g c g a t a c g t a a t g c g a a t t g c a g a a t t c a g t g a g t c a t c g a
P.i._13-7 c t g c g a a c t g c g a t a c g t a a t g c g a a t t g c a g a a t t c a g t g a g t c a t c g a
P.i._13-10 c t g c g a a c t g c g a t a c g t a a t g c g a a t t g c a g a a t t c a g t g a g t c a t c g a
P.i._13-59 c t g c g a a c t g c g a t a c g t a a t g c g a a t t g c a g a a t t c a g t g a g t c a t c g a
P.ci._Wei2017 c t g c g a a c t g c g a t a c g t a a t g c g a a t t g c a g a a t t c a g t g a g t c a t c g a
P.ci._P50 c t g c g a a c t g c g a t a c g t a a t g c g a a t t g c a g a a t t c a g t g a g t c a t c g a
P.ci._325393 c t g c g a a c t g c g a t a c g t a a t g c g a a t t g c a g a a t t c a g t g a g t c a t c g a
P.ci._13-12 c t g c g a a c t g c g a t a c g t a a t g c g a a t t g c a g a a t t c a g t g a g t c a t c g a
P.ci._13-32 c t g c g a a c t g c g a t a c g t a a t g c g a a t t g c a g a a t t c a g t g a g t c a t c g a
P.ci._13-58 c t g c g a a c t g c g a t a c g t a a t g c g a a t t g c a g a a t t c a g t g a g t c a t c g a
410 420 430 440 450
P.i._363670R a a t t t t g a a c g c a t a t t g c a c t t c c g g g t t a t g c c t g g a a g t a t g t c t g t
P.i._2076-80 a a t t t t g a a c g c a t a t t g c a c t t c c g g g t t a t g c c t g g a a g t a t g t c t g t
P.i._13-7 a a t t t t g a a c g c a t a t t g c a c t t c c g g g t t a t g c c t g g a a g t a t g t c t g t
P.i._13-10 a a t t t t g a a c g c a t a t t g c a c t t c c g g g t t a t g c c t g g a a g t a t g t c t g t
P.i._13-59 a a t t t t g a a c g c a t a t t g c a c t t c c g g g t t a t g c c t g g a a g t a t g t c t g t
P.ci._Wei2017 a a t t t t g a a c g c a t a t t g c a c t t c c g g g t t a t a c c t g g a a g t a t g t c t g t
P.ci._P50 a a t t t t g a a c g c a t a t t g c a c t t c c g g g t t a t g c c t g g a a g t a t g t c t g t
P.ci._325393 a a t t t t g a a c g c a t a t t g c a c t t c c g g g t t a t a c c t g g a a g t a t g t c t g t
P.ci._13-12 a a t t t t g a a c g c a t a t t g c a c t t c c g g g t t a t g c c t g g a a g t a t g t c t g t
P.ci._13-32 a a t t t t g a a c g c a t a t t g c a c t t c c g g g t t a t a c c t g g a a g t a t g t c t g t
P.ci._13-58 a a t t t t g a a c g c a t a t t g c a c t t c c g g g t t a t g c c t g g a a g t a t g t c t g t
460 470 480 490 500
P.i._363670R a t c a g t g t c c g t a a a t c a a a c t t g c g t t t c t t c c t t c c g t g t a g t c g g t g
P.i._2076-80 a t c a g t g t c c g t a a a t c a a a c t t g c g t t t c t t c c t t c c g t g t a g t c g g t g
P.i._13-7 a t c a g t g t c c g t a a a t c a a a c t t g c g t t t c t t c c t t c c g t g t a g t c g g t g
P.i._13-10 a t c a g t g t c c g t a a a t c a a a c t t g c g t t t c t t c c t t c c g t g t a g t c g g t g
P.i._13-59 a t c a g t g t c c g t a a a t c a a a c t t g c g t t t c t t c c t t c c g t g t a g t c g g t g
P.ci._Wei2017 a t c a g t g t c c g t a a a t c a a a c t t g c g t t t c t t c c t t c c g t g t a g t c g g t g
P.ci._P50 a t c a g t g t c c g t a a a t c a a a c t t g c g t t t c t t c c t t c c g t g t a g t c g g t g
P.ci._325393 a t c a g t g t c c g t a a a t c a a a c t t g c g t t t c t t c c t t c c g t g t a g t c g g t g
P.ci._13-12 a t c a g t g t c c g t a a a t c a a a c t t g c g t t t c t t c c t t c c g t g t a g t c g g t g
P.ci._13-32 a t c a g t g t c c g t a a a t c a a a c t t g c g t t t c t t c c t t c c g t g t a g t c g g t g
P.ci._13-58 a t c a g t g t c c g t a a a t c a a a c t t g c g t t t c t t c c t t c c g t g t a g t c g g t g

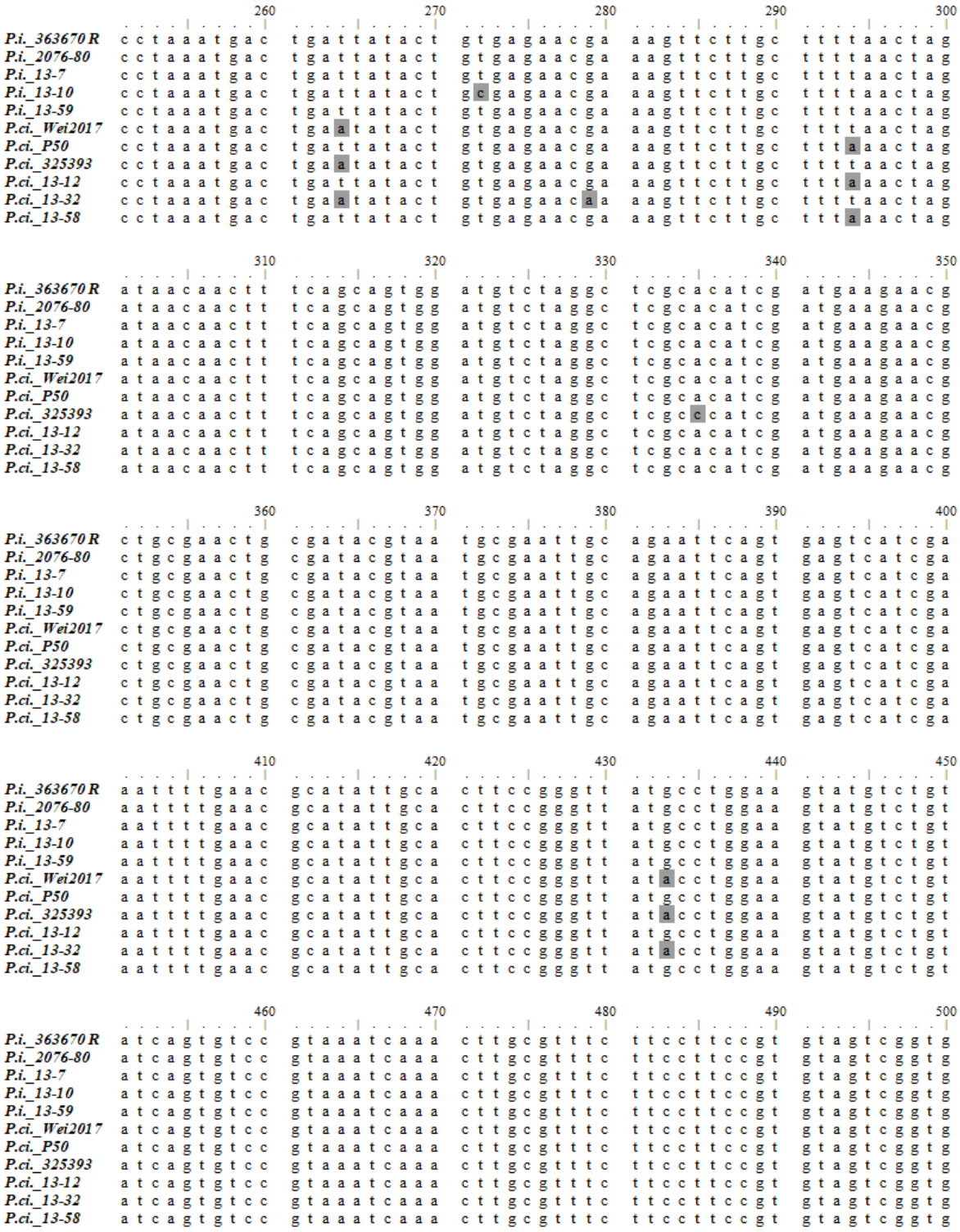
260 270 280 290 300
P.i._363670R c c t a a a t g a c t g a t t a t a c t g t g a g a a c g a a a g t t c t t g c t t t t a a c t a g
P.i._2076-80 c c t a a a t g a c t g a t t a t a c t g t g a g a a c g a a a g t t c t t g c t t t t a a c t a g
P.i._13-7 c c t a a a t g a c t g a t t a t a c t g t g a g a a c g a a a g t t c t t g c t t t t a a c t a g
P.i._13-10 c c t a a a t g a c t g a t t a t a c t g c g a g a a c g a a a g t t c t t g c t t t t a a c t a g
P.i._13-59 c c t a a a t g a c t g a t t a t a c t g t g a g a a c g a a a g t t c t t g c t t t t a a c t a g
P.ci._Wei2017 c c t a a a t g a c t g a a t a t a c t g t g a g a a c g a a a g t t c t t g c t t t t a a c t a g
P.ci._P50 c c t a a a t g a c t g a t t a t a c t g t g a g a a c g a a a g t t c t t g c t t t a a a c t a g
P.ci._325393 c c t a a a t g a c t g a a t a t a c t g t g a g a a c g a a a g t t c t t g c t t t t a a c t a g
P.ci._13-12 c c t a a a t g a c t g a t t a t a c t g t g a g a a c g a a a g t t c t t g c t t t a a a c t a g
P.ci._13-32 c c t a a a t g a c t g a a t a t a c t g t g a g a a c a a a g t t c t t g c t t t t a a c t a g
P.ci._13-58 c c t a a a t g a c t g a t t a t a c t g t g a g a a c g a a a g t t c t t g c t t t a a a c t a g
310 320 330 340 350
P.i._363670R a t a a c a a c t t t c a g c a g t g g a t g t c t a g g c t c g c a c a t c g a t g a a g a a c g
P.i._2076-80 a t a a c a a c t t t c a g c a g t g g a t g t c t a g g c t c g c a c a t c g a t g a a g a a c g
P.i._13-7 a t a a c a a c t t t c a g c a g t g g a t g t c t a g g c t c g c a c a t c g a t g a a g a a c g
P.i._13-10 a t a a c a a c t t t c a g c a g t g g a t g t c t a g g c t c g c a c a t c g a t g a a g a a c g
P.i._13-59 a t a a c a a c t t t c a g c a g t g g a t g t c t a g g c t c g c a c a t c g a t g a a g a a c g
P.ci._Wei2017 a t a a c a a c t t t c a g c a g t g g a t g t c t a g g c t c g c a c a t c g a t g a a g a a c g
P.ci._P50 a t a a c a a c t t t c a g c a g t g g a t g t c t a g g c t c g c a c a t c g a t g a a g a a c g
P.ci._325393 a t a a c a a c t t t c a g c a g t g g a t g t c t a g g c t c g c c a t c g a t g a a g a a c g
P.ci._13-12 a t a a c a a c t t t c a g c a g t g g a t g t c t a g g c t c g c a c a t c g a t g a a g a a c g
P.ci._13-32 a t a a c a a c t t t c a g c a g t g g a t g t c t a g g c t c g c a c a t c g a t g a a g a a c g
P.ci._13-58 a t a a c a a c t t t c a g c a g t g g a t g t c t a g g c t c g c a c a t c g a t g a a g a a c g
360 370 380 390 400
P.i._363670R c t g c g a a c t g c g a t a c g t a a t g c g a a t t g c a g a a t t c a g t g a g t c a t c g a
P.i._2076-80 c t g c g a a c t g c g a t a c g t a a t g c g a a t t g c a g a a t t c a g t g a g t c a t c g a
P.i._13-7 c t g c g a a c t g c g a t a c g t a a t g c g a a t t g c a g a a t t c a g t g a g t c a t c g a
P.i._13-10 c t g c g a a c t g c g a t a c g t a a t g c g a a t t g c a g a a t t c a g t g a g t c a t c g a
P.i._13-59 c t g c g a a c t g c g a t a c g t a a t g c g a a t t g c a g a a t t c a g t g a g t c a t c g a
P.ci._Wei2017 c t g c g a a c t g c g a t a c g t a a t g c g a a t t g c a g a a t t c a g t g a g t c a t c g a
P.ci._P50 c t g c g a a c t g c g a t a c g t a a t g c g a a t t g c a g a a t t c a g t g a g t c a t c g a
P.ci._325393 c t g c g a a c t g c g a t a c g t a a t g c g a a t t g c a g a a t t c a g t g a g t c a t c g a
P.ci._13-12 c t g c g a a c t g c g a t a c g t a a t g c g a a t t g c a g a a t t c a g t g a g t c a t c g a
P.ci._13-32 c t g c g a a c t g c g a t a c g t a a t g c g a a t t g c a g a a t t c a g t g a g t c a t c g a
P.ci._13-58 c t g c g a a c t g c g a t a c g t a a t g c g a a t t g c a g a a t t c a g t g a g t c a t c g a
410 420 430 440 450
P.i._363670R a a t t t t g a a c g c a t a t t g c a c t t c c g g g t t a t g c c t g g a a g t a t g t c t g t
P.i._2076-80 a a t t t t g a a c g c a t a t t g c a c t t c c g g g t t a t g c c t g g a a g t a t g t c t g t
P.i._13-7 a a t t t t g a a c g c a t a t t g c a c t t c c g g g t t a t g c c t g g a a g t a t g t c t g t
P.i._13-10 a a t t t t g a a c g c a t a t t g c a c t t c c g g g t t a t g c c t g g a a g t a t g t c t g t
P.i._13-59 a a t t t t g a a c g c a t a t t g c a c t t c c g g g t t a t g c c t g g a a g t a t g t c t g t
P.ci._Wei2017 a a t t t t g a a c g c a t a t t g c a c t t c c g g g t t a t a c c t g g a a g t a t g t c t g t
P.ci._P50 a a t t t t g a a c g c a t a t t g c a c t t c c g g g t t a t g c c t g g a a g t a t g t c t g t
P.ci._325393 a a t t t t g a a c g c a t a t t g c a c t t c c g g g t t a t a c c t g g a a g t a t g t c t g t
P.ci._13-12 a a t t t t g a a c g c a t a t t g c a c t t c c g g g t t a t g c c t g g a a g t a t g t c t g t
P.ci._13-32 a a t t t t g a a c g c a t a t t g c a c t t c c g g g t t a t a c c t g g a a g t a t g t c t g t
P.ci._13-58 a a t t t t g a a c g c a t a t t g c a c t t c c g g g t t a t g c c t g g a a g t a t g t c t g t
460 470 480 490 500
P.i._363670R a t c a g t g t c c g t a a a t c a a a c t t g c g t t t c t t c c t t c c g t g t a g t c g g t g
P.i._2076-80 a t c a g t g t c c g t a a a t c a a a c t t g c g t t t c t t c c t t c c g t g t a g t c g g t g
P.i._13-7 a t c a g t g t c c g t a a a t c a a a c t t g c g t t t c t t c c t t c c g t g t a g t c g g t g
P.i._13-10 a t c a g t g t c c g t a a a t c a a a c t t g c g t t t c t t c c t t c c g t g t a g t c g g t g
P.i._13-59 a t c a g t g t c c g t a a a t c a a a c t t g c g t t t c t t c c t t c c g t g t a g t c g g t g
P.ci._Wei2017 a t c a g t g t c c g t a a a t c a a a c t t g c g t t t c t t c c t t c c g t g t a g t c g g t g
P.ci._P50 a t c a g t g t c c g t a a a t c a a a c t t g c g t t t c t t c c t t c c g t g t a g t c g g t g
P.ci._325393 a t c a g t g t c c g t a a a t c a a a c t t g c g t t t c t t c c t t c c g t g t a g t c g g t g
P.ci._13-12 a t c a g t g t c c g t a a a t c a a a c t t g c g t t t c t t c c t t c c g t g t a g t c g g t g
P.ci._13-32 a t c a g t g t c c g t a a a t c a a a c t t g c g t t t c t t c c t t c c g t g t a g t c g g t g
P.ci._13-58 a t c a g t g t c c g t a a a t c a a a c t t g c g t t t c t t c c t t c c g t g t a g t c g g t g

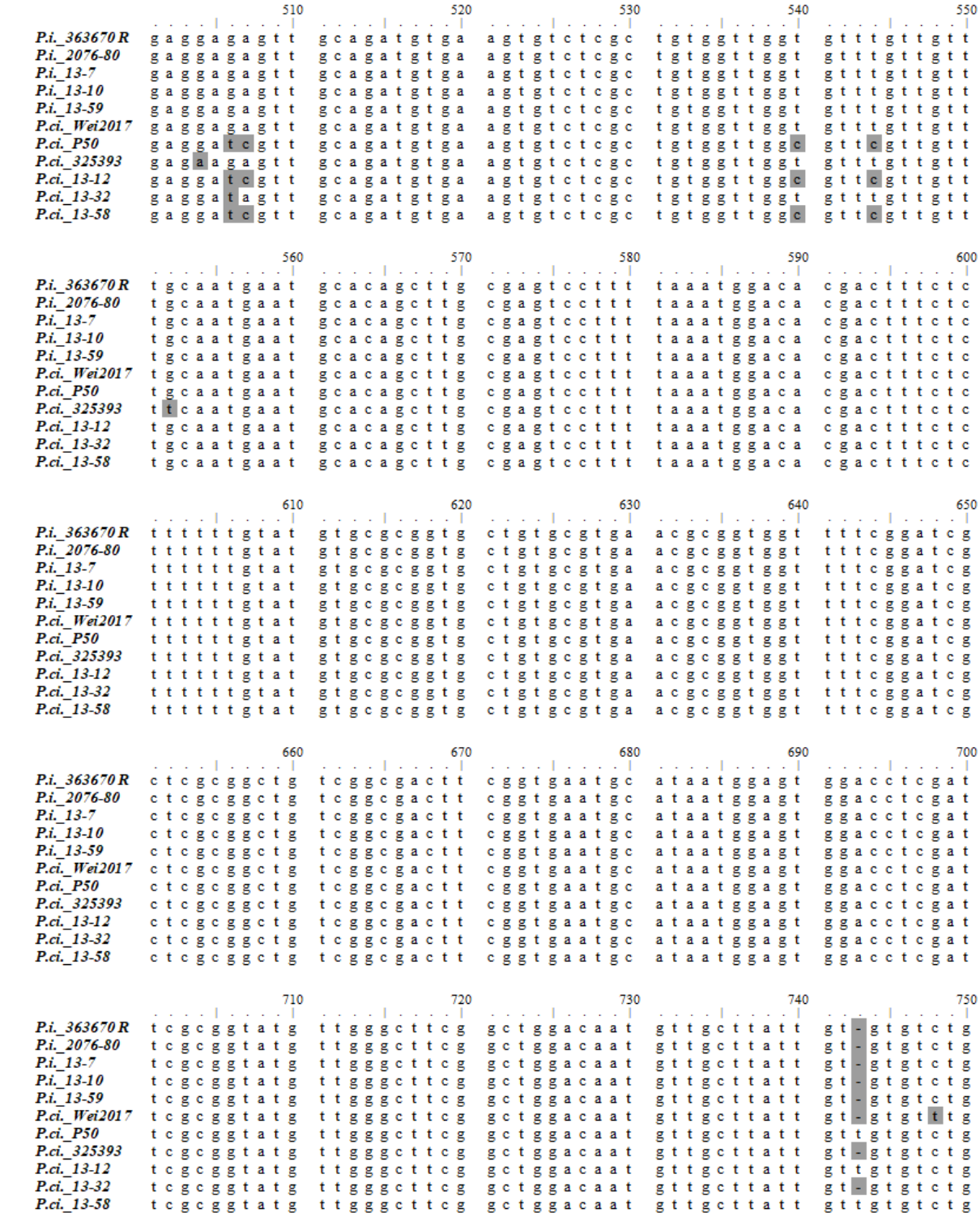
510 520 530 540 550
P.i._363670R g a g g a g a g t t g c a g a t g t g a a g t g t c t c g c t g t g g t t g g t g t t t g t t g t t
P.i._2076-80 g a g g a g a g t t g c a g a t g t g a a g t g t c t c g c t g t g g t t g g t g t t t g t t g t t
P.i._13-7 g a g g a g a g t t g c a g a t g t g a a g t g t c t c g c t g t g g t t g g t g t t t g t t g t t
P.i._13-10 g a g g a g a g t t g c a g a t g t g a a g t g t c t c g c t g t g g t t g g t g t t t g t t g t t
P.i._13-59 g a g g a g a g t t g c a g a t g t g a a g t g t c t c g c t g t g g t t g g t g t t t g t t g t t
P.ci._Wei2017 g a g g a g a g t t g c a g a t g t g a a g t g t c t c g c t g t g g t t g g t g t t t g t t g t t
P.ci._P50 g a g g a t c g t t g c a g a t g t g a a g t g t c t c g c t g t g g t t g g c g t t c g t t g t t
P.ci._325393 g a g a a g a g t t g c a g a t g t g a a g t g t c t c g c t g t g g t t g g t g t t t g t t g t t
P.ci._13-12 g a g g a t c g t t g c a g a t g t g a a g t g t c t c g c t g t g g t t g g c g t t c g t t g t t
P.ci._13-32 g a g g a t a g t t g c a g a t g t g a a g t g t c t c g c t g t g g t t g g t g t t t g t t g t t
P.ci._13-58 g a g g a t c g t t g c a g a t g t g a a g t g t c t c g c t g t g g t t g g c g t t c g t t g t t
560 570 580 590 600
P.i._363670R t g c a a t g a a t g c a c a g c t t g c g a g t c c t t t t a a a t g g a c a c g a c t t t c t c
P.i._2076-80 t g c a a t g a a t g c a c a g c t t g c g a g t c c t t t t a a a t g g a c a c g a c t t t c t c
P.i._13-7 t g c a a t g a a t g c a c a g c t t g c g a g t c c t t t t a a a t g g a c a c g a c t t t c t c
P.i._13-10 t g c a a t g a a t g c a c a g c t t g c g a g t c c t t t t a a a t g g a c a c g a c t t t c t c
P.i._13-59 t g c a a t g a a t g c a c a g c t t g c g a g t c c t t t t a a a t g g a c a c g a c t t t c t c
P.ci._Wei2017 t g c a a t g a a t g c a c a g c t t g c g a g t c c t t t t a a a t g g a c a c g a c t t t c t c
P.ci._P50 t g c a a t g a a t g c a c a g c t t g c g a g t c c t t t t a a a t g g a c a c g a c t t t c t c
P.ci._325393 t t c a a t g a a t g c a c a g c t t g c g a g t c c t t t t a a a t g g a c a c g a c t t t c t c
P.ci._13-12 t g c a a t g a a t g c a c a g c t t g c g a g t c c t t t t a a a t g g a c a c g a c t t t c t c
P.ci._13-32 t g c a a t g a a t g c a c a g c t t g c g a g t c c t t t t a a a t g g a c a c g a c t t t c t c
P.ci._13-58 t g c a a t g a a t g c a c a g c t t g c g a g t c c t t t t a a a t g g a c a c g a c t t t c t c
610 620 630 640 650
P.i._363670R t t t t t t g t a t g t g c g c g g t g c t g t g c g t g a a c g c g g t g g t t t t c g g a t c g
P.i._2076-80 t t t t t t g t a t g t g c g c g g t g c t g t g c g t g a a c g c g g t g g t t t t c g g a t c g
P.i._13-7 t t t t t t g t a t g t g c g c g g t g c t g t g c g t g a a c g c g g t g g t t t t c g g a t c g
P.i._13-10 t t t t t t g t a t g t g c g c g g t g c t g t g c g t g a a c g c g g t g g t t t t c g g a t c g
P.i._13-59 t t t t t t g t a t g t g c g c g g t g c t g t g c g t g a a c g c g g t g g t t t t c g g a t c g
P.ci._Wei2017 t t t t t t g t a t g t g c g c g g t g c t g t g c g t g a a c g c g g t g g t t t t c g g a t c g
P.ci._P50 t t t t t t g t a t g t g c g c g g t g c t g t g c g t g a a c g c g g t g g t t t t c g g a t c g
P.ci._325393 t t t t t t g t a t g t g c g c g g t g c t g t g c g t g a a c g c g g t g g t t t t c g g a t c g
P.ci._13-12 t t t t t t g t a t g t g c g c g g t g c t g t g c g t g a a c g c g g t g g t t t t c g g a t c g
P.ci._13-32 t t t t t t g t a t g t g c g c g g t g c t g t g c g t g a a c g c g g t g g t t t t c g g a t c g
P.ci._13-58 t t t t t t g t a t g t g c g c g g t g c t g t g c g t g a a c g c g g t g g t t t t c g g a t c g
660 670 680 690 700
P.i._363670R c t c g c g g c t g t c g g c g a c t t c g g t g a a t g c a t a a t g g a g t g g a c c t c g a t
P.i._2076-80 c t c g c g g c t g t c g g c g a c t t c g g t g a a t g c a t a a t g g a g t g g a c c t c g a t
P.i._13-7 c t c g c g g c t g t c g g c g a c t t c g g t g a a t g c a t a a t g g a g t g g a c c t c g a t
P.i._13-10 c t c g c g g c t g t c g g c g a c t t c g g t g a a t g c a t a a t g g a g t g g a c c t c g a t
P.i._13-59 c t c g c g g c t g t c g g c g a c t t c g g t g a a t g c a t a a t g g a g t g g a c c t c g a t
P.ci._Wei2017 c t c g c g g c t g t c g g c g a c t t c g g t g a a t g c a t a a t g g a g t g g a c c t c g a t
P.ci._P50 c t c g c g g c t g t c g g c g a c t t c g g t g a a t g c a t a a t g g a g t g g a c c t c g a t
P.ci._325393 c t c g c g g c t g t c g g c g a c t t c g g t g a a t g c a t a a t g g a g t g g a c c t c g a t
P.ci._13-12 c t c g c g g c t g t c g g c g a c t t c g g t g a a t g c a t a a t g g a g t g g a c c t c g a t
P.ci._13-32 c t c g c g g c t g t c g g c g a c t t c g g t g a a t g c a t a a t g g a g t g g a c c t c g a t
P.ci._13-58 c t c g c g g c t g t c g g c g a c t t c g g t g a a t g c a t a a t g g a g t g g a c c t c g a t
710 720 730 740 750
P.i._363670R t c g c g g t a t g t t g g g c t t c g g c t g g a c a a t g t t g c t t a t t g t - g t g t c t g
P.i._2076-80 t c g c g g t a t g t t g g g c t t c g g c t g g a c a a t g t t g c t t a t t g t - g t g t c t g
P.i._13-7 t c g c g g t a t g t t g g g c t t c g g c t g g a c a a t g t t g c t t a t t g t - g t g t c t g
P.i._13-10 t c g c g g t a t g t t g g g c t t c g g c t g g a c a a t g t t g c t t a t t g t - g t g t c t g
P.i._13-59 t c g c g g t a t g t t g g g c t t c g g c t g g a c a a t g t t g c t t a t t g t - g t g t c t g
P.ci._Wei2017 t c g c g g t a t g t t g g g c t t c g g c t g g a c a a t g t t g c t t a t t g t - g t g t t t g
P.ci._P50 t c g c g g t a t g t t g g g c t t c g g c t g g a c a a t g t t g c t t a t t g t t g t g t c t g
P.ci._325393 t c g c g g t a t g t t g g g c t t c g g c t g g a c a a t g t t g c t t a t t g t - g t g t c t g
P.ci._13-12 t c g c g g t a t g t t g g g c t t c g g c t g g a c a a t g t t g c t t a t t g t t g t g t c t g
P.ci._13-32 t c g c g g t a t g t t g g g c t t c g g c t g g a c a a t g t t g c t t a t t g t - g t g t c t g
P.ci._13-58 t c g c g g t a t g t t g g g c t t c g g c t g g a c a a t g t t g c t t a t t g t t g t g t c t g

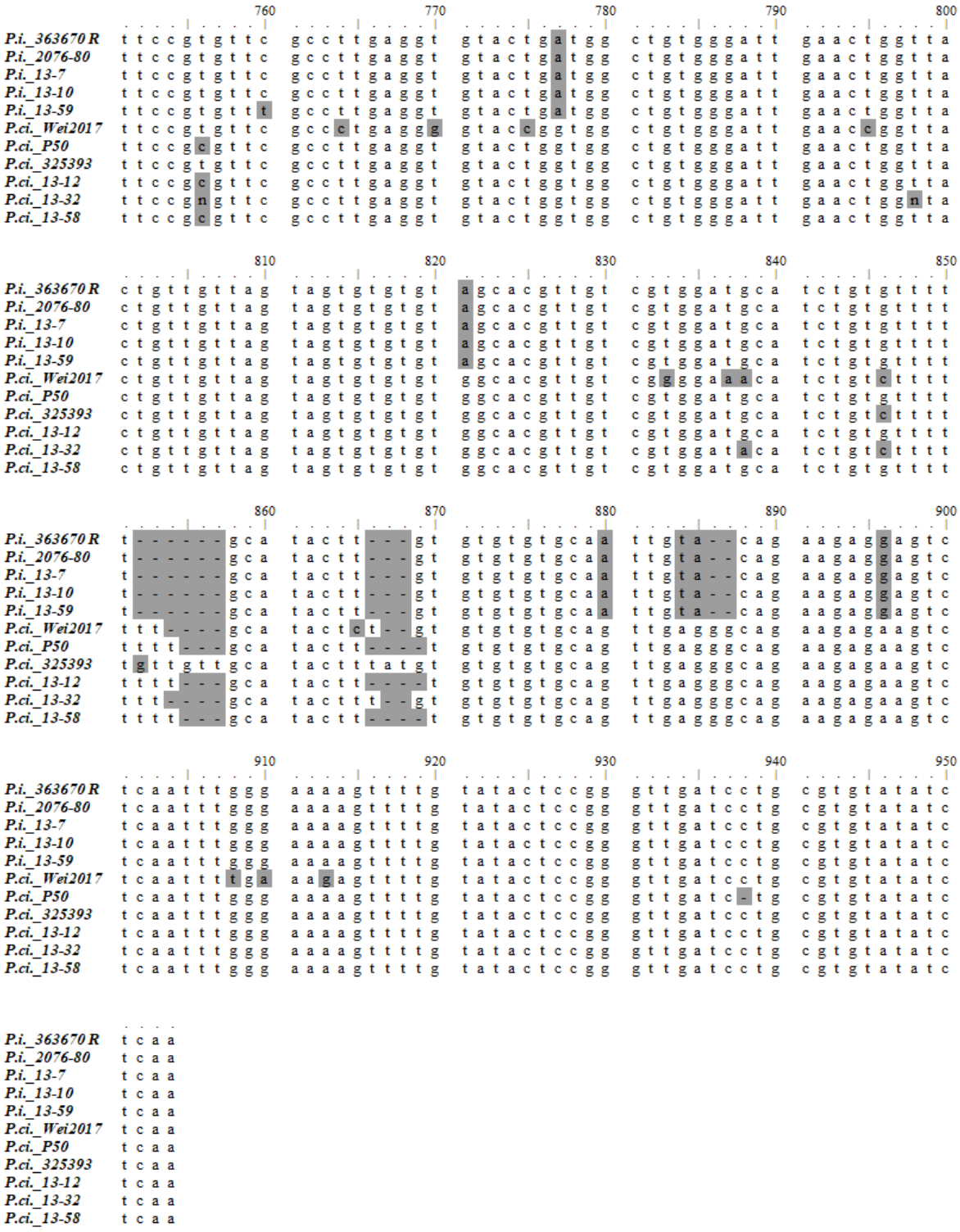
760 770 780 790 800
P.i._363670R t t c c g t g t t c g c c t t g a g g t g t a c t g a t g g c t g t g g g a t t g a a c t g g t t a
P.i._2076-80 t t c c g t g t t c g c c t t g a g g t g t a c t g a t g g c t g t g g g a t t g a a c t g g t t a
P.i._13-7 t t c c g t g t t c g c c t t g a g g t g t a c t g a t g g c t g t g g g a t t g a a c t g g t t a
P.i._13-10 t t c c g t g t t c g c c t t g a g g t g t a c t g a t g g c t g t g g g a t t g a a c t g g t t a
P.i._13-59 t t c c g t g t t t g c c t t g a g g t g t a c t g a t g g c t g t g g g a t t g a a c t g g t t a
P.ci._Wei2017 t t c c g t g t t c g c c c t g a g g g g t a c c g g t g g c t g t g g g a t t g a a c c g g t t a
P.ci._P50 t t c c g c g t t c g c c t t g a g g t g t a c t g g t g g c t g t g g g a t t g a a c t g g t t a
P.ci._325393 t t c c g t g t t c g c c t t g a g g t g t a c t g g t g g c t g t g g g a t t g a a c t g g t t a
P.ci._13-12 t t c c g c g t t c g c c t t g a g g t g t a c t g g t g g c t g t g g g a t t g a a c t g g t t a
P.ci._13-32 t t c c g n g t t c g c c t t g a g g t g t a c t g g t g g c t g t g g g a t t g a a c t g g n t a
P.ci._13-58 t t c c g c g t t c g c c t t g a g g t g t a c t g g t g g c t g t g g g a t t g a a c t g g t t a
810 820 830 840 850
P.i._363670R c t g t t g t t a g t a g t g t g t g t a g c a c g t t g t c g t g g a t g c a t c t g t g t t t t
P.i._2076-80 c t g t t g t t a g t a g t g t g t g t a g c a c g t t g t c g t g g a t g c a t c t g t g t t t t
P.i._13-7 c t g t t g t t a g t a g t g t g t g t a g c a c g t t g t c g t g g a t g c a t c t g t g t t t t
P.i._13-10 c t g t t g t t a g t a g t g t g t g t a g c a c g t t g t c g t g g a t g c a t c t g t g t t t t
P.i._13-59 c t g t t g t t a g t a g t g t g t g t a g c a c g t t g t c g t g g a t g c a t c t g t g t t t t
P.ci._Wei2017 c t g t t g t t a g t a g t g t g t g t g g c a c g t t g t c g g g g g a a a c a t c t g t c t t t t
P.ci._P50 c t g t t g t t a g t a g t g t g t g t g g c a c g t t g t c g t g g a t g c a t c t g t g t t t t
P.ci._325393 c t g t t g t t a g t a g t g t g t g t g g c a c g t t g t c g t g g a t g c a t c t g t c t t t t
P.ci._13-12 c t g t t g t t a g t a g t g t g t g t g g c a c g t t g t c g t g g a t g c a t c t g t g t t t t
P.ci._13-32 c t g t t g t t a g t a g t g t g t g t g g c a c g t t g t c g t g g a t a c a t c t g t c t t t t
P.ci._13-58 c t g t t g t t a g t a g t g t g t g t g g c a c g t t g t c g t g g a t g c a t c t g t g t t t t
860 870 880 890 900
P.i._363670R t - - - - - - g c a t a c t t - - - g t g t g t g t g c a a t t g t a - - c a g a a g a g g g a g t c
P.i._2076-80 t - - - - - - g c a t a c t t - - - g t g t g t g t g c a a t t g t a - - c a g a a g a g g g a g t c
P.i._13-7 t - - - - - - g c a t a c t t - - - g t g t g t g t g c a a t t g t a - - c a g a a g a g g g a g t c
P.i._13-10 t - - - - - - g c a t a c t t - - - g t g t g t g t g c a a t t g t a - - c a g a a g a g g g a g t c
P.i._13-59 t - - - - - - g c a t a c t t - - - g t g t g t g t g c a a t t g t a - - c a g a a g a g g g a g t c
P.ci._Wei2017 t t t - - - - g c a t a c t c t - - g t g t g t g t g c a g t t g a g g g c a g a a g a g a a g t c
P.ci._P50 t t t t - - - - g c a t a c t t - - - - t g t g t g t g t g c a g t t g a g g g c a g a a g a g a a g t c
P.ci._325393 t g t t g t t g c a t a c t t t a t g t g t g t g t g c a g t t g a g g g c a g a a g a g a a g t c
P.ci._13-12 t t t t - - - - g c a t a c t t - - - - t g t g t g t g t g c a g t t g a g g g c a g a a g a g a a g t c
P.ci._13-32 t t t - - - - g c a t a c t t t - - g t g t g t g t g t g c a g t t g a g g g c a g a a g a g a a g t c
P.ci._13-58 t t t t - - - - g c a t a c t t - - - - t g t g t g t g t g c a g t t g a g g g c a g a a g a g a a g t c
910 920 930 940 950
P.i._363670R t c a a t t t g g g a a a a a g t t t t g t a t a c t c c g g g t t g a t c c t g c g t g t a t a t c
P.i._2076-80 t c a a t t t g g g a a a a a g t t t t g t a t a c t c c g g g t t g a t c c t g c g t g t a t a t c
P.i._13-7 t c a a t t t g g g a a a a a g t t t t g t a t a c t c c g g g t t g a t c c t g c g t g t a t a t c
P.i._13-10 t c a a t t t g g g a a a a a g t t t t g t a t a c t c c g g g t t g a t c c t g c g t g t a t a t c
P.i._13-59 t c a a t t t g g g a a a a a g t t t t g t a t a c t c c g g g t t g a t c c t g c g t g t a t a t c
P.ci._Wei2017 t c a a t t t t g a a a g a g t t t t g t a t a c t c c g g g t t g a t c c t g c g t g t a t a t c
P.ci._P50 t c a a t t t g g g a a a a a g t t t t g t a t a c t c c g g g t t g a t c - t g c g t g t a t a t c
P.ci._325393 t c a a t t t g g g a a a a a g t t t t g t a t a c t c c g g g t t g a t c c t g c g t g t a t a t c
P.ci._13-12 t c a a t t t g g g a a a a a g t t t t g t a t a c t c c g g g t t g a t c c t g c g t g t a t a t c
P.ci._13-32 t c a a t t t g g g a a a a a g t t t t g t a t a c t c c g g g t t g a t c c t g c g t g t a t a t c
P.ci._13-58 t c a a t t t g g g a a a a a g t t t t g t a t a c t c c g g g t t g a t c c t g c g t g t a t a t c
P.i._363670R t c a a
P.i._2076-80 t c a a
P.i._13-7 t c a a
P.i._13-10 t c a a
P.i._13-59 t c a a
P.ci._Wei2017 t c a a
P.ci._P50 t c a a
P.ci._325393 t c a a
P.ci._13-12 t c a a
P.ci._13-32 t c a a
P.ci._13-58 t c a a

# APPENDIX B

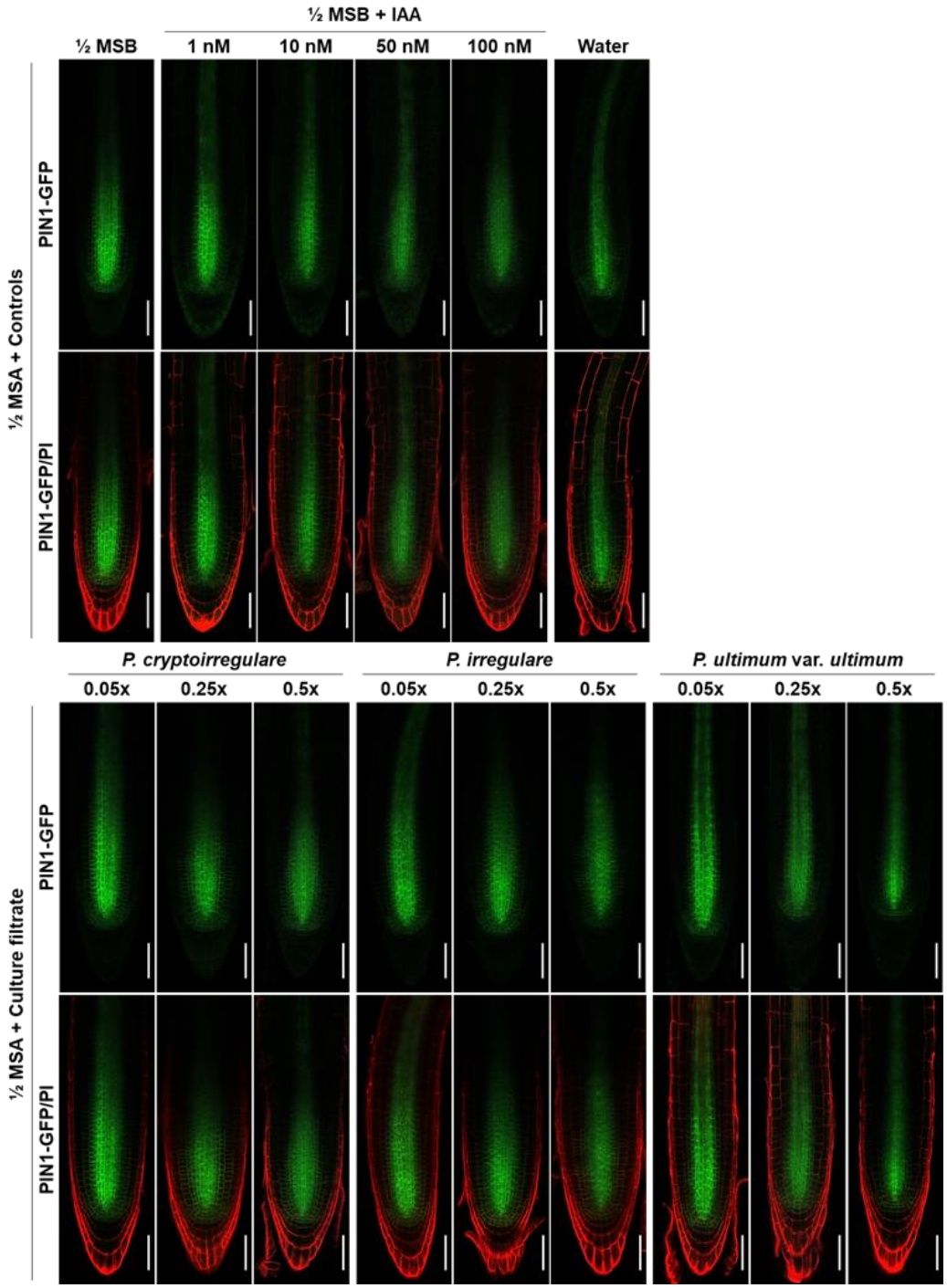


**Figure B1 Auxin transport in root tissues of *Arabidopsis* seedling PIN1-GFP upon exposure to culture filtrates of *Pythium* spp. or IAA.** Photos were taken of propidium iodide(PI)-stained *Arabidopsis* seedlings expressing the auxin reporter construct PIN1-GFP after 6 days of incubation at 22 ºC on ½ Murashige and Skoog agar (MSA) mixed 1:1 with *P. cryptoirregulare*, *P irregulare*, or *P. ultimum* var. *ultimum* culture filtrates, ½ Murashige and Skoog broth (MSB), MSB with indole-3-acetic acid (IAA) or water. Fluorescence signals were detected using the Argon laser of the Zeiss LSM 880 confocal microscope with the following excitation/emission settings: 488/505-530 nm for GFP and 488/>560 for PI detection. Scale bars = 50 µm.

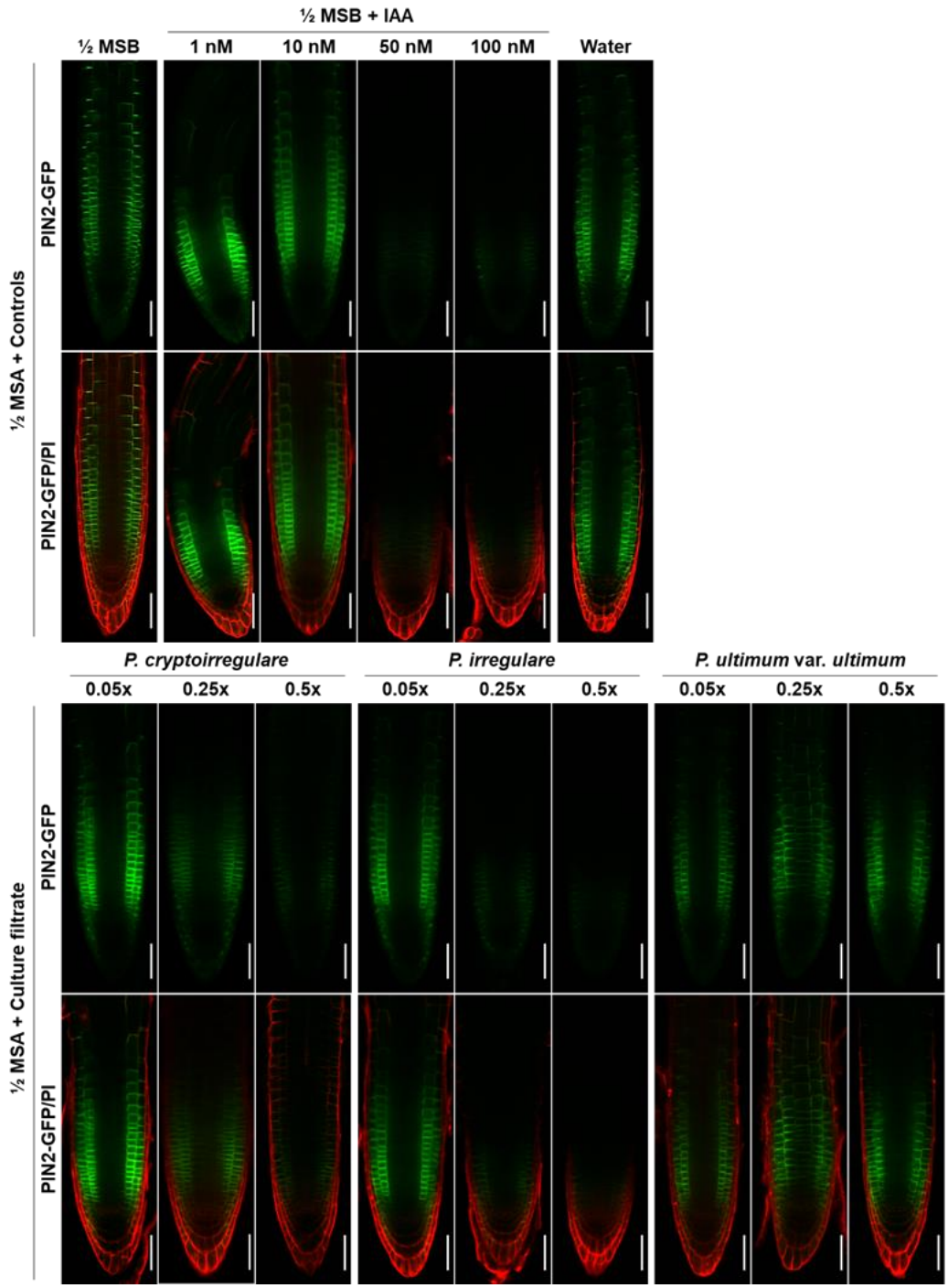


**Figure B2 Altered auxin transport in root tissues of *Arabidopsis* seedling PIN2-GFP upon exposure to culture filtrates of *Pythium* spp. or IAA.** Photos were taken of propidium iodide(PI)-stained *Arabidopsis* seedlings expressing the auxin reporter construct PIN2-GFP after 6 days of incubation at 22 ºC on ½ Murashige and Skoog agar (MSA) mixed 1:1 with *P. cryptoirregulare*, *P. irregulare*, or *P. ultimum* var. *ultimum* culture filtrates, ½ Murashige and Skoog broth (MSB), MSB with indole-3-acetic acid (IAA) or water. Fluorescence signals were detected using the Argon laser of the Zeiss LSM 880 confocal microscope with the following excitation/emission settings: 488/505-530 nm for GFP and 488/>560 for PI detection. Scale bars = 50 μm

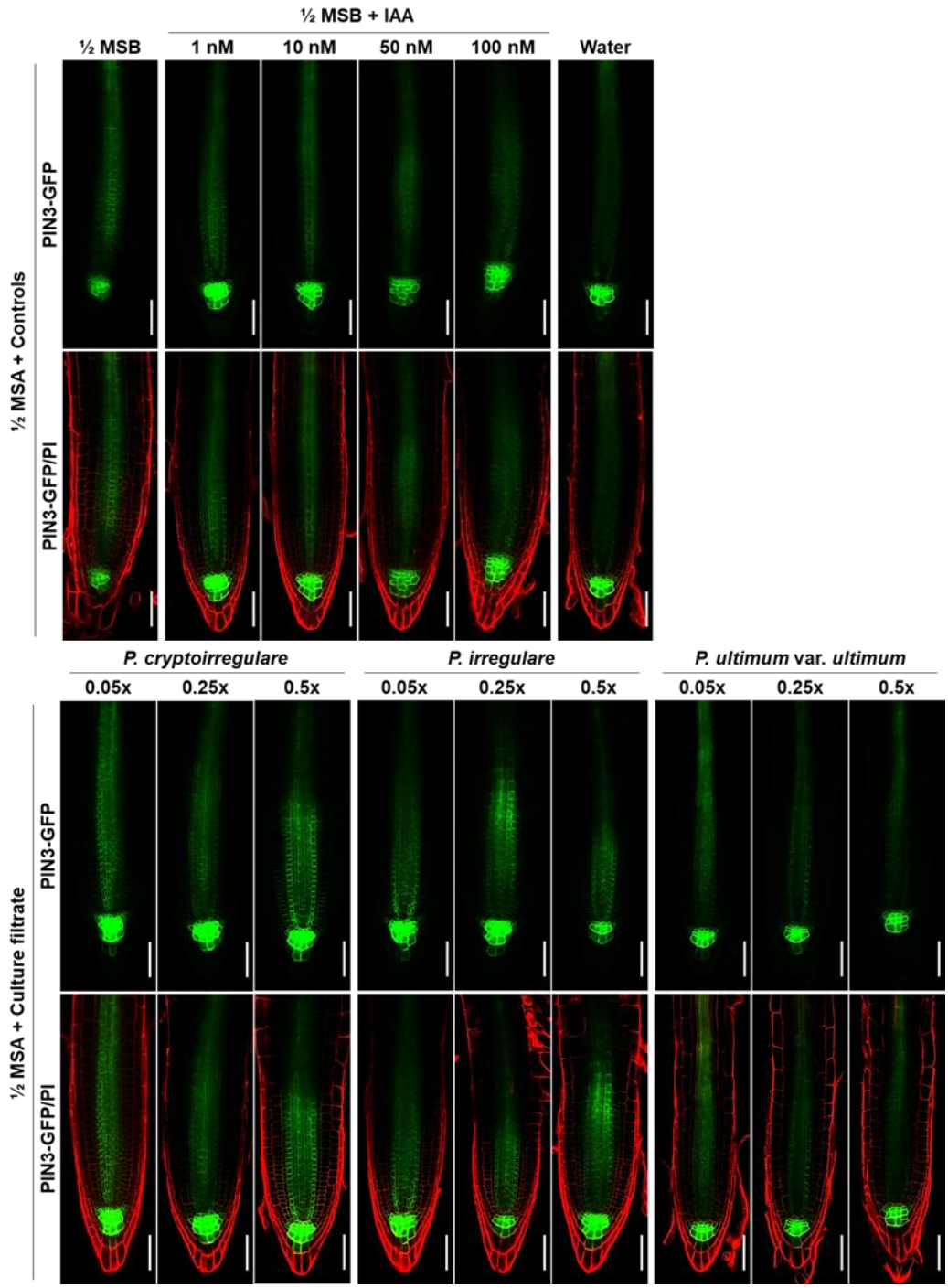


**Figure B3 Altered auxin transport in root tissues of *Arabidopsis* seedling PIN3-GFP upon exposure to culture filtrates of *Pythium* spp. or IAA.** Photos were taken of propidium iodide(PI)-stained *Arabidopsis* seedlings expressing the auxin reporter construct PIN3-GFP after 6 days of incubation at 22 ºC on ½ Murashige and Skoog agar (MSA) mixed 1:1 with *P. cryptoirregulare*, *P irregulare*, or *P. ultimum* var. *ultimum* culture filtrates, ½ Murashige and Skoog broth (MSB), MSB with indole-3-acetic acid (IAA) or water. Fluorescence signals were detected using the Argon laser of the Zeiss LSM 880 confocal microscope with the following excitation/emission settings: 488/505-530 nm for GFP and 488/>560 for PI detection. Scale bars = 50 μm

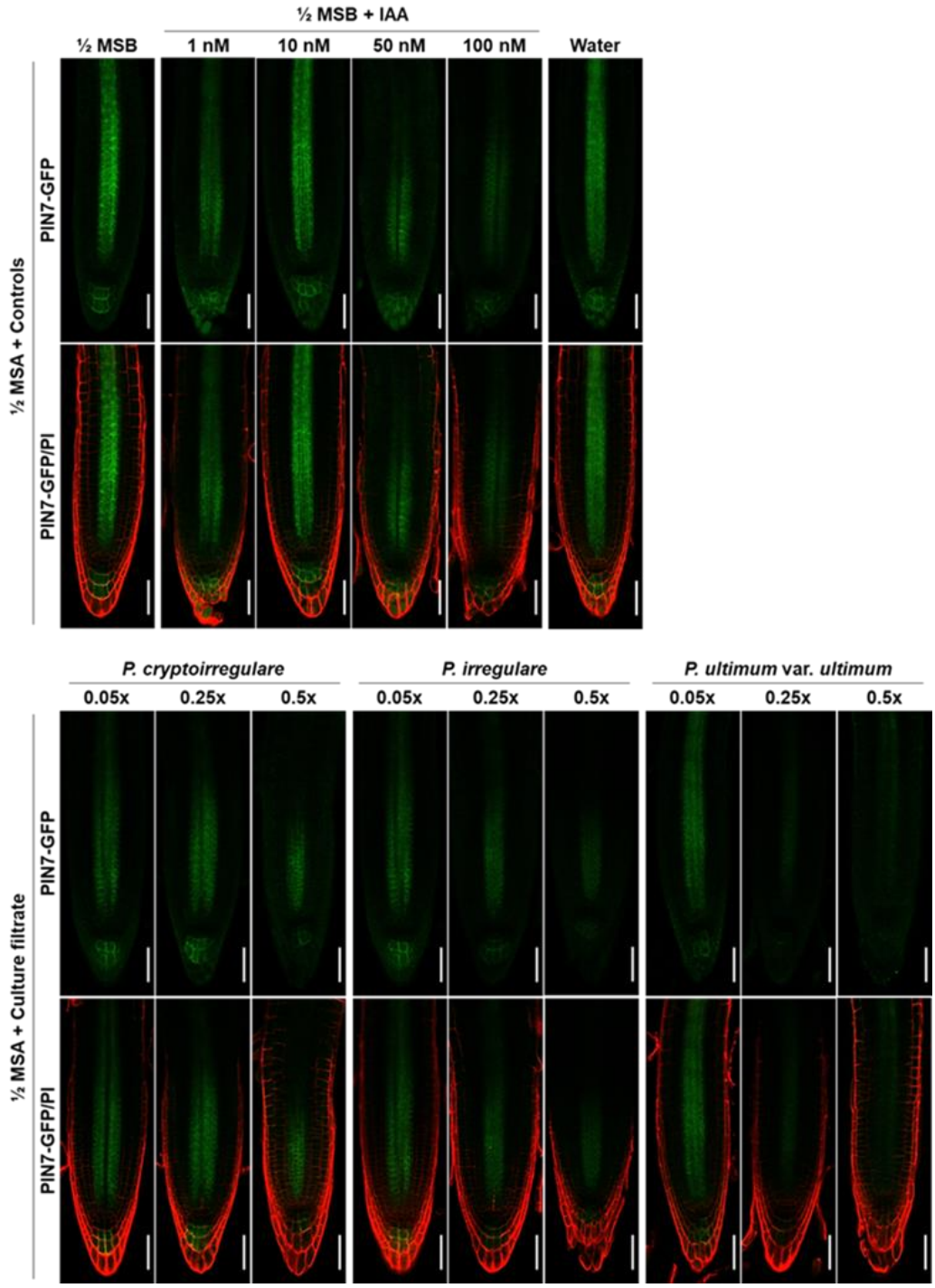


**Figure B4 Altered auxin transport in root tissues of *Arabidopsis* seedling PIN7-GFP upon exposure to culture filtrates of *Pythium* spp. or IAA.** Photos were taken of propidium iodide(PI)-stained *Arabidopsis* seedlings expressing the auxin reporter construct PIN7-GFP after 6 days of incubation at 22 ºC on ½ Murashige and Skoog agar (MSA) mixed 1:1 with *P. cryptoirregulare*, *P irregulare*, or *P. ultimum* var. *ultimum* culture filtrates, ½ Murashige and Skoog broth (MSB), MSB with indole-3-acetic acid (IAA) or water. Fluorescence signals were detected using the Argon laser of the Zeiss LSM 880 confocal microscope with the following excitation/emission settings: 488/505-530 nm for GFP and 488/>560 for PI detection. Scale bars = 50 μm

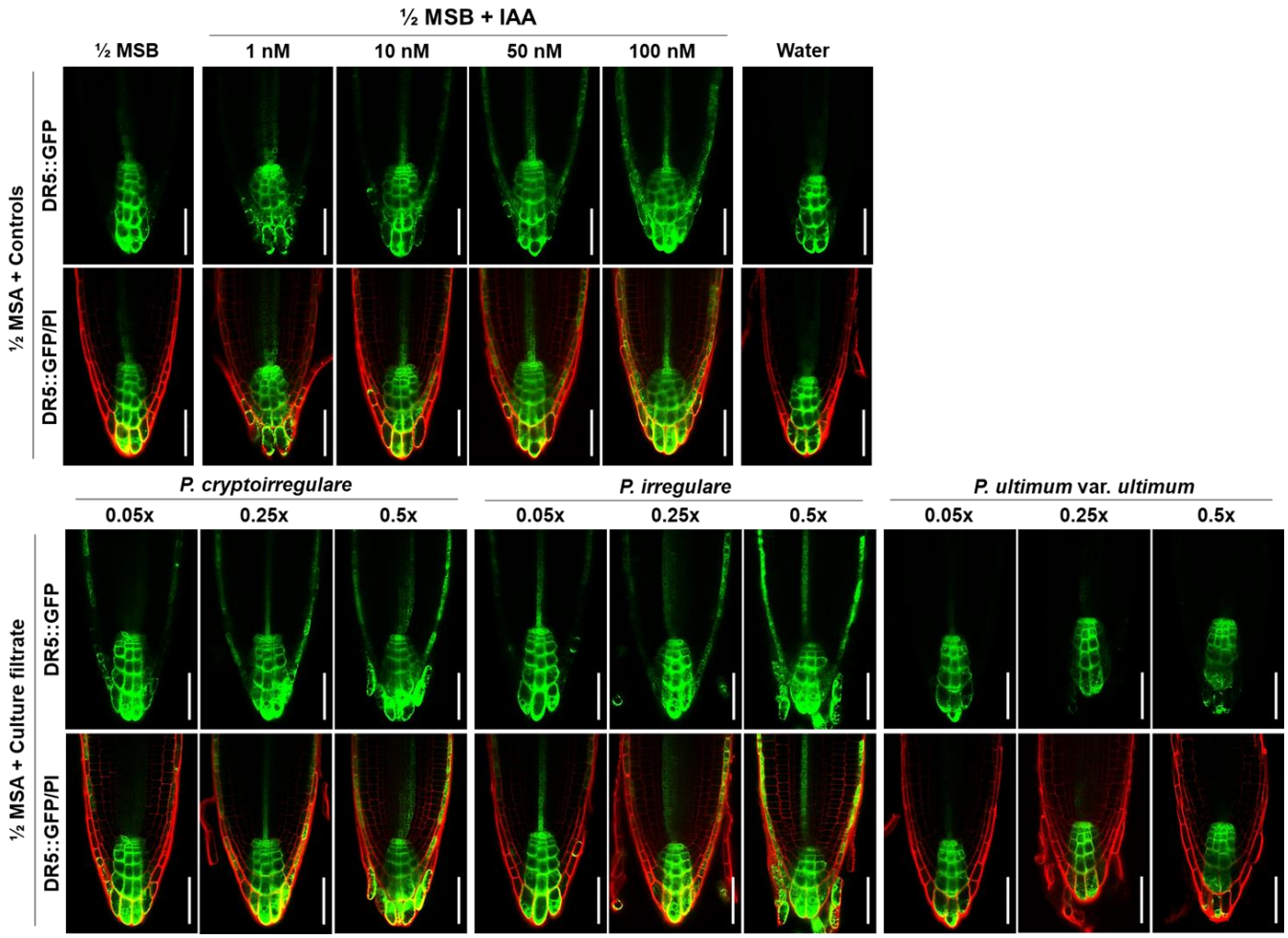


**Figure B5 Altered auxin transport in root tissues of *Arabidopsis* seedling DR5::GFP upon exposure to culture filtrates of *Pythium* spp. or IAA.** Photos were taken of propidium iodide(PI)-stained *Arabidopsis* seedlings expressing the auxin reporter construct DR5::GFP after 6 days of incubation at 22 ºC on ½ Murashige and Skoog agar (MSA) mixed 1:1 with *P. cryptoirregulare*, *P irregulare*, or *P. ultimum* var. *ultimum* culture filtrates, ½ Murashige and Skoog broth (MSB), MSB with indole-3-acetic acid (IAA) or water. Fluorescence signals were detected using the Argon laser of the Zeiss LSM 880 confocal microscope with the following excitation/emission settings: 488/505-530 nm for GFP and 488/>560 for PI detection. Scale bars = 50 µm

# APPENDIX C

**Table C1 List of significant differences according to R using the cld function for generating letter lines to compare treatment combinations**

| Treatments | Length estimate | Letter group |
|---|---|---|
| P.u:0.25x:*aux1-7* | 5.476 | A |
| P.u:0.25x:axr2-4 | 6.3954 | AB |
| P.i:0.5x:Col-0 | 6.465626 | ABC |
| P.u:0.5x:*aux1-7* | 6.7026 | AB |
| P.u:0.25x:*axr1-3* | 7.0024 | ABC |
| P.u:0.5x:*axr1-3* | 7.0094 | ABC |
| P.ci:0.5x:Col-0 | 7.7302 | ABCD |
| P.u:0.5x:Col-0 | 7.8984 | ABCDE |
| P.ci:0.5x:*aux1-7* | 8.2072 | ABCDE |
| P.u:0.5x:axr2-4 | 8.3258 | ABCDEF |
| P.u:0.25x:Col-0 | 9.3138 | ABCDEF |
| P.i:0.25x:Col-0 | 10.4534 | ABCDEFG |
| P.i:0.5x:axr2-4 | 11.3188 | ABCDEFGH |
| P.i:0.5x:*axr1-3* | 11.355 | ABCDEFGH |
| P.i:0.5x:*aux1-7* | 11.9504 | ABCDEFGHI |
| P.ci:0.5x:*axr1-3* | 12.1522 | ABCDEFGHIJ |
| IAA:100nM:Col-0 | 13.0896 | ABCDEFGHIJK |
| P.ci:0.5x:axr2-4 | 13.6822 | ABCDEFGHIJK |
| P.ci:0.25x:Col-0 | 14.5008 | ABCDEFGHIJKL |
| IAA:1nM:*axr1-3* | 15.0254 | ABCDEFGHIJKLM |
| IAA:50nM:Col-0 | 16.2952 | ABCDEFGHIJKLMN |
| IAA:100nM:*aux1-7* | 17.08738 | ABCDEFGHIJKLMNO |
| IAA:1nM:axr2-4 | 17.4028 | ABCDEFGHIJKLMNO |
| IAA:1nM:*aux1-7* | 17.695 | ABCDEFGHIJKLMNO |
| P.u:0.05x:axr2-4 | 17.8794 | ABCDEFGHIJKLMNO |
| P.ci:0.25x:axr2-4 | 18.0164 | ABCDEFGHIJKLMNOP |
| IAA:1nM:Col-0 | 18.3658 | BCDEFGHIJKLMNOP |
| P.i:0.25x:axr2-4 | 18.7484 | BCDEFGHIJKLMNOP |
| P.ci:0.25x:*aux1-7* | 20.24363 | CDEFGHIJKLMNOPQ |
| P.u:0.05x:*aux1-7* | 20.3144 | DEFGHIJKLMNOPQ |
| P.u:0.05x:*axr1-3* | 20.461 | EFGHIJKLMNOPQ |
| P.i:0.25x:*aux1-7* | 20.9558 | FGHIJKLMNOPQ |
| P.i:0.05x:Col-0 | 21.14027 | DEFGHIJKLMNOPQR |
| IAA:50nM:*aux1-7* | 22.3842 | GHIJKLMNOPQR |
| P.i:0.25x:*axr1-3* | 22.7902 | GHIJKLMNOPQR |
| IAA:10nM:Col-0 | 22.98052 | GHIJKLMNOPQR |
| P.i:0.05x:*aux1-7* | 23.014 | GHIJKLMNOPQR |
| P.u:0.05x:Col-0 | 23.3416 | HIJKLMNOPQR |

| | | |
|---|---|---|
| P.ci:0.05x:Col-0 | 23.581 | HIJKLMNOPQR |
| P.ci:0.25x:*axr1-3* | 23.7334 | HIJKLMNOPQR |
| ½ MSB:1x:Col-0 | 23.8516 | HIJKLMNOPQR |
| IAA:10nM:*aux1-7* | 24.5902 | IJKLMNOPQR |
| IAA:50nM:axr2-4 | 24.644 | JKLMNOPQR |
| ½ MSB:1x:*aux1-7* | 25.2208 | KLMNOPQR |
| P.ci:0.05x:*axr1-3* | 25.4084 | KLMNOPQR |
| P.i:0.05x:axr2-4 | 26.9804 | LMNOPQR |
| ½ MSB:1x:*axr1-3* | 27.6834 | MNOPQR |
| P.ci:0.05x:*aux1-7* | 28.1084 | NOPQR |
| IAA:10nM:*axr1-3* | 28.2522 | NOPQR |
| IAA:100nM:axr2-4 | 28.7274 | NOPQR |
| IAA:100nM:*axr1-3* | 29.0158 | OPQR |
| P.ci:0.05x:axr2-4 | 29.2432 | OPQR |
| P.i:0.05x:*axr1-3* | 30.0634 | OPQR |
| IAA:10nM:axr2-4 | 30.6036 | PQR |
| ½ MSB:1x:axr2-4 | 31.926 | QR |
| IAA:50nM:*axr1-3* | 34.4214 | R |